FUSION OF MULTISCALE REGION-BASED FUZZY FEATURES FOR GAIT RECOGNITION

BY

AMER GHAZI ABDULLAH BINSAADOON

A Thesis Presented to the
DEANSHIP OF GRADUATE STUDIES

KING FAHD UNIVERSITY OF PETROLEUM & MINERALS

DHAHRAN, SAUDI ARABIA

In Partial Fulfillment of the
Requirements for the Degree of

MASTER OF SCIENCE

In

COMPUTER SCIENCE

JANUARY, 2017

KING FAHD UNIVERSITY OF PETROLEUM & MINERALS
DHAHRAN 31261, SAUDI ARABIA

DEANSHIP OF GRADUATE STUDIES

This thesis, written by **AMER GHAZI ABDULLAH BINSAADOON** under the direction of his thesis adviser and approved by his thesis committee, has been presented to and accepted by the Dean of Graduate Studies, in partial fulfillment of the requirements for the degree of **MASTER OF SCIENCE IN COMPUTER SCIENCE**.

Thesis Committee

Dr. El-Sayed M. El-Alfy (Adviser) 15/1/17

Dr. Tarek A. El-Bassuny (Member)

Dr. Wasfi G. Al-Khatib (Member)

Jan 16, 2017
Dr. Khalid Abdullah Aljasser
Department Chairman

Dr. Salam A. Zummo
Dean of Graduate Studies

19/1/17
Date

To my mother and father for all their love and support and putting me through the best education possible. To all my brothers and sisters whose encouragement and prays make me able to get such sucess and honor. I appreciate their sacrifices and I wouldn't have been able to get to this stage without them.

ACKNOWLEDGMENTS

First and foremost, I am grateful to Allah, the Most Merciful and the Most Gracious, for His guidance and blessings without which this thesis would not have been possible.

My greatest appreciation to my thesis advisor, Dr. El-Sayed M. El-Alfy, for his guidance, patience, and invaluable assistance to complete this thesis work. Also, I would like to thank my thesis committee members, Dr. Tarek A. El-Bassuny and Dr. Wasfi G. Al-Khatib for their helpful comments and discussions. Special thanks to my parents without their help and support I can't go through this thesis.

TABLE OF CONTENTS

LIST OF TABLES

LIST OF FIGURES

THESIS ABSTRACT

NAME: AMER GHAZI ABDULLAH BINSAADOON

TITLE OF STUDY: Fusion of Multiscale Region-Based Fuzzy Features for Gait Recognition

MAJOR FIELD: COMPUTER SCIENCE

DATE OF DEGREE: January, 2017

Gait recognition has become a popular research problem gaining importance for human identification based on walking style. It has emerged as an attractive research problem due to possessing several desirable merits. Unlike other biometrics, gait biometric can be computed from long distance and there is no need to prior configuration for targeted subjects. However, a gait recognition method can suffer from numerous challenging covariates that degrade its reliability and performance for human identification. This thesis explores three gait recognition fuzzy features that address various challenging covariates to reliably identify subjects with low computational complexity: Kernel-based Fuzzy Local Binary Patterns (KFLBP), Multi-kernel Fuzzy Local Gabor-Based Binary Patterns (MFLGBP), and Fuzzy Local Gabor-Based Binary Patterns (FLGBP). In KFLBP, instead of sampling

all points over one radius as in Fuzzy Local Binary Pattern (FLBP), multiple radii (kernels) with multiple neighbors are utilized and the information provided by multiple operators is combined. To overcome storage and computation burden, we adopt Gait Energy Image (GEI) as the spatio-temporal gait representation. GEI represents the human walking in a single image conserving motion temporal properties over an average gait cycle. Gabor filter is also utilized due to its robustness against local distortion and noise. The GEI image is convolved with a Gabor filter bank of different orientations and different scales. Most of the existing gait recognition methods that involve Gabor-based filters suffer from the curse of dimensionality, even with the use of a dimensionality reduction technique. This adds more computational and storage burdens and may cause difficulties to identify subjects with a high degree of confidence. Therefore, we propose two Gabor-based fuzzy feature (MFLGBP) and (FLGBP) that extract discriminative gait information by analyzing the Gabor responses. Instead of utilizing the whole Gabor responses, the proposed features encode the whole Gabor response into a histogram of 256 bins. Moreover, to enhance the performance of the proposed features, we propose to partition the GEI into different-sized regions. The partitioning has been conducted as a fraction of the subject's height and width. Intensive experiments are carried out to evaluate the performance of the proposed methods against several gait recognition methods. Linear-kernel Support Vector Machine (SVM) classifier is used for classification. The experimental results have shown that promising performance can be achieved with the proposed approaches under a variety of covariates.

ملخص الرسالة

الاسم الكامل: عامر غازي عبدالله بن سعدون

عنوان الرسالة: دمج سمات ضبابية متعددة النطاقات للتعرف على الأشخاص عن طريق المشي

التخصص: علوم حاسوب

تاريخ الدرجة العلمية: يناير، 2017

أصبح استخدام طريقة المشي للتعرف على هوية الأشخاص مشكلة بحثية ذات أهمية بالغة. فقد ظهرت كمشكلة بحثية جاذبة نظراً لامتلاكها عدة خصائص مميزة. على عكس القياسات الحيوية الأخرى، استخدام طريقة المشي كقياس حيوي يمكن حسابها من مسافات طويلة، وليس هناك حاجة إلى اعداد مسبق للأهداف تحت الدراسة. ومع ذلك، طريقة المشي كقياس حيوي يعاني من العديد من التحديات والمتغيرات الصعبة التي تقلل من موثوقيتها وأدائها لتحديد هوية الأشخاص. هذه الرسالة البحثية تستعرض ثلاث طرق لاستخراج سمات ضبابية من طريقة المشي والتي تعالج أنواع متعددة من المتغيرات المصاحبة للمشي لتحديد موثوق لهوية الأشخاص مع انخفاض التعقيد الحسابي. هذه الطرق هي: الأنماط الثنائية المحلية الضبابية متعددة الأقطار، الأنماط الثنائية المحلية الضبابية المبنية على تحويل قابور، الأنماط الثنائية المحلية الضبابية متعددة الأقطار المبنية على تحويل قابور. في الطريقة الأولى باستخدام الأنماط الثنائية المحلية الضبابية متعددة الأقطار، فبدلاً من أخذ كل العينات باستخدام قطر واحد كما هو الحال في الأنماط الثنائية المحلية الضبابية، توزع العينات باستخدام عدة أقطار ولكل قطر يتم استخدام الطريقة المقترحة ويتم دمج المعلومات الناتجة. ليتم التغلب على الأعباء الحسابية والتخزينية، تم استخدام صورة طاقة المشي كتمثيل مكاني وزماني للمشي. صورة طاقة المشي تعبر عن المشي البشري في صورة واحدة للحفاظ على الخصائص الزمانية للحركة كمتوسط لدورة مشي كاملة. تم استخدام مرشح قابور وذلك لثباته ضد التشوهات المحلية وعدم الانتظام. تتم عملية الالتفاف الرياضي بين صورة طاقة المشي مع مجموعة من مرشحات قابور باستخدام اتجاهات وتدرجات مختلفة. معظم الطرق الحالية للتعرف على هوية الأشخاص والتي تستخدم مرشحات قابور تعاني من مشكلة لعنة الأبعاد، حتى مع استخدام تقنيات التقليل من الأبعاد. وهذا يضيف المزيد من الأعباء الحسابية والتخزينية مما قد يسبب صعوبات في التعرف على هوية الأشخاص بدرجة عالية من الثقة. لذلك، تقترح هذه الرسالة نوعين من السمات الضبابية السابق ذكرها المعتمدة على مرشح قابور والتي تقوم باستخراج معلومات مميزة عن طريقة مشي الأشخاص عن طريق تحليل استجابات قابور. بدلاً من استخدام استجابات قابور بأكملها، السمات المقترحة تقوم بترميز استجابة قابور إلى مجمع تكراري يتكون من مائتان وستة وخمسون فئة. علاوة على ذلك، ولزيادة أداء السمات المقترحة، تم تقسيم صورة طاقة المشي إلى عدة مناطق مختلفة الأبعاد. تم إجراء التقسيم كنسبة من ارتفاع وعرض الشخص تحت الدراسة. تم إجراء العديد من التجارب لتقييم أداء السمات المقترحة ومقارنتها بالطرق المستخدمة حالياً للتعرف على هوية الأشخاص عن طريق دراسة طريقة المشي. تم استخدام الة متجه الدعم أحادية النواة للقيام بعملية التمييز بين عينات الاختبار. وقد أظهرت النتائج التجريبية أن أداءً واعداً من الممكن أن يتحقق باستخدام الطرق المقترحة وفي وجود العديد من المتغيرات المصاحبة للمشي.

CHAPTER 1

RESEARCH PROBLEM AND OBJECTIVES

1.1 Introduction

Human biometrics are used as a powerful tool to automate human identification and authentication. The word *biometrics* is originally a Greek word that consists of two parts: *bio* which means life, and *metron* which means measurement [10]. Biometrics relate to science and technology in order to identify humans based on their biological features.

Biometrics can generally fit into two categories: physiological or behavioral biometrics [11]. Physiological biometrics deal with the physical characteristics of the subject's attributes such as face, iris, fingerprint, palm print, etc. Moreover, they require the subject to cooperate in a predefined manner such as standing at a certain angle. On the other hand, behavioral biometrics study the subject behavior or action during a definite period of time. For example, gait is a famous instance of behavioral biometrics.

In large scale biometric-based authentication systems, using one biometric is

not enough. Most of intensively used biometrics require close-distance cooperation and require large size databases [12]. Besides, the recent trend is to use at least two different biometrics for fast processing. For example, face and iris recognition strict subjects to set directly in the front of the acquisition device. Gait biometric is used as a first check authentication to operate at distance in order to reduce the computation as well as the search space of identities. Then another close-distance biometric is used for high recognition rate achievement. Consequently, fusing multi-biometrics together is a promising area in recognition [13].

Techniques and algorithms for gait analysis are generally inspired from the knowledge of human motion analysis. A lot of motion analysis methods were inapplicable for human gait recognition due to the lack of video capturing and other necessary technologies. Nowadays, with the fast development in related technologies, it becomes possible to investigate and deploy more sophisticated methods and enhance the overall performance of gait recognitions.

1.2 Research Problem and Motivation

Recently, gait biometric is extensively utilized in forensics and criminal investigation purposes [14, 15, 16]. Also, gait recognition has great contribution in visual surveillance application, authentication and identification systems, access control related products, etc.

Unlike gait biometric, biometrics like face, iris, and fingerprints request the targeted subject to interact in a predefined way, be close, and stand at a predefined

angle. Gait biometric identifies people by their way of walking. In gait-based authentication systems, the process of image acquisition is non-intrusive; it can be done in public areas without attracting the attention of subjects under observation and no need for their cooperation. Also the system can work at long distance (e.g. 10 m or more) unlike most of other biometrics. Moreover, gait doesn't need high resolution sequences to operate in satisfactory performance.

Most of the gait-based identification approaches can be classified into two main categories [17]: model-free and model-based. The model-free approaches construct the gait by using static and dynamic building blocks. The shape and size of a human body represent the static part and the movement dynamics reflects the dynamic part. Gait static features include the height and width of the person's silhouette bounding box. Frequency and phase of movement are examples of dynamic features. Model-based approaches create knowledge about images before using it in feature extraction. Model-based approaches either use frequency and amplitude merged together with extracted features, or use a collection of images directly. Time is an important factor and generally research on model based is much less than that on model free because of the computationally expensive process.

Gait recognition has become a hot research area [18]. However, there are several challenges that directly affect the recognition performance of existing approaches. Gait recognition can be greatly affected by a number of variations like type of shoes, clothes, hair style, illness, carrying conditions, speed, etc. The

discriminating power of walking style can also be degraded by certain physical factors such as injuries. Moreover, there are several ambient conditions such as weather conditions, shadows near feet, etc. Nevertheless, gait is still a potential choice for intelligent visual surveillance and tracking of subjects at distance [19].

Despite the huge effort and research work that has been conducted, there is still an urgent need for more advanced methodologies to address these challenges and build more effective gait recognition methods.

1.3 Thesis Objectives

Our goal in this thesis is to conduct a basic and applied research on gait recognition. In order to achieve this goal, the following summarizes our research objectives:

1. Survey and analyze the strengths and weaknesses of existing methods.
2. Explore novel methods for feature extraction of gait images based on fuzzy logic.
3. Introduce a robust multiscale partitioning with region-based features for gait recognition.
4. Develop and evaluate the proposed methods on different gait covariates such as carrying objects, wearing coats, and varying walking speeds.
5. Publish papers to make our research and achieved results available to other interested researchers.

1.4 Thesis Organization

The following chapters of this thesis are organized as follows. In Chapter 2, we describe the state-of-the-art gait recognition approaches and summarize their main strengths and weaknesses. Chapter 3 briefly reviews Local Binary Patterns (LBP) and Fuzzy Local Binary Patterns (FLBP) for texture feature extraction. It also includes our proposed extensions for extracting relevant features to represent the gait energy image. We evaluate the performance of the proposed methods and discuss the attained results in Chapter 4. Finally, the thesis is concluded in Chapter 5 with suggestions for future work.

CHAPTER 2

BACKGROUND & LITERATURE REVIEW

2.1 Gait Recognition System Overview

A typical gait recognition system is composed of five main components. Figure 2.1 illustrates the main building blocks of silhouette-based gait recognition system.

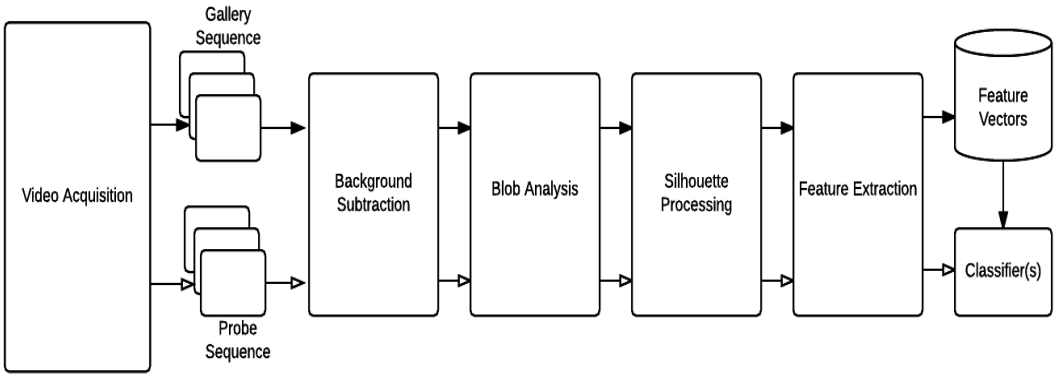

Figure 2.1: Silhouette-based gait recognition system

- **Video acquisition**: The process of capturing the raw data of the walking subjects through acquisition devices such as cameras.

- **Background subtraction**: The process of separating the static back-

ground to enable the focus on moving subjects.

- **Blob analysis**: In this component, the object of interest is isolated and passed into next component for silhouette formation.
- **Silhouette processing**: The foreground is binarized to form the subject silhouette. Then, if necessary, silhouettes are aligned and normalized to remove camera depth and view variations.
- **Feature extraction**: The process to convert the high dimensionality video data into a low-dimensionality representative set of features.
- **Feature vectors**: A database that stores the extracted features of gait sequences.
- **Classifier(s)**: Using extracted features from gallery sequences, a classification model is built and then used to identify probe subjects.

2.2 Taxonomy of Existing Approaches

Literature contains a number of reviews and surveys on gait recognition methods. However, they either focus on specific category of gait recognition methods [20] [21] [22] [23] or conduct the survey based on general classification [17] [24] [25] [26]. Other surveys present gait within a set of biometric modalities and illustrate the influence of emerging multiple modalities on the overall system accuracy [27] [28] [29] [30]. In this thesis, we provide a detailed taxonomy of existing gait recognition methods.

Figure 2.2 provides an overview of the surveyed approaches. In general, all gait recognition techniques can fit into three main categories: model-based, model-free, and fusion-based approaches. Each category has its characteristics and mechanism for extracting and utilizing gait features. The details of each category and examples from the literature are explained and described in the following subsections.

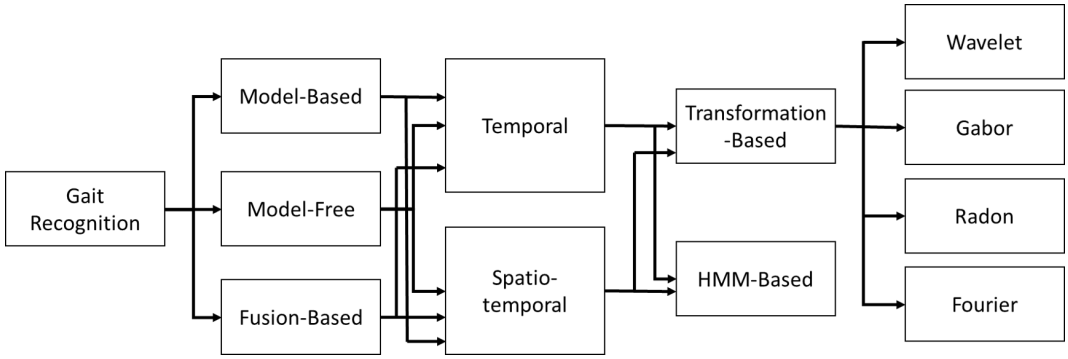

Figure 2.2: Taxonomy of existing gait recognition approaches

2.3 Model-Based Approaches

Model-based gait recognition methods calculate a set of static or dynamic human body parameters through modelling or tracking different body components such as limbs, legs, arms and thighs. Gait features derived from these parameters are then employed for humans identification and recognition purposes. However, model-based methods are sensitive to the quality of gait sequences and also computationally expensive due to parameters calculation.

Cunado et al. [1] modelled the lower limbs as two inter-connected pendulums. Hough transform was applied on image sequence to extract libs as shown in Figure 2.3a. Then, Fourier transform was used by processing the change of slope

with time by least-squares fitting to make data suitable for transformation. The features were represented by computing the magnitude spectra of the frequency content of the change in angle. In [31], the authors extended the work by extracting gait features directly from the evidence gathering process. Fourier series (FS) and Velocity Hough transform (VHT) techniques were used to model the hip rotation and extract the gait model, respectively. Moreover, a genetic algorithm (GA) was implemented to reduce the computational time in extracting model parameters. The experimental results showed that the method improved the correct classification rate and immunity to noise. However, the inter-connected pendulum model did not include full human motion. In Figure 2.3b, Yam et al. [2] used a dynamically coupled pendulums to describe full limb movement. Results showed that this model could be utilized to describe walking and running gaits.

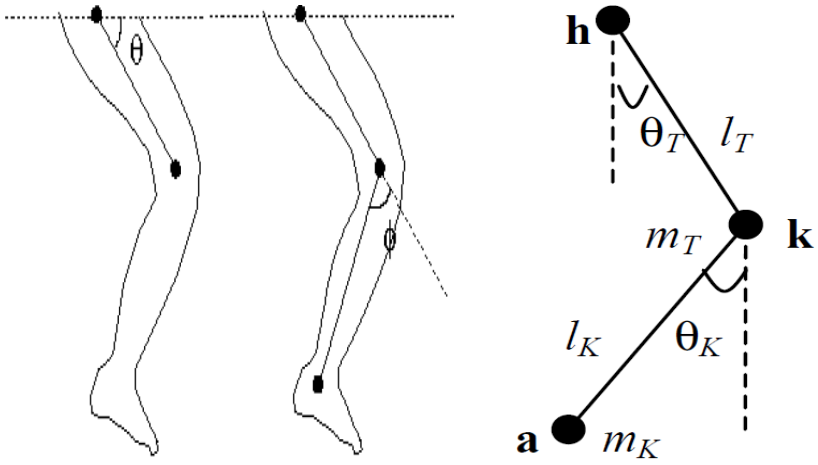

(a) (b)

Figure 2.3: The inter-connected pendulum model of a leg [1] (b) The dynamically coupled pendulums model [2]

Using human anatomical knowledge, Yoo and Hwang [3] [32] used contours of the human body to extract nine coordinates which were utilized to calculate

trajectory-based kinematic features from gait sequences for analyzing the gait motion as illustrated in Figure 2.4. Enhanced back propagation neural network was used to recognize humans. This method has the ability to predict a gait motion by using the phase-space portrait. Recently, it was extended in [33] to describe a new approach and an automated system to analyze and classify human gait motion using the 2D stick figures model features.

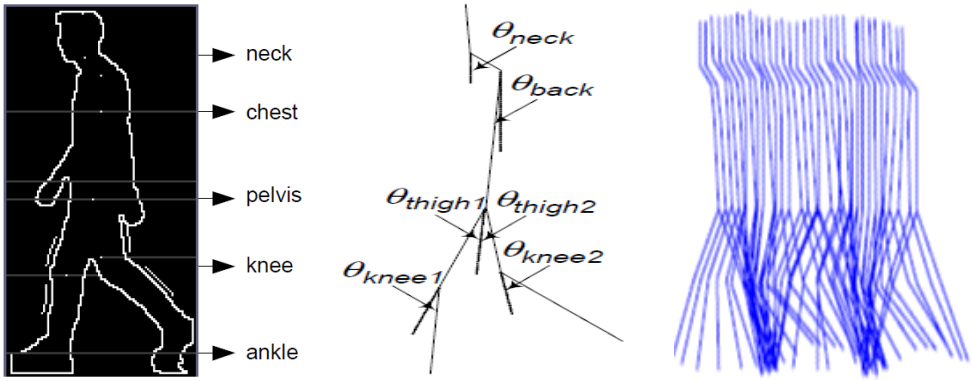

(a) body contour (b) stick figure (c) gait signatures

Figure 2.4: Gait stick figures constructed from gait silhouettes [3]

Lee and Grimson [4] constructed an elliptic gait model by dividing the gait silhouettes into 7 regions as illustrated in Figure 2.5a. The gait features were represented as the parameters of the ellipses and used for human recognition. As illustrated in Figure 2.5b, Zhang et al. [5] employed a five-link biped locomotion human model together with the base-to-height ratio and the relative height vector to effectively represent both the physical structure and movement characteristics of the person's body. This method was robust to different types of covariates such as clothes.

Tanawongsuwan and Bobick [34] used the angles between left and right hips

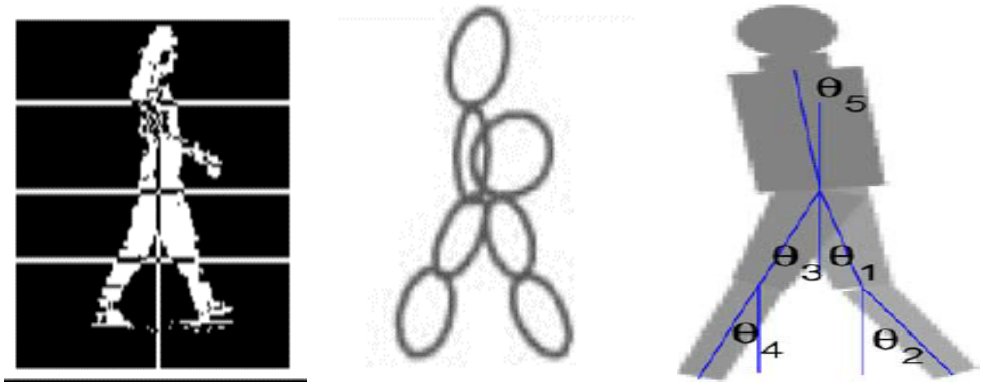

(a) (b) (c)

Figure 2.5: (a) The silhouette of a foreground walking person is divided into 7 regions [4], (b) and ellipses are fitted [4], (c) and the five-link biped human model [5]

and the knee joints angles as dynamic features for gait recognition. Magnetic sensors were attached to subjects and the obtained signals were normalized. Dynamic Time Wrapping (DTW) was used for time alignment and a feature vector of 240 dimensions was obtained. PCA dimensionality reduction analysis was applied to get a 4-dimensional feature vector. In Dockstader et al. [6], a hierarchical model was proposed using a set of thick lines joined at a single point to represent the legs and a periodic pendulum motion model to describe the gait pattern; this is illustrated in Figure 2.6a.

Haiping Lu et al. [7] recently proposed a full-body layered deformable model. The proposed model was designed for the fronto-parallel gait and the human body part shapes (widths and heights) and dynamics (positions and orientations) were described using 22 different parameters as illustrated in Figure 2.6b. The reported results demonstrated that the proposed method could benefit from both lower and upper limbs dynamics, as well as the shoulders and the head.

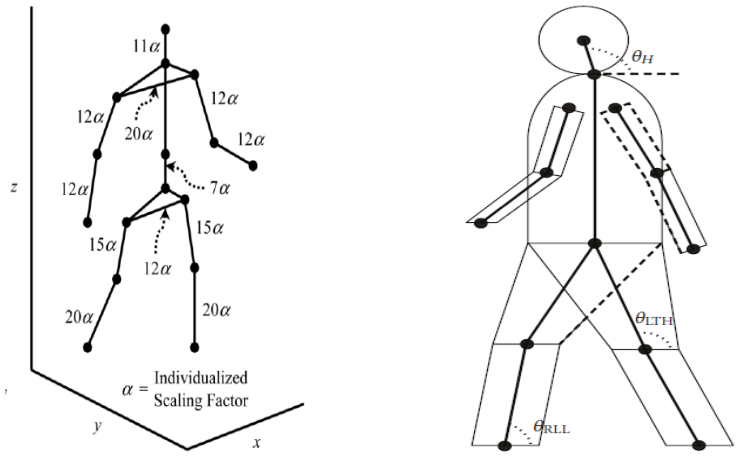

(a) (b)

Figure 2.6: (a) Hierarchical model [6] (b) Layered deformable model [7]

Four different static features were investigated in Bobick and Johnson [35]. These four features are: the distance from the head to the pelvis, the distance between the pelvis and right/left foot, the distance between the right and left foot, and finally the bounding box around the subject. As a trial to reduce noise, they divided the silhouette into five regions and used the centroids of those regions. Gaussian models were also used to remove shadows. Expected confusion was used to study the significance of recognition and the method's performance in the presence of huge datasets.

BenAbdelkader et al. [36] tracked the walker in video surveillance using the bounding box. Frequency of walking and stride length were then extracted through these bounding boxes. To reduce the effect of the pose of the walker, another feature was included which is the height. The recognition rate was 51% and enhanced to 65% using 2-dimensional and 4-dimensional feature vectors respectively.

Niyogi and Adelson [37] modeled the image sequence of a person in three dimensions: X, Y, and T; where X and Y are the dimensions of images and T represents the time dimension. The model was seen as a cube XYT. The XT plane was investigated and they found that the head behaves as a line and ankles give twisted pattern. Active contours were used to discover edges of ankle pattern. The silhouette of the walker was formed from averaging of the contours at various slices of XT plane of the cube, and that silhouette was used as an exemplar figure. From the stick figure, four joint angles were extracted and their derivatives were used to generate a feature vector of size 40 dimensions. Recognition rate of 79% was obtained using L2 norm for matching.

2.4 Model-Free Approaches

Model-free methods describe gait motion of the walking human based on either shapes of silhouettes or the whole motion of human bodies without considering the underlying structure. They have the advantage of low computational costs as they need not to calculate parameters to model the accurate motion patterns. As a result, model-free approaches are generally insensitive to the quality of silhouettes but usually not robust to changes of viewing angles and variations in scales. In the following section, we are reviewing some of relevant model-free approaches.

Wang et al. [38] proposed simple and efficient silhouette-based gait recognition method that has the ability for capturing the structural and temporal characteristics of gait. It depends on transforming the 2D binary silhouette into 1D distance

signal. After background subtraction and silhouette generation, the outer contour of subject was traced and the shape center (x_c, y_c) was determined. Then, the algorithm unwrap the contour in a counterclockwise manner to get the distance signal that is composed of distances between contour pixels and the shape center (x_c, y_c). To eliminate the discrepancies in size and magnitude between different distance signals, L1-norm was used to normalize the magnitude and re-sampling (360 samples) to normalize different sizes. Moreover, all sequences with lateral view were regularized by unifying their direction from left to right. In order to reduce the huge dimensionality of distance signals, PCA technique was applied on training and probe gait samples. Due to the spatio-temporal discrepancies between training and probe samples, dynamic time wrapping algorithm and normalized Euclidean distance (NED) were used to get the similarities between vectors. Nearest neighbor (NN) and exemplars nearest neighbor (ENN) classifiers carry out the classification process. The evaluation process was carried out using NLPR CASIA A gait database. It contains 20 subjects with three different viewing angles laterally (0°), obliquely (45°), and frontally (90°) and four sequences for each angle per subject. Performance evaluation was done through leave-one-out cross validation scheme. The best performance was 93.75% which obtained using NED with ENN classifier under frontal view (90°). The authors compared their method with other closely related algorithms and showed that their method outperform them in term of recognition rate and computation cost. It is clear that the proposed method is insensitive to noise such as color and texture due to the

use of silhouette of subjects. Also, it is simple to comprehend and to implement. The authors showed that it has relatively low computational cost. The proposed method is view dependent and unable to perform on multi-view applications. The variety in cloths may extremely degrade the overall performance.

Kale et al. [39] introduced a new gait feature. They proposed a width vector representation for the gait by computing the difference between boundary pixels of subject's contour for each row of the binary silhouette. The width vector retains the physical structure of the subject. Dynamic time wrapping (DTW) was used to wrap the discrepancies in gait cycles. Local distance between width vectors of test and training gallery was computed by using Euclidean distance. Three gait databases were used for performance evaluation: UMD, CMU, and USF with high recognition rates. Hong et al. [40] inspired their work from the idea of width vector and they called it mass vector representation. They tried to overcome some of the limitations in the gait representation using width vector. Mass vector is the number of nonzero-valued pixels in each row of a binarized silhouette. To evaluate the method, the author reimplement the width vector algorithm and applied both algorithms on CASIA A dataset. The obtained results showed the outperformance of mass vector over width vector in term of recognition rate (96.25%). Both algorithm lack the generality of viewing angles capabilities. They conducted their experiments in a view-dependent manner.

Ng et al. [41] proposed a silhouette-based gait recognition approach. It represents the subject's gait by using the height and width of the silhouette and six

joint angles extracted from the enhanced Hough-based human skeleton. First, morphological opening was applied on the noisy silhouette for clearing purposes. Then the width and height were extracted from the enhanced human silhouette. Six regions were then extracted among the silhouette: head and neck, torso, right hip and thigh, right lower leg, left hip and thigh, and left lower leg. To get the skeleton for each region, a morphological skeleton was applied on silhouette and joint angles were computed through Hough transform. The height and width with the six joint angles represent the feature vector to be used in the classification process. USF dataset with nine subjects was used for evaluate the proposed method. Classification process was performed through KNN and fuzzy KNN classifiers. Fuzzy KNN obtained the highest recognition rate of 72.07%. The main drawback of the proposed approach is that it is a view dependent and lack the generality of dealing with multiple covariates. Also. The extracted features may not reflect temporal and dynamic gait features that can enhance the accuracy to notable level.

Shaikh et al. [42] proposed a partial silhouette-based gait recognition approach in which the dynamic feature in swinging hands were extracted. First, the noise in binarized silhouette frames was removed through morphological processing and boundary filling. Then, the gait cycle was detected by using the ratio of height and width of the bounding box. The bounding box was divided into four quarters and the two mid-quarters were selected to represents the swinging hands. In feature extraction phase, the boundary of the segmented silhouette was converted into

1D signal by computing the distance between boundary pixels and the silhouettes centroid. PCA and Multiple Discriminant Analysis (MDA) were then applied on extracted feature vectors respectively for dimensionality reduction purpose. In the evaluation process, CASIA A and CMU-MoBo gait datasets were used. The proposed method was compared with the fully-used silhouette and the best performance was obtained over the lateral and frontal view of the partial silhouette with 85% and 96% for CASIA A and CMU-MoBo respectively. The proposed method can perform well in case of incomplete or noisy silhouette as long as the portion of hands in silhouette is retained and hand dynamics can be extracted clearly. Moreover, it is scale invariant due to the use of normalized distance. Also, the proposed method is costly low in term of computation and memory as just a portion of silhouette is used in computation process. As most of the literature gait recognition methods, it conducts all experiments on a view-dependent basis and give no attention to multi-view environment and applications.

Sabir et al. [43] applied Haar wavelet on human silhouette to extract and fuse three gait features. For each gait cycle, the LL1 wavelet sub-band was used and the distances between different parts of the body were computed and summarized through max, min, mean, and standard deviation to get a spatio-temporal feature vectors. The second feature is called Leg Motion Detection (LMD) feature and extracted by computing the hamming distance between legs in each consecutive frames for each leg separately. The obtained feature was Right Leg Hamming Distances (RLHD) for right leg and Left Leg Hamming Distances (LLHD). Mean,

standard deviation and least square were then gathered to represent the feature vector. The last features was statistical parameters that generated from the LL3 sub-band. The silhouette was divided into upper and lower parts and then mean and standard deviation were calculated for each part. Due to the high dimensionality of the three fused feature vectors, LDA algorithm was applied to map the feature space into a new low-dimensional space. The training and classification process was performed over CASIA B gait database and using the nearest neighbor classifier. Only side view (angle 90) was involved in experiments and the highest recognition rate of 97.98% was obtained from the fusion of the three features. The main drawback of the proposed method is the highly required computational power. Moreover, the proposed method is only applicable for view-dependent applications where in real environment the multi-view based gait method is inevitable.

Yang et al. [44] utilized the concept of histogram of gradient (HOG) to come up with efficient gait recognition feature. Silhouettes were first binarized and HOG method applied on two different scales of the binary silhouette. HOG window was divided into cells and an 8-bits histogram of the accumulative gradient of pixels at different direction was constructed for each cell. Due to the use of HOG at different levels and different block sizes of the binary silhouette, it regarded as an extension of HOG and called pyramid HOG. The total length of pHOG was 648 for each binary silhouette. The Gaussian mixture model (GMM) based HMM was then trained and a model for each subject was constructed. Experiments

were conducted using CASIA B (only 31 subjects) dataset on a view-dependent basis. HMM with 5 states showed the best recognition rate of 95.81%. Also, the authors compared their proposed method with two other common approach which are GEI and MMSI and the results showed the outperformance of the proposed method. It is clear that the proposed method may not be applicable for multiple view environments and applications.

Lee et al. [45] proposed a novel image weighting approach to detect the noise-free silhouette over those noisy silhouettes. Probabilistic SVM was used to classify silhouette frames into noise-free and noisy images. The output of PSVM was used to construct common implemented gait representations such as GEI, HTI, AEI, etc. to test the performance of the proposed method. Two benchmark gait datasets were exposed to the proposed method; CASIA A and SOTON. For simplicity, NN classifier performed the classification process. Obtained results showed the outperformance of the proposed method over the original gait representation used methods. It is costly in term of computation time.

Collins et al. [46] proposed a baseline gait recognition approach to provide a benchmark lower bound recognition rate for all silhouette-based gait methods. First, the silhouettes were extracted and a gait cycle extraction method was adopted. Silhouettes were then normalized. For each cycle, double support frames (with max stride) and midstance frames (with min stride) were extracted and established as templates for that subjects. Normalized correlation was applied to get matching scores for double support frames and midstances frame separately.

Then, NN classifier performed the classification process. Four gait databases were involved in experiments and method evaluation: CMU-MoBo, MIT, UMD, and USH. Results were reported with different conditions over different ranks.

Sengupta et al. [47] proposed a Fourier Transform based gait recognition method from binary silhouette sequences. Fast Fourier Transform (FFT) was first applied on binary silhouette images of a gait cycle sequence. As a result, a gait image was constructed at each frequency components. Due to the high number of these components, a threshold was used to select all frequencies components above that threshold. Pearson correlation was then applied for each gait image and a score was obtained. Based on the rank r used, the probe gait image is regarded as correctly classified if the correct class (subject) was within the returned r classes. The process was repeated for all gait images of a probe sequence. Last, a binary vector B was generated which indicates if a gait image at certain frequency is recognized correctly. Final decision was obtained through OR voting rule; we get correct recognition if one element of B is 1. USF dataset was used to evaluate the performance of the proposed method. Also, other peer methods were presented to show the outperformance of the proposed method.

Benbakreti and Benyettou [48] presented a new silhouette-based gait recognition from the contour and angles of different parts among the binary silhouette. The binary human silhouette was divided into seven parts based on anatomical prior knowledge. The lengths and distances were extracted among these parts to represents the gait. Moreover, the perimeter and area of the silhouettes contour

were extracted and added to the feature vector. PCA was then applied for dimensionality reduction purpose. Experiments were conducted using CASIA B dataset and results reported. The proposed method showed good results especially over the lateral view (degree 90). However, no comparison with other related gait recognition methods was conducted to show the effectiveness of the proposed method over other approaches. Also, the proposed method is view-dependent and may not be applicable to real environments and applications.

Kochhar et al. [49] utilize the naturally observable features in silhouette to recognize humans in high rates. Three silhouette-based gait features were extracted. First, the aspect ratio between height and width of human silhouette was computed through bounding box technique. Second, cubic Bezier curve was constructed and utilized to give unique insight to the human identity. Four control points were chosen to construct the curve: centroid, the knee outer contour, the heel and the toe. Standard deviation of these four points was computed and involved as a feature. Finally, the area between the right and left legs was observed and involved as a unique gait feature. All Experiments were conducted on the lateral view (degree 90) of CASIA A database and SVM was adopted for classification. Each feature was studied separately and compared with two other gait recognition approaches. The highest accuracy of 87.5% was obtained out of the Bezier curve feature. The obtained recognition rate was not that satisfactory although the used gait dataset is small and the literature has many outperformed methods.

Liu and Sarkar [50] proposed an averaged silhouette representation for gait recognition purpose. The silhouettes were first extracted and gait periodicity was detected for gait sequences. For each cycles in a gait sequence, the silhouettes were averaged to generate the proposed representation. Method evaluation was conducted using the USF gait challenge database. The set of averaged silhouettes in a gait sequence of a probe sample were compared to all gallery set sequences through the Euclidean distance and the negative median was selected as the similarity score. The proposed method was then compared with the baseline algorithm and the obtained results showed that the averaged silhouette method outperform in term of recognition rate in most established experiments. The authors reported that their proposed average silhouette method is also a 30 time improved in term of time. Moreover, the needed storage was also utilized.

Dadashi et al. [51] proposed a new wavelet-based gait recognition method. It describes the contour of silhouettes using wavelet packets. First, the authors used a threshold based method to subtract the background and extract the binary silhouettes. Then, the outer contour was detected to be used in the next procedures. The generated 2D contours were then unwrapped to 1D signal by finding the distance between the centroid of body and the contour boundary points starting clockwise from the top point. Due to the scale variations of the silhouette, the generated distance signals were then normalized. Discrete wavelet transform was then used to decompose the silhouette signals into 3 levels. Each signal is then projected onto atoms of the wavelet packet and 5 biggest coefficients using

Matching Pursuit algorithm are kept to represent each distance signal. Therefore, each gait sequence is mapped in a space of 380 dimensions. Due to the high dimensionality obtained, PCA and LDA was then used to reduce the dimensionality to 18 eigenvalues. Just 6 views out of 11 of CAISA B and CASIA C datasets were used to evaluate the proposed method. Transductive SVM was trained and tested and a classification rate of 96% of view 90 was obtained. This method gives no attention to the variation in views or even the different covariate factors. It was applied on 6 views separately.

Kellokumpu et al. [52] proposed a new gait recognition method based on using Local Binary Patterns from Three Orthogonal Planes (LBP-TOP) that spatiotemporally analyzes the human movements and extract LBP-based gait features. LBP-TOP is an extension of the basic LBP. It is a dynamic textures descriptor and has the ability to capture the appearance and the motion characteristics of human walking. The gait sequence is regarded as a space time volume and three planes were formed: xy (appearance plane), xt and yt (temporal planes). The authors have used elliptical sampling of neighboring pixels for both temporal planes, and circular sampling for the appearance plane xy. The LBP-TOP features were generated by concatenating the output histograms through the three planes. For unfitting pixels, bilinear interpolation was used to estimate them. Furthermore, the authors proposed a multi-kernels LBP codes in which more than one circular sampling radius with any number of points were used and regarded as one binary pattern. In the previous analogous work, the histograms of multiple radii were

concatenated. The proposed method used just the uniform LBP codes and removed the collection bin (bin of non-uniform codes) and bins of all white or black regions. Also, the volume was divided into four rough regions of legs and hands. Using of multiple kernels with merging sampling points as one LBP code definitely preserves the structural information in better way than the traditional method. And that is will not increase the size of the histogram that much. The division of the main volume into subvolumes will give more detailed description but, on the other hand, will increase the computations burden and produce more histograms. Experiments were conducted using CMU MoBo gait dataset due to its temporal variations (different speeds) and spatial variations (different covariates). Different setups were used and the obtained results compared with other methods in the literature. It was concluded that using appearance only is better than motion only. Combining both appearance and motion improve the performance slightly. Also, the proposed method is always better than the traditional multiresolution approach in case of regarding all bins; not only the uniform patterns. But, of course, that will be taken with the risk of increasing the histogram size.

Kusakunniran et al. [53] adopted the Procrustes Shape Analysis (PSA) to describe gait signature and to measure similarities between constructed signatures. The authors adapted the traditional PSA to tackle the problem of gait change due to the change in walking speeds. They proposed a higher order shape configuration (HSC) as an extension the traditional centroid shape configuration (CSC). Moreover, they introduced the differential composition model (DCM) to discrim-

inate the changes in shape caused by the changes in walking speeds. Also, DCM reflects the discrimination abilities of different body parts. Weights were given for different body parts using the Fisher discriminant ratio. Experiments were conducted on OU-ISIR A dataset and the experimental results demonstrated that the proposed approach are effective for cross-speed gait recognition.

2.5 Fusion-Based Approaches

Human vision perception system usually does not depend on a single gait feature to identify humans. There are many characteristics of the subject that might serve as alternatives. As a way to enhance the recognition performance, an effective strategy can be applied by combining or fusing multi-source information. These include model-free gait features fusion, model-based gait features fusion, and hybrid-based gait features fusion (fusing features from both model-free and model-based approaches). Relevant techniques are discussed as follows.

Wang et al. [54] fused static features extracted by the Procrustes Shape analysis and dynamic features extracted by tracking and recovering walkers joint-angle trajectories of low limbs. They got four signals: two from the left and right knees, and two from the left and right hips. Signals generated from several sequences of the same subject were averaged to get an exemplar for that subject. These signals were aligned to a fixed phase using dynamic time wrapping (DTW). The matching scores were computed for static and dynamic features separately then fused using different fusion strategies: sum, max, min, mean, and product. Their

method was applied on their own small dataset of 20 subjects and 80 sequences on total.

Bazin and Nixon [55] proposed a probabilistic framework for data fusion. Static and dynamic gait features were extracted from different sources. Wagg and Nixon [56] approach was applied to extract the dynamic features using model-based estimation. The static features were extracted using the method of Veres et al. [57]. Nandini et al [58] combined the maximal information compression index and the periodicity of the gait for recognition. The results demonstrated that the performance of the fusion approach was better than that when static or dynamic features were used separately.

Nandini et al. [59] proposed a new gait recognition method in which they combine wavelet coefficients with three silhouette geometrical features. Firstly, Haar wavelet transform was applied on each silhouette image of gait sequence and the approximation coefficients of the low frequency sub-band were stored as the first feature vector. Also, three silhouette geometrical features were extracted which are width, height, and area of the silhouette. These features were extracted from each frames in the gait sequence and then the mean feature vector was computed for each frame sequence. All experiments were conducted on CASIA A gait dataset and a recognition rate of 92.24% was obtained which is better than two other compared gait recognition methods.

Nandini and Sindhu [60] combined three gait features to come up with new gait recognition method. Wavelet approximation coefficient and Hough peaks as well

as the width and height of silhouette were combined together to recognize humans through gait features. First, a threshold-based background subtraction was used to get human silhouette. The approximation coefficients of the Haar wavelet were used as the first features of the proposed combination. Then, the silhouette skeleton was extracted and exposed to Hough transform. Hough transform detects the straight lines and describe them in two parameters: r (distance from origin to the line) and θ (the angle generated by the vector from the origin to the closet point to the line). The peaks of r were used directly as features. Beside the two features, width and height of silhouette were computed. For each gait sequence, the three features were extracted from each frame and then averaged to get the mean feature vectors. The authors compared their proposed method with their earlier work and with two peer gait recognition methods that used wavelet alone, Hough alone. The proposed method were outperformed and achieved 95% recognition rate using KNN classifier.

Nizami et al. [61] proposed to fuse multiple gait cycles by extracting GEI and motion silhouette image (MSI) images from each cycle. Autocorrelation was used to estimate the gait cycle length. Then for every cycle of a gait sequence, GEI and MSI images were extracted and used for training and testing. They adopted Extreme Learning Machine (ELM) to do classification. They performed fusion in the decision level not the features level. Outputs from ELM for each GEI and MSI images from the probe gait sequences were checked and the maximum output (max fusion rule) was chosen to indicate the predicted class. In [62] the authors

repeated the experiment but with a different classifier. The nearest neighbor (NN) was used to classify each GEI or MSI. The outputs from these NN classifiers were passed over majority voting mechanism to find the final decision. A small scaled CASIA A dataset and SOTON dataset were used for validation of the method. They conducted their experiments only on one view which is the canonical view (angle 0°). To analyze their method, they did not fuse features from different representations. Instead, they conducted experiments on each representation separately and they claimed that GEI led to better results. The fusion was actually done in the decision level not the feature level. Secondly, the dataset used in their experiments was small and only one view (angle 0°) was tested. The authors came up with a new gait recognition system in [63] and they called it motion contour image (MCI). The contour of each silhouette in the cycle is extracted using dilation mask and then they summed and averaged to get the MCI image.

Lam et al. [64] proposed a novel gait recognition model in which they combined two gait representations: motion silhouette contour templates (MSCTs) and static silhouette templates (SSTs). MSCT captured the characteristics of the motion of humans and SST focuses on the static features of human gait. The gait sequence was divided into cycles and MSCT and SST were extracted for each cycle. So, a set of MSCTs and SSTs were generated for each gait sequence. To avoid the variety of the numbers of MSCTs and SSTs in each gait sequence, the exemplar of MSCT and SST was computed as the average of the set of MSCTs and SSTs, respectively. Also in this study, the fusion was done on the decision level not the

feature level. Similarity score was computed for the MSCT and SST separately. The minimum sum of the two scores indicated the predicted class. They achieved a recognition rate of 85% on the SOTON dataset and 80% in the USF dataset which is not that promising.

Lu and Zhang [65] proposed a fusion strategy to improve the classification performance in gait-based human identification. Three features were used: Fourier descriptor [66], wavelet descriptor, and pseudo-Zernike moment. First, the silhouettes were extracted and binarized. Then the three types of features were extracted from the binary silhouettes and ICA was used for dimensionality reduction. The authors performed the fusion on the decision level not the feature level. Genetic fuzzy SVM (GFSVM) was used as the classifier. The experiments were conducted on small gait datasets (CASIA A with 20 subjects and AUXT with 50 subjects). Each subject has 3 different views and 4 sequences for each view. They obtained 95% recognition rate.

Han and Bhanu [67] used both real GEI template with distorted synthetics version of the real GEI templates. The distortion was to immune the system against the noise that may be generated in real life conditions. GEI images were extracted for each gait cycle in the gait sequence and then averaged to get exemplar template for both real and synthetic template. Then, principal component analysis (PCA) was applied on the both templates and followed by multiple discriminant analysis (MDA). The training and testing were done separately. In other words, for every probe gait sequence, real and synthetic templates was computed and

matched with the gait gallery. The scores obtained for both templates were fused to improve the performance of the system. The small USF HumanID dataset were used with 122 sequences.

Hong et al. [68] proposed a feature level fusion strategy to improve the performance of gait classification. They came up with a new feature called multi-bipolarized contour mean (MBCM) which is actually the process of extraction four mean vectors of subject contour in four different direction: vertical positive, vertical negative, horizontal positive, and horizontal negative. The authors simply used the four vectors in classification and that what they meant by fusion. CASIA A (20 subjects) dataset was used to conduct experiments and the nearest neighbor NN was adopted as the main classifier. The best obtained recognition rate is 96% from applying the fusion but that was only true for the oblique view (45°).

2.6 Temporal Comparison

The word 'temporal' comes from the nature of feature extraction and comparison mechanism. Feature extraction and recognition are performed on frame by frame basis. Each frame of gait image sequence is investigated to get the features and then matching these features between the test inputs and training patterns gallery (image sequences). The following sections describe some examples from the literature.

Kale et al.[69] proposed a new algorithm to track the walker and extract its

canonical pose. They track the walker using optical flow to discover the walking angle and then wrapping the image to the new canonical pose (fronto-paralle) projection. They used the height and leg dynamics feature and achieved encouraging recognition rate using the baseline algorithm of Sarkar et al. [70].

Some other gait recognition approaches use the period of gait cycles as gait feature. Ran et al. [71] used two different methods to extract the period: Maximal Principal Gait Angle (MPGA) and the Fourier transform. They used the input and output signals generated by Voltage Controlled Oscillator (VCO) to get the cycle period as the phase difference of the two signals. Ho et al. [72] used both static and dynamic features to determine the gait cycle period. The used static feature is the motion vector histograms and the used dynamic feature is the Fourier descriptors. They used Principal Component Analysis (PCA) and Multiple Discriminant Analysis to reduce the feature dimensionality. For the recognition process, they used the nearest neighbor classifier.

Kale et al. [73] used the width vector feature analysis proposed in [74] to identify humans through their gaits. Width vector is the difference between the left and right boundaries in the binary silhouette representation space. As a classifier, they used Hidden Markov Model (HMM) for recognition process. The main drawback in their approach is that it requires huge training data (more than 5,000) and this is not practical in gait application where the data is very limited. Moreover, HMM performance is sensitive to parameters initialization such as the number of states. Also, the viewing angle affects the overall recognition

performance.

2.7 Spatio-Temporal Summary

Spatio-temporal Approaches attempt to mitigate the computations expensiveness in the frame by frame comparison of temporal methods. The walking cycle can be summarized temporally, spatially or both. Temporal summary can be done by gathering statistics from the motion in the whole image sequence. Spatially we can do it by extracting a single quantity from the silhouettes of the image sequence. We describe some spatio-temporal examples in the following section.

Zhang et al. [8] proposed a new gait feature representation and called it Active Energy Image (AEI). AEI shows the actively moving regions. Successive frames are subtracted from each other and then all differences are summed and normalized. AEI reduces the effect of noise on the silhouette images. The authors applied two-dimensional Locality Preserving Projections (2DLPP) to reduce dimensionality and they got high rate of recognition on the CASIA B dataset. Figure 2.7 shows an example of an AEI image.

Wang et al. [75] combined static and dynamic features to get high accuracy on the Soton gait database. The bidimensional silhouette is converted into unidimensional distance signal. For each silhouette, the distance from the origin into predefined points on the boundary of the silhouette is computed to represent the dynamic features. All distance signals are normalized using the magnitude and then exposed to eigen-based analysis for dimensionality reduction. Features like

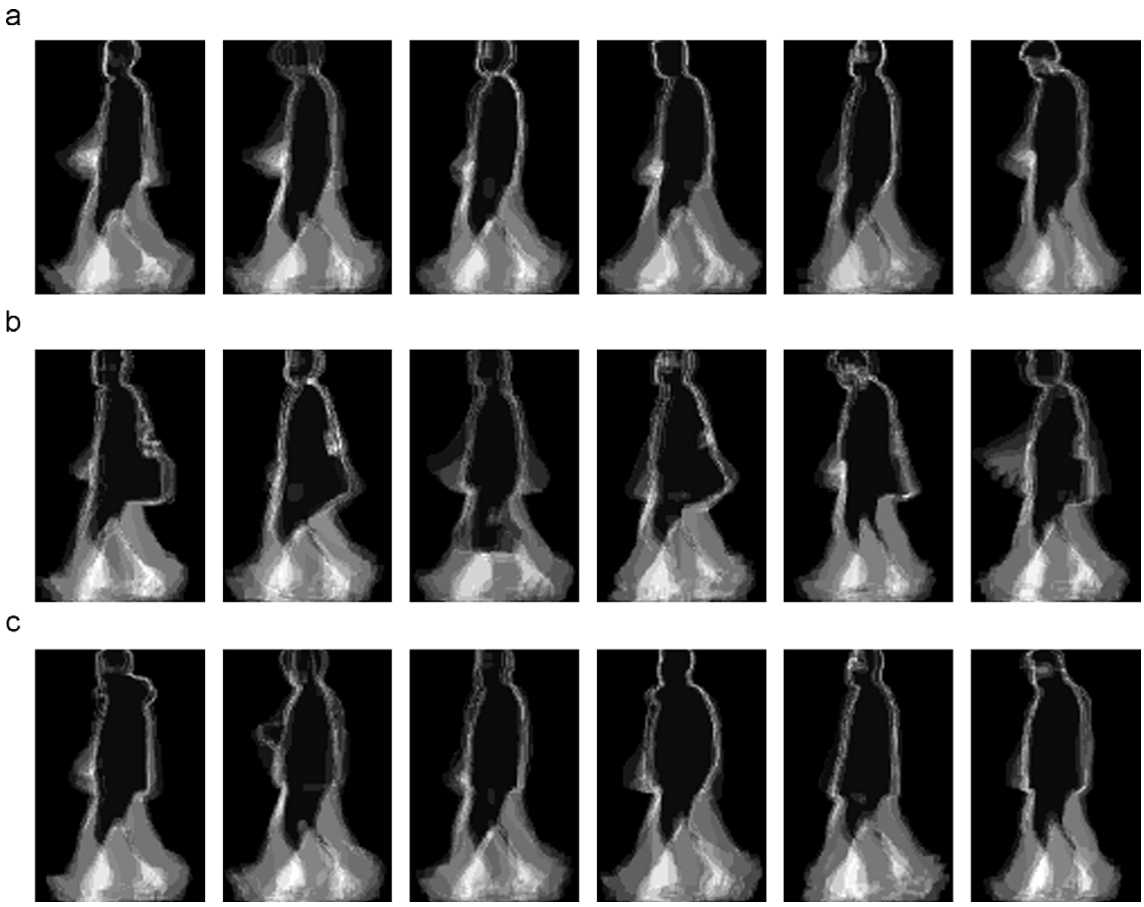

Figure 2.7: AEI samples [8]

height and aspect ratios of the silhouette were used as static features and combined with the dynamic features to get the benefits of both. For recognition, a nearest neighbor technique is used and the recognition rate was 100% on Soton database.

BenAbdelkader et al. [76] used video streams to discover subject motion and extract that motion using bounding box. Series of these bounding boxes are generated and scaled to common size. Then for each pair of frames the difference between each pixel is computed pixel by pixel. Cutler and Davis [77] used BenAbdelkader's approach to plot the two-dimensional similarity of the sum of all

frames differences and represent the summary features. Eigen space is used for analysis.

Lee [78] divided the binary silhouette of a walking human into seven elliptical-shaped regions. The walking person is perpendicular to the image plane. A view and appearance based approach is used to transform the person image into the image plane. Features are extracted from seven ellipses in form of parameters. However, the parameters are exposed to noise and it is difficult to find the periodicity using these features. As an efficient solution, mean and standard deviation of the features are computed to be used as the final summary features.

Han and Bhanu [9] proposed a new effective method to summarize the silhouette sequence spatiotemporally into a Gait Energy Image (GEI). Gait cycle is extracted from the gait sequence of silhouette and then all involved frames are summed and normalized to get the GEI image. GEI describes how motion proceeds. The more region is involved in motion, the brighter it is in the GEI image. In similar way with a relatively little difference, the Motion History Image (MHI) [79] is generated. MHI uses logical OR between successive silhouette frames to identify moving pixels. Figure 2.8 shows a GEI image generated from a silhouette sequence.

Chen et al. [80] proposed a dimensionality reduction method called tensor-based Riemannian manifold distance-approximating projection (TRIMAP). A graph is constructed from the given data in a way that preserves the geodesic distance between data points. Then the graph is projected into a lower dimen-

sional space by tensor-based optimization methods. The authors used Gabor filter to extract features from GEI representation of gait image sequences and applied a dimensionality reduction on the extracted features. They obtained promising gait recognition rate on the University of South Florida human gait database.

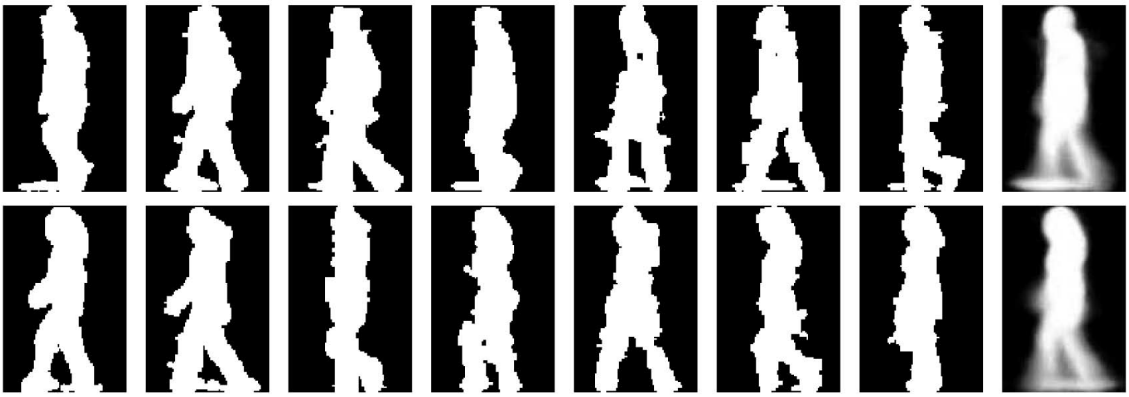

Figure 2.8: GEI image (rightmost) generated from silhouette sequence (HumanID gait database) [9]

Nizami et al. [81] divided the whole gait sequence into subsets and derived their own summarization method which is called the Moving Motion Silhouette Images (MMSI) for each subset. Independent Component Analysis (ICA) was used for dimensionality reduction purpose. Probabilistic Support Vector Machine (SVM) was used to classify the independent components and the obtained probabilities are merged to get the final recognition. They applied the method on CASIA A with 100% accuracy and with 98.67% for SotonBig dataset.

2.8 Transformation-Based Approaches

Some gait-based approaches transform the original silhouettes from its current domain into more informative domain. There are several transformation techniques

such as wavelet, Fourier, Radon, and Gabor which are utilized in the gait-based human identification approaches. We explain some of these transformation-based gait recognition approaches in the following section.

2.8.1 Wavelet-Based Methods

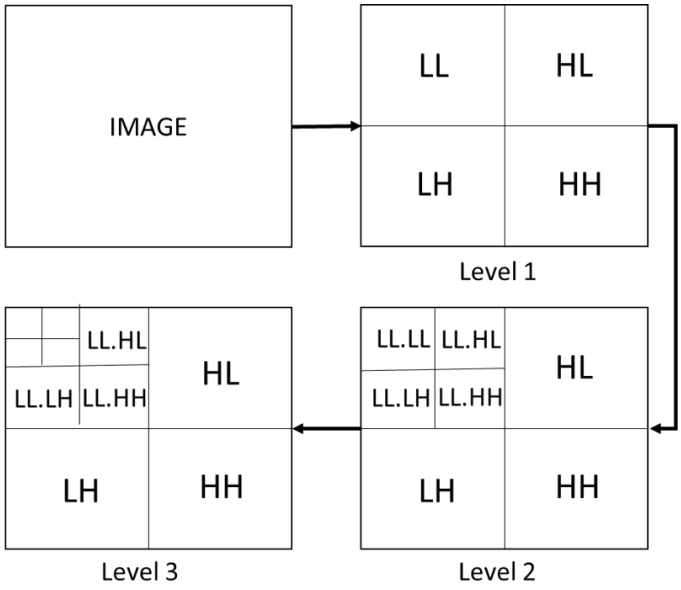

Figure 2.9: Wavelet Scheme

Rahati et al. [82] used wavelet transformation as a feature extraction technique on a frame basis style. Simply, they subtracted background from video tape and create the silhouette of the corresponding subject. Then, the exterior contour were detected and extracted out of the silhouettes to produce boundaries signals. To keep the size of the feature vector the same for all gait sequence frames, a linear interpolation was used to extract 100 data points for each frame of image. Wavelet transform of basis functions were then used to extract wavelet descriptors which in turn were used as gait feature vector. The authors conduct experiments on USF

dataset with 10400 gait frames; 7000 frames were used for training and 3400 frames were used for testing. KNN and multilayer perceptron neural network classifiers were used for training and classification. The authors used Fourier descriptors to evaluate their method. The results show that their wavelet-based approach outperform that based on Fourier descriptors in term of error rates. Also, they applied the approach on single resolution and multiresolution basis. The results show that wavelet perform well on decomposition level 4 in the case of single resolution with a recognition rate of 91%. Multiresolution had the best results over single resolution with a recognition rate of 94%. They claimed that wavelet descriptors are insensitive to variations and deformations of human body walking style. That is because of the choice of the coefficients of the low-frequency bands of transformation result. Also, multiresolution wavelet-based recognition is a reliable approach to be used in gait problem. On the other hand, it is computationally expensive to use multiresolution.

Wei et al. [83] proposed a novel gait image representation that captures both spatial and temporal characteristics of human gait style. They called it Spatial-Temporal Energy (STE). To generate STE image, first the contour of each frame in an image sequence is detected and extracted. Then, just one gait cycle is used and frames of that cycle are averaged to get the STE image representation. They have proved mathematically that STE is insensitive to noise attached to frames contours. Also, if the gait cycle includes unrelated frames,i.e. frames belonging to adjacent gait cycle, the influence on the recognition rate is negligible. Wavelet

transformation was then used with different configuration to generate four sub-images with different characteristics as follows: sub-image A captures the body expression, sub-image H captures the forward motion, sub-image V captures the undulation of the human body, and sub-image D captures the motion detail. Then, the four sub-images were linearly combined together to get the combined feature $f(x, y)$. After that, the concept of mutual information were applied to get the mutual information between the STE and its combined features.

Arai and Andrie [84] proposed a gait recognition approach based on a combination of wavelet sub-bands of two different gait features. Two preprocessing techniques were used: model-based and model-free. A human skeleton from each silhouette frame in the image sequence of a person was extracted by determining eight feature points: head, neck, waist, two knees, and two ankles. By connecting these points using straight line, the skeleton is created. The model-free preprocessing performs background subtraction to get the motion body per frame of sequence. Then, the authors applied Discrete Haar-based wavelet transform on each frame for both skeleton and motion representations as well as on the averaged frame sequence for both skeleton and motion. Wavelet at level 1 decomposes each frame into four sub-bands images: an approximation and three detail coefficients. The authors combined these four bands to generate 6 different feature combinations and use them in classification. 60 persons from CASIA dataset were used for evaluating the proposed method and compared with other peer approaches. Their method showed recognition rate of 95% which outperform other compared

gait approaches. Using model-based for extracting the skeleton of human body is very computationally expensive. Also, skeleton representations leads to lose other gait movement information. Motion representation is less costly and reflect more information than the skeleton-based model.

Du and Shao [85] proposed a novel gait recognition approach based on Haar wavelet and using SVM classifier. First, video sequences for subjects were processed and background was subtracted using Gaussian Mixture Model (GMM) to get the binary silhouette frames. Then, outer contour was detected and extracted out of the generated binary silhouettes. Then, Haar wavelet transform was applied on the extracted contours and four sub-images were generated. The authors claimed that the cH component carries the motional information of the human walking behavior. So, they used only the cH sub-images as the signature points for classification process. Due to the high dimensionality of the cH image (quarter of the original contour image), PCA technique was used to reduce the features dimensionality. CASIA and SOTON gait datasets were used to evaluate the proposed method and SVM classifier was trained and tested. A recognition rate of 91% and 94% were obtained from CASIA and SOTON respectively. This method suffers from the curse of dimensionality even after applying PCA for reduction purpose. Also, the method was compared against non-wavelet-based approaches.

Ming et al. [86] proposed a fusion strategy of two model-based gait features: skeleton-based and contour-based features. The skeleton model was determined using eight predefined key points: the mid of head, the mid of shoulder, the mid

of neck, the mid of hip, the mid of both knees, and the mid of both malleolus. The feature vector was then generated by computing the six angles between the joints of the human skeleton. Also, the ten coordinates were included in the feature vector. For the silhouette contour-based feature, the authors came up with their own modified edge tracking algorithm and the distances between the centroid and the edge points were computed. Then, the DB2 wavelet transform was applied on the distance signals to generate 64 points of the wavelet descriptors. Then, the authors performed simple fusion by concatenating the two feature vectors together to get the global feature vector. Three views of 80 subjects of the CAISA B were used; 36, 54, and 90. The training and testing was conducted using SVM classifier based on RBF kernel function. The experiments showed best performance on the fusion of features and angles with 87.50%. It is a simple process to get the contour but, on the other hand, contour cannot deal with self-occlusion and doesn't reflect the motion details. Skeleton model is more useful in representing the joints in motion than the contour representation and more suitable for multi-view gait analysis. DB2 wavelet transform is simple and less computationally expensive than other versions of wavelet transform.

Lu et al. [87] adopted wavelet descriptors to represent the human silhouettes. Firstly, the silhouettes were extracted for each gait sequence using background subtraction. Then, the contours were detected and extracted to represents the silhouettes. These contours were then unwrapped into 1D distance signals by computing the distance between the centroid and the boundary points. To fix

the length of the distance signals, only 256 boundary points were selected using resampling of the contour points. Then, discrete wavelet transform was conducted on the distance signals to get the wavelet descriptors. Only 64 points of the lowest frequencies of the generated wavelet descriptors were selected because the lowest frequencies include most of the energy. Independent Components Analysis (ICA) was then used to reduce the feature dimensionality in such a way the ratio of within-class distance and between-class distance is minimized. NN and SVM classifiers were adopted and experiments were conducted on two gait datasets: XAUT and CASIA A. The experiments were run on several ranks and different number of ICA selected components. SVM Recognition rates of 85, 95, and 100% were obtained using Rank 1, 5, and 10 respectively on the CASIA A dataset. Discrete wavelet transform is a robust tool against scales, linear transformation, and rotation. Despite of the high recognition rates obtained out of their proposed method, both XAUST (10 subjects) and CASIA A (20 subjects) don't reflect the compatibility of the proposed method with large gait datasets with many subjects, views, and covariate factors.

Li et al. [88] proposed a novel combination of gait features based on Quaternion Wavelet Transform (QWT) which is an improved version of the discrete wavelet transform. Unlike previous wavelet-based approaches, the proposed method combine the magnitude of the low frequency sub-band with the phases of the other three high frequency sub-bands after applying QWT on the GEIs. The low frequency band includes the energy and more smooth than the other three sub-bands.

The other three sub-bands include the details and represent the intensity of the features. The features were constructed by the low frequency sub-band (magnitude) and the other three high frequency sub-bands (phases) column-wise and then normalize to zero mean and variance of the unity. To alleviate the effect of the curse of dimensionality, PCA and MDA were executed on the feature space to obtain low dimensional feature space. All experiments were conducted on the USF gait dataset. The proposed method was compared with baseline method as well as with the methods that use magnitude only or phase only. The recognition rate of the proposed method outperformed other methods in some probes of USF. The average rate was 57.08% which is better than the baseline method. QWT is a good tool for analyzing magnitude and phases of images. Also, QWT is suitable tool for multi-view applications like gait because of its shift invariant properties. The main drawback of the proposed method is the heavy computations and the effect of high dimensionality features on the recognition performance.

Zhang and Liu [89] proposed the use of Haar wavelet and Radon transform consecutively on the binary silhouette of gait sequence. First, GMM-based background subtraction was performed and binary silhouettes were generated. One gait cycle was extracted out of the whole sequence to be used in the subsequent operations. The silhouettes were then bounded using a rectangular box and the area outside that box was deleted out. Secondly, Haar wavelet transform was performed and the two high frequency sub-bands cH and cV were selected. cH and cV are the horizontal and vertical frequency components of the binary silhouette

respectively. The gait cycle are then divided into four similar state using Hu moments similarity measure. Then, radon transform was performed on the cH and cV wavelets and used for classification. The experiments were conducted using cH only, cV only, and the synthesized of both respectively. CAISA B and SOTON were the source of gait data. The higher recognition rate was obtained out of the synthesized representation with 94% and 93% on CAISA B and SOTON datasets respectively.

Sabir et al. [90] proposed a gender classification system in which three types of gait features were fused: spatiotemporal and two wavelet-based features. Wavelets transform was applied and two of the obtained frequencies sub-bands were used to extracted leg motion model and wavelet statistical features. First, CASIA B videos were preprocessed and background subtraction was used to extract binary silhouettes. Then, gait cycles were estimated and then silhouettes were normalized and aligned. The spatiotemporal features were extracted from each silhouette across on gait cycle by computing five distances as follows: distance between both hands, knees, feet, and shoulders as well as the height of the silhouette. Leg Motion was the second set of features and computed by tracking each leg in each frame and then compute the hamming distance between legs in each consecutive frames. Mean and standard deviation were then used to construct the feature vector. For the last and third feature, wavelet transform was applied on the silhouette and the sub-band LL3 was chosen and divided into upper and lower parts. Mean and standard deviation were found for each part and used as feature

vectors. To evaluate the proposed method, one viewing angle (90°) of CASIA B was used. KNN and SVM were trained and tested. Spatiotemporal features were the best in term of recognition rate than the two other features. Combining the spatiotemporal and statistical wavelet features outperformed the other tested features combinations. In case of fusing the three features together, three fusion methods were use: score fusion, feature fusion, and voting fusion. Score fusion outperformed both feature and voting fusion. The recognition rate was 96.47% on average. A heavy computational process was performed across the proposed method and high dimensionality feature vectors were obtained due to the feature fusion even the authors tried to alleviate its effect through LDA dimensionality reduction algorithm. Moreover, all experiments were conducted across only one viewing angle (90°) which is unpractical and not follow the multi-viewing nature of gait-based applications.

Amin and Hatzinakos [91] proposed a new appearance based gait feature through the wavelet gait analysis. The lower part of the human body was targeted and analyzed based on wavelet transform. Three main steps were followed to get the gait signatures. First, the Georgia Tech silhouette database was passed through median filter to remove the possible outliers and binarized smoothed silhouettes were obtained. Secondly, the gait cycle was estimated through the analysis of the lower part of silhouettes area (number of silhouette pixels). Signal of the motion was derived and the cycle was detected accordingly. Thirdly, the area signal of silhouettes across gait cycle were exposed to the 1-D discrete

wavelet transform with Daubechies 4 (db4) kernel. Four statistical information was computed for each frequency subbands: mean, standard deviation, kurtosis and skewness. Then feature vector of length 16 was created and normalized. The proposed method was evaluated using nearest neighbor and Georgia Tech gait dataset of 15 subjects. 5 probe sets were created and used. Three peer gait recognition methods were compared with the proposed method in terms of recognition rate and computation expensiveness. In most cases, the wavelet-based method outperformed the Baseline algorithm which uses the silhouette directly in matching. Also, the mass vector method outperformed the proposed method in most experimental cases. In term of computation, the wavelet-based method has lower time complexity than the Baseline algorithm and mass vector method. Moreover, the proposed method is more compacted than Baseline and mass vector method. The proposed method has only 16 dimensions whereas Baseline algorithm uses the whole silhouette and mass vector method uses set of feature vectors equals to the number of frames in gait cycle each of length 128 features. The wavelet-based proposed method is less sensitive to the noise in silhouette due to the preprocessing median filtering.

Arai and Asmara [92] used 3D skeleton model to extract gait features based on the 3D Discrete Wavelet Transform (3D DWT) for the sake of gender classification. The authors created their own gait dataset using Kinect Camera and Ipisoft motion capture software. First, the Kinect camera captures the depth data. And then the Ipisoft uses the recorded data to track the motion and create the 3D

skeleton after removing noises. After that, the 3D skeleton was exported into Ipisoft (BVH) file format. 3D Haar Discrete Wavelet was then exposed to the 3D skeleton data and 8 frequency subbands were obtained. To get the feature vector, three statistics were extracted out of each subband: mean, standard deviation and energy. Two version of the dataset were used: raw data and resized version of data. SVM and Nave Bayes classifiers were trained and tested for specific set of features and the classification rates were reported for each scenario. The highest recognition rate of 83.75% was using SVM when using the raw data. Unlike 2D analysis of human gait skeleton, 3D skeleton has more accurate 3D coordinates of the extracted human skeleton which may help in enhance the accuracy. The rareness of 3D gait dataset makes it difficult to conduct valuable and comprehensive experiments. Also, the proposed 3D methods suffer from the curse of data dimensionality and they are costly in term of storage.

Chen et al. [93] proposed a wavelet-based gait recognition method in which motion templates called Stride History Images (SHI) were analyzed. First, background subtraction algorithm was applied on gait sequences and silhouettes were extracted and binarized. To make things simple, the silhouette moving from right to left was converted left to right movement using horizontal mirror. To estimate gait cycle, the contour points were first detected and the three histogram bins were constructed by computing the number of contour points in each of the three halves in the lower quarter of the silhouette. Then, two subsequence of consecutive strides (left foot forward and right foot forward) were extracted starting from a

trough in the plotted histogram bins signal. Then, for each stride, the SHI, which represents the cumulative image of the difference between consecutive frames in the stride sequence, was generated to get two motion templates forward SHI and rear SHI to be used later in feature extraction and classification. Then, the SHI images were first mapped to polar coordinates in which the center of SHI images are the origin using the unit disc. After that, the cubic B-spline wavelet moments were extracted to be used in classification. To evaluate the proposed approach, SOTON dataset was used and it consists of 115 different subjects. Experiments were conducted using NN classifier and a recognition rate of 88.20% was achieved.

2.8.2 Radon-Based Methods

Boulgouris and Chi [94] proposed a Radon-transformed silhouettes templates as a new gait recognition system. The binary silhouettes of USF dataset were exposed to Radon transform after estimating the cycle of each gait sequence and perform silhouette alignment. Unlike other transformation-based gait recognition methods, Radon-based method does not need a prior noise filtering of binary silhouettes and that is because each Radon coefficients involves the contribution of several silhouette pixels and, consequently, the generated transformed is less vulnerable to variations in pixels values due to possible noises. Radon transform uses the center of the binary silhouette as the reference point and sum the pixels intensities across lines determined by two parameters p and θ. (x, y) coordinated binary silhouettes were mapped to (p, θ) Radon coordinates and each point (p_i, θ_i)

corresponds to Radon coefficient which is the sum of pixels along a line in a silhouette determined by the parameters p and θ. Then, the Radon-transformed template was constructed by first applying continuum transform function on each Radon coefficient image and then summing and averaging. The authors assumed that the frequency for all gait sequences (training and testing) were the same and this is not practical. However, this will not affect the performance of the proposed method due to the summing process along template construction. LDA algorithm was then used to get low-dimensional feature space. The proposed method was evaluated using seven different test sets of USF gait dataset. The authors compared their method with four different peer gait recognition methods and reported the performance. Also, they conducted experiments using feature vectors of two lengths: with length 50 and 70 and with Rank 1 and Rank 5. The proposed method using feature vector of length 50 was generally outperformed all other methods with an averaged accuracy of 56%.

2.8.3 Gabor-Based Methods

Huang et al. [95] proposed a gait recognition method based on the application of Gabor wavelet and using a proposed modified version of the GEI gait representation under the existence of overlapping walkers. Also, the authors gave more attention to shadows and their effects on gait recognition. Firstly, background subtraction was performed on the gait sequences to extract all walkers. As an improvement step, adaptive background model was then executed to alleviate the

effect of illumination and slow walking. Then, shadows were removed to generate the complete silhouettes. Secondly, in the case of overlapping walkers, a three step search (TSS) was performed to prevent the confliction of using multi-walkers in silhouettes as on person which negatively the classification performance. Then, one gait cycle was used to generate a modified version of GEI. Gabor wavelet was then executed over the modified GEIs to create Gabor gait feature vectors. The Gabor vectors were with high dimensionality, so PCA was utilized to get low-dimensionality projection of the feature space. SVM with RBF-kernel function was trained and gait classification was then conducted to evaluate the proposed method. Experiments were conducted using CAISA A gait dataset and a recognition rate of 90% for lateral view (0 angle) was obtained and reported as better than existing comparable methods. As it is clear, this method is more real than many of the existing gait recognition methods because it gives attention to shadows and walkers overlapping scenarios. However, it is computationally expensive and may have low response time in real-system application in which time is a critical factor.

Hu et al. [96] utilized the Gabor filters on gait silhouette to get Gabor-based gait features. Gabor filters with different orientations and scales were first applied on silhouettes to represents body shapes. PCA and Maximization of Mutual Information (MMI) were used to reduce the dimensionality of Gabor features. Then, Gaussian Mixture Model-Hidden Markov Models (GMM-HMMs) was trained and used to classify the new test samples. The proposed method was evaluated using

CASIA B and compared to other state-of-the-art similar approaches. Gabor filter is insensitive to changes of covariates such as carrying condition and clothing.

Chen et al. [80] proposed a dimensionality reduction method called tensor-based Riemannian manifold distance-approximating projection (TRIMAP). A graph is constructed from the given data in a way that preserve the geodesic distance between data points. Then the graph is projected into a lower dimensional space by tensor-based optimization methods. The authors use Gabor filter to extract features from GEI representation of gait image sequences and applied their dimensionality reduction on the extracted features. They obtained promising gait recognition rate on the University of South Florida human gait database.

Tao et al. [97] proposed a novel solution for the undersample problem (USP) and they called it the general tensor discriminant analysis (GTDA). (USP) refers to the problem in which the dimensionality of the extracted features is much higher than the training samples. (GTDA) was used as a preprocessing step for the linear discriminant analysis (LDA) classification method. They have claimed that their reduction method outperforms most of the popular and frequently used methods such as the principle components analysis (PCA) and two-dimensional LDA (2DLDA). GTDA reduces the effect of USP problem. Also, it preserves the discriminative information in the training dataset. The solution of GTDA converges due to the use of projection optimization algorithm and this leads to stable classification accuracy. The authors used Gabor-based gait images representation to test and evaluate their new method. Three different versions of Gabor are

used: 1) the sum of Gabor filters over directions (GaborD), 2) the sum of Gabor filters over scales (GaborS), and 3) GaborSD which the sum of both GaborD and GaborS. The USF gait dataset was used for conducting several number of experiments to test the recognition rate stability of the GTDA.

Yang et al. [98] propose a Gabor-based representation of GEI gait images using discriminative common vectors (DCV). First, GEI image is convolved with 40 Gabor kernels. Then, DCV is applied on the Gabor responses to reduce the dimensionality and enhance the distinguishing ability of GEI. The proposed method is evaluated on the benchmark USF HumanID database and experimental results demonstrated that the proposed approach can help in improving the overall performance.

Similarly in [99], Yang et al. proposed an enhanced version of GEI called Enhanced GEI (EGEI). Dynamic region analysis based on variance analysis is proposed to segment the GEI into several discriminative dynamic regions. To alleviate the noise effect, a dynamic weight mask is applied. The obtained EGEI was then convolved with Gabor filters and then Gabor responses were passed over discriminative common vectors (DCV) for dimensionality reduction purpose. Experimental results over USF HumanID demonstrated the effectiveness of the proposed method in term of accuracies.

Zhang et al. [100] proposed LBP-based approach to reduce the dimensionality of obtained Gabor responses. LBP operator encodes each Gabor response into histogram of binary codes. Each pixel is tested with respect to its neighbors by

using hard thresholding. Similarly, the same authors use the same mechanism on the pahse of Gabor responses [101].

Zhang et al. [102] proposed Local Gabor Phase Patterns (LGPP) based on applying the Local XOR Patterns (LXP) operator on both real and imaginary parts of Gabor responses. LXP operator first quantizes the values into different ranges and then thresholds the interest point with its neighbors. Similarly, Xie et al. [103] proposed local Gabor-based LXP patterns (LGXP). They applied LXP on the Gabor phase to generate binary patterns which in turn are represented using histogram distribution.

Guan et al. [104] proposed a cross-speed gait recognition approach using classifiers ensemble framework based on Random Subspace Method (RSM). First, GEI images were constructed by averaging all frames within one complete gait cycles. Then, the constructed GEI images were convolved with Gabor filters with five scales and eight orientations to generate more robust Gabor-GEI gait representation. A two-dimensional Principle Component Analysis (2DPCA) was applied on Gabor-GEI to reduce the high dimensional constructed images. Authors came up with the claim that speeds variations only affects part of the human body and can be tackled with series of week classifiers based on RSM. Each base classifier was generated by randomly sampling on the original feature set before the final classifier combination using majority voting. Experiments were conducted on OU-ISIR A dataset and results demonstrated that higher speeds are more efficient to be used as gallery set for cross-speed walker and runner identification.

2.8.4 Fourier-Based Methods

Tian et al. [105] proposed an appearance gait feature for gait recognition based on Fourier transform. First, the silhouettes of humans were extracted from gait sequences through background subtraction algorithm. A 3×3 low-pass filter and a bench of morphological operations were then applied on the extracted silhouettes to filter the noise and fill the gaps respectively. Then, the silhouette contour was traced and described as complex numbers for each frame in the gait sequence. Equal points resampling technique was then used over the extracted contour points to unite their size for all samples. To generate the 1-D distance signal, the Euclidean distance from the contour center to each arbitrary boundary point was discovered. To relive the effect of size difference of dataset gait images, all generated distance signals were normalized. Discrete Fourier Transform (DFT) was then applied on the extracted distance signals to generate the Fourier gait descriptors. Only the 30 lowest frequency components were chosen as gait features and involved in training and classification process. Experiments and evaluation were investigated using CMU and Body DataBase gait databases. Results showed that proposed method has encouraging performance.

Ling et al. [106] used Fourier transform to describe the shape of movement for gait-based human identification. The contour central distance signal was first extracted and normalized to 256 point samples. Then, the fast Fourier transform was applied over these distance signals for each frame image to get Fourier coefficients. The 15 coefficients with lower frequencies were chosen to represents

the human gait. Two different classification methods were investigated. Due to the temporal differences which cause differences in the length of gait sequences length, Hausdorff distance with NN classifier were used in the classification process. Also, HMM was trained and tested due to its great capabilities of capturing temporal transition and analyzing time-varying data. The proposed method was evaluated using CASIA A gait dataset and compared with another gait recognition method. A recognition rate of above 85% was obtained using HMM classifier. Fourier descriptor has the advantage of controlling the invariances of the proposed gait feature. That is obtained through the manipulating of the Fourier extracted coefficients. On the other hand, Hausdroff method is sensitive to the noise in gait sequences.

Huang et al. [107] proposed a Fourier-based gait recognition approach. Silhouettes were extracted by passing the gait sequences over set of operations in order: background modeling, background subtraction, shadow removal. Then, Fourier descriptors were discovered by applying Fourier transform over the boundary of human silhouette of each frame within the targeted gait sequence. The proposed method used three different number of lowest frequency components: 10, 15, and 20. The authors created their own database with 15 image sequences for 5 different groups of people: children, pregnant, adult, with stick, and aged. The best recognition rate of 81% was achieved using 20 frequency components as gait features and SVM as the classifier. The proposed approach achieved his merit from the characteristics of the Fourier transform which is scale, rotation, and translation

invariant.

Some other gait recognition approaches use the period of gait cycles as gait feature. Ran et al. [108] used two different methods to extract the period: Maximal Principal Gait Angle (MPGA) and the Fourier transform. They used the input and output signals generated by Voltage Controlled Oscillator (VCO) to get the cycle period as the phase difference of the two signals. Ho et al. [109] uses both static and dynamic features to determine the gait cycle period. Static feature is the motion vector histograms and the dynamic feature used is the Fourier descriptors. They used Principal Component Analysis (PCA) and Multiple Discriminant Analysis to reduce the feature dimensionality. And for recognition process they used the nearest neighbor classifier.

2.9 HMM-Based Approaches

Iwamoto et al. [110] proposed a HHM-base gait recognition approach in which the persons outline (contour) was used as the gait feature. As a common gait preprocessing step, the silhouette was first extracted using background subtraction and then binarized. By analyzing the gait sequence and computing the distances between feet, the gait cycle can be extracted and then used as the identification unit. The contour of a person was then extracted and resampled to get the same numbers of points for each silhouette. P-expression which is used for expressing the curvilinear of P-style Fourier Description uses the outline curve and convert its points into a complex-valued set of points. The real and imaginary part were then

linearly combined together to form the feature vector. Due to the high dimensionality of the generated feature vector, PCA algorithm was applied and set to 10, 20, 30, 50, 100 set of dimensions. Due to the time-serial characteristics of gait cycle, HMM was used as the identification tool to get benefits of its superiority of capturing the dynamic and temporal features characteristics. HMM needs first to be trained its parameters. For each person, feature vectors series out of each gait cycle was used to train that persons HMM model. For each feature vector series, Baum-Welch algorithm performed the training by calculating the optimal values of those parameters (probabilities) that makes the probability of observing that series in this HMM model the maximum. Three probe sets were prepared and experiments with different setups were conducted. The results showed the compatibility and robustness of HMM for gait recognition application in case of using more than two states and two or more Gaussian mixtures. The authors claimed the validity of their proposed method based on conducting experiments of only one viewing angle of walking (0°). In practical applications, cameras are capturing walking in different angles. Multi-view examination should be performed. Identification process is exploiting just one gait cycle whereas information of two or more gait cycles is captured through cameras in real life (wasted information). Also, more sophisticated gait features than silhouette contour can be investigated.

Kale et al. [111] used the width vector feature analysis proposed in [112] to identify humans through their gaits. Width vector is the difference between the left and right boundaries in the binary silhouette representation space. As a clas-

sifier, they used Hidden Markov Model (HMM) for recognition process. The main drawbacks in their approach that it requires huge training data (more than 5,000) and this is not practical in gait application where the data is very limited. Moreover, HMM performance is sensitive to parameters initialization such as number of states. Also, the viewing angle affects the overall recognition performance.

2.10 Cross-View Gait Recognition Approaches

Wang et al. [113] proposed a cross-view gait recognition method based on the couple metric learning (CML) approach. The authors incorporate the concept of separable criteria to avoid the limitations in CML. The basic idea of CML is to map the data points into couple subspace in which points from the same class are close to each other; reducing the within-class distance. However, distance between classes may be also small. So, the separable criteria was applied to CML to solve the problem of between-class distance. Experiments were conducted based on GEI feature of CASIA B gait dataset. Classification was performed using NN classifier. The proposed method was compared with two approaches: CML and Canonical Correlation Analysis (CCA). The obtained results demonstrate the outperformance of SCML.

Kusakunniran et al. [114] utilized the proposed view transformation model (VTM) with optimized version of GEI gait representation. The authors here applied LDA over GEI to get an optimized version of GEI with less dimensionality and more discriminating separability. Then VTM was trained using a reduced

version of Singular Value Decomposition (SVD) which is called Truncated SVD (TSVD). The probe gait sequence and the gallery set gait sequences were transformed using the VTM into the same viewing angle. CASIA B dataset was used to train and construct the VTMs. The proposed method was compared with similar VTM method [115] with Fourier features and using standard SVD. The obtained results showed that VTM with optimized GEI and TSVD outperformed VTM with Fourier feature and standard SVD for all tested cases (one view transformation and multiple view transformation). The proposed multi-view gait recognition method achieved better recognition rate compared to similar approaches. Moreover, the proposed method reduced dimensionality of the gait features as well as the size of the VTM models. However, it requires high computational process especially for constructing the VTM models.

Kusakunniran et al. [116] proposed a cross-view gait recognition method. The proposed method passes through two main stages: view-normalization and recognition stages. In the first stage, gait silhouettes were used to construct a new proposed Gait Texture Image (GTI). Then, Transform Invariant Low-Rank Textures (TILT) was applied on the constructed GTIs to obtain the domain transformation of the gait information in the new common canonical view. And to better recognize human through gait in different views, the authors applied Procrustes Shape Analysis (PSA) on the gait silhouettes on their new canonical view to extract a PSA-based view-invariant gait feature. In PSA, shape boundaries were first detected through the Border Following algorithm. The size of extracted boundary

was then resampled into 100 sample points. Then, the Pairwise Shape Configuration (PSC) was used to describe the resampled shape by measuring the relation between each boundary point and its consecutive neighbor. Finally, Procrustes Mean Shape (PMS) was applied on the extracted PSCs vectors to extract gait feature which incorporates shape and motion information. PMS has several advantages. It preserve the similarity between different samples of the same subject under the same viewing angle. And it also give discriminative power between different subjects under the same viewing angle. The Procrustes Distance (PD) was performed to measure the similarity between probe and gallery sequences. Five views of the CASIA B gait database and the USF were used through the evaluation experiments. Results showed that the proposed method has better performance in term of accuracy in most tested cases. The performance of the proposed method highly degrade when the viewing angle of the targeted gait sequences is frontal or close to the frontal view.

Hu et al. [117] proposed a linear unitary feature projection method for cross-view gait recognition called View-invariant Discriminative Projection (ViDP). The main objective of ViDP is to map the gait feature of a subject under certain view into a subspace in which gait features from the same subject under different views are close to each other and apart from gait features of different subjects. Two benchmark gait databases were used in the evaluation process: CASIA B and USF. 24 subjects of CASIA B were used to train the ViDP and the rest 100 subjects for method evaluation. Experiments were conducted first with one viewing angle in

the gallery data and then with multiple views in the gallery data. The obtained results showed that ViDP give better performance in term of recognition rate over similar compared cross-view gait recognitions and projection methods. ViDP performed the best in case of using three different views of CASIA B in the gallery set (18, 90, and 162) with average recognition rate of 90%. Also, a recognition rate of 83% was obtained in case of USF gait database which exceeded other similar compared methods. The advantage of using ViDP for cross-view gait recognition that it maps the original features to lower dimensional subspace in a way that feature of same subjects are close to each other and apart enough from features of other subjects. On the other hand, ViDP require a preprocess stage in which gait sequences of different subjects were used to train and generate the projection matrix.

Han et al. [118] proposed a multi-view gait recognition method based on GEI feature. The authors concluded that the GEIs extracted from a subject through different view may overlapping or adjacent if the difference between views angle is not too large. The authors constructed a series of GEIs out of each gait sequence by overlapping 3/4 of frames between consecutive GEIs. They showed that similarity can be generated among GEIs in the extreme frames of different sequences of different views for the same subject. The authors constructed their own dataset of 8 subjects and 10 directions for each. Minimum Euclidean distance classifier was used to perform classification. Results showed that the proposed method obtained good performance.

Al Mansur et al. [119] Proposed a cross-view gait recognition based on Multi-view Discriminative Analysis (MvDA). Unlike other cross-view projection methods, MvDA analyses the gait data and come up with view-dependent projection matrices for each gait view. CASIA Band OU-LP benchmark gait databases were used to conduct experiments and evaluate the proposed framework. GEI feature was extracted over the two databases and then exposed to MvDA. Partial set of subjects were used to train the MvDA and to construct the projection set of matrices. NN classifier was used for similarity measurements. Results showed that for small difference between probe and gallery views, LDA outperformed MvDA due to the fact that LDA can absorb the variation in views. However, MvDA outperformed other approaches in case of large views differences. Also, MvDA requires large training data to perform at high rate. So, MvDA performed better for the large data OU-LP that for the CASIA B.

Muramatsu et al. [120] proposed a view transformation cross-view gait recognition approach. First, subset of the gait dataset was used to train and extract the transformation matrix through the SVD algorithm. The transformation matrix was then applied on probe and gallery data to transform the view of one to the other. In the recognition phase, transformation consistency measure was used to measure the dissimilarity between the reconstructed probe and gallery features. Based on the linear logistic regression (LLR), the obtained scores were used to calculate the likelihood ratio (LR). To evaluate the proposed method, OU-LP gait dataset was utilized and similar approaches were involved. The viewing angle of

55 degree was used as a gallery and a different view of 85 degree as a probe. The authors utilized the frequency domain features (FDF) as the gait features. The proposed method had the best accuracy over other involved approaches.

Kusakunniran et al. [121] proposed a view transformation SVD based method for multi-view gait recognition. Unlike similar approaches, the view transformation problem was reformulated into a regression problem and each view transformation model consisted of set of regression processes. First the well-known GEI gait features were constructed. Then, SVD matrix factorization was applied to generate set of view-dependent sub-matrices. Then, Support Vector Regression (SPR) with three different kernels was utilized to generate series of regression processes which used to predict a pixel value under the targeted view from relevant pixel value on region of interest (ROI) area on the source view. The proposed method was evaluated using CASIA B gait database and Euclidean distance was used to measure the similarity among gait features. 24 subjects were used to train the SVD based VTM and 100 for evaluation. The proposed method was compared to other SVD based approaches as well as with different kernels of SVR. The best performance of 93% was obtained using RBF-SVR and outperform all involved similar methods and other used kernels. SVR tool give generalization performance and sparse due to the use of view-dependent training. Also, it gives global optimal solution unlike other regression techniques. Due to the use of linear kernel, SVR can work with large feature space.

Huang and Boulgouris [122] proposed a weight-based multi-view gait recogni-

tion method. The distance is computed along all available views and then weights was given for each viewing angle. Part of the gait dataset was used in the process of determining the appropriate weights by formulating it as optimization problem. GEI was used as the gait feature and extracted from five different views of the CMU-MoBo gait dataset. Dissimilarity was measured using Euclidean distance. For each probe sequence under certain view, the distance was computed along all available views of each subject. Then, a fusion rule was applied to get the final similarity score. Experiments were conducted for all views separately and for different fusion rules and compared to the proposed weighting method. The obtained recognition rates clarify the outperformance of the proposed method.

Chen et al. [123] proposed a cross-view gait recognition method based on projection of Gravity Center Trajectory (GCT) feature. After estimating the parameters of 3-D GCT using only one probe gait sequence, the coefficients of the constructed model were projected into different view planes. Then, the projection curves on different planes were obtained and used as an appropriate cross-view gait feature. Then, the view transformation matrix was constructed based on the projection feature of curve and plane. To improve the accuracy and fill the gaps, the body part trajectory (BPJ) was also extracted as gait feature and investigated separately during experiments. Finally, the scores of both features obtained using correlation strength similarity measure were cumulated and the final score obtained. The evaluation was based on CASIA B gait database. Several scenarios were implemented: one-view to one-view, multi-view to one-view, and extreme

views scenarios. The performance of the combined feature matching was better than using the two feature separately. And the GCT achieved better performance than BPJ when used separately. The proposed method outperformed state-of-the-art similar approaches. It achieved that improvement and efficiency with less than 80 dimensions and with computation due to the linear projection.

Kale et al. [124] proposed a novel approach in which all arbitrary views were translated to a common side view. Subjects were tracked using perspective projection and optical flow to estimate the azimuth of the walker. The authors conducted experiment on their own created dataset of 12 subjects. The Sarkar et al. [70] baseline algorithm was adopted to evaluate the proposed method end encouraging results were obtained.

Table 2.1 shows main information of the main gait recognition approaches in the literature.

2.11 Comparison of Gait Approaches

2.11.1 General Comparison

Model-based methods require an intensive computational process to build model and extract gait features. Consequently, Research related to this category doesn't attract interested community and can't compete with model-free approaches. On the other hand, model-free methods is simple to extract and formulate as well as less expensive in term of computation cost. We believe that publications towards

Table 2.1: Summary of Main Gait Recognition Approaches

Authors	Feature Extraction	Gait Dataset	Classifier(s)	Recognition Rate
Rahati et al. [82]	Wavelet	USF	KNN MNP	94%
Wei et al. [83]	Basis Wavelet	SOTON	NN	High
Arai and Andrie [84]	Haar Wavelet	CASIA	n.a.	95%
Du and Shao [85]	Haar Wavelet	CAISA B SOTON(large) SOTON(small)	SVM	CAISA B 91% SOTON(large) 94% SOTON(small) 90%
Dadashi et al. [51]	Basis Wavelet	CAISA B CAISA C	TSVM	96%
Ming et al. [86]	DB2 Wavelet	CASIA B	SVM-RBF	87.50%
Lu et al. [87]	Discrete Wavelet	XAUT CAISA A	KNN SVM	(85,95,100)%
Li et al. [88]	Quaternion Wavelet	USF	KNN	57.08%
Guan et al. [104]	Random Subspace Method (RSM)	OU-ISIR A	Classifier Ensemble	100%(6km/h)
Nandini et al. [59]	Haar Wavelet Geometrical features	CASIA A	Sum Rule	92.24%
Huang et al. [95]	Gabor Wavelet	CASIA A	SVM-RBF	90%
Nandini and Sindhu [60]	Haar Wavelet Hough Geometrical features	CASIA A Real data	KNN	95%
Zhang and Liu [89]	Haar Wavelet Radon	CASIA B SOTON	Hu moment	94% CASIA B 93% SOTON
Sabir et al. [90]	Spatiotemporal Statistical Wavelet Leg motion	CASIA B	KNN SVM	96.47%
Amin and Hatzinakos [91]	Discrete Wavelet	GeorgiaTech	NN	94.32%
Arai and Asmara [92]	3D Discrete Wavelet	Own Dataset	Naive Bayes SVM	83.75%
Chen et al. [93]	Cubic B-spline Wavelet	SOTON	NN	88.20%
Kusakunniran et al. [53]	PSA HSC	OU-ISIR A	Procrustes Distance (PD)	100%(6km/h)
Arai and Asmara [92]	3D Discrete Wavelet	Own Dataset	Naive Bayes SVM	83.75%
Boulgouris and Chi [94]	Radon Template	USF	Euclidean	56%
Iwamoto et al. [110]	Geometrical Fourier	Own Dataset	HMM	High
Kellokumpu et al. [52]	Multiresolution LBP-TOP	CMU MoBo	Histogram Similarity	88%
Wang et al. [38]	Signal distance	NLPR CASIA A	NN ENN	93.75%
Kale et al. [39]	Width vector	UMD CMU USF	DTW ED	80% 95.8%
Hong et al. [40]	Mass vector	NLPR CASIA A	DTW	96.25%
Ng et al. [41]	Height width six joint angles	USF (9 subjects)	KNN Fuzzy KNN	72.07%
Shaikh et al. [42]	Partial silhouette 1D distance signal	CAISA A CMU-MoBo	ED	85% 96%
Sabir et al. [43]	Wavelet	CASIA B	NN	97.98% (view 90)
Yang et al. [44]	pHOG	CASIA B	HMM	95.81%
Lee et al. [45]	Image-weighting	CASIA A SOTON	PSVM	98.23%
Collins et al. [46]	Baseline method (Body shape)	CMU-MoBo MIT UMD USH	Normalized Correlation NN	High
Sengupta et al. [47]	Fourier Transform	USF	Pearson correlation	High
Benbakreti and Benyettou [48]	Perimeter Area Angles	CASIA B	DTW	High
Kochhar et al. [49]	Aspect ratio Bezier curve area between legs	CASIA A	SVM	87.5%
Liu and Sarkar [50]	Averaged Silhouette	USF	Median of ED	Moderate
Ling et al. [106]	Fourier Descriptor	CASIA A	Hausdroff with NN HMM	Greater than 85%(view 90) HMM

new mode-based features for gait recognition are very rare. We can say that the current deployed features lack the enough discriminative capability that may attract interested researchers. Also, it should be taken in first considerations of any new attempts to develop more distinctive feature, that it will consume a lot of computations and, consequently, resources.

The main notable problem with the model-based methods that they are inapplicable for real time applications and scenarios. Construction of models and extraction of features require considerable time that violate minimum requirements of real time systems.

On the other hand, model-free methods are simple and more intuitive. Features can be extracted in frame by frame basis or as a bench of summary features. It generally outperforms model-based approaches with the advantage of less time and resources requirements. Under the category of spatiotemporal gait sequence representations such as MHI [79], GEI [9], and AEI [8], apparent recognition rates were achieved. Later, gait features were proposed and applied over these spatiotemporal summary representations and proved better performance. As model-based methods are not suitable choice for real time scenarios, also model-free suffers in some cases. When gait method capture gait features on a frame-based manner, this arise need for aligning feature vectors due to the difference in the number of frames in each gait sequences and, as an intuitive result, violate real time requirements.

2.12 Influential Factors and Challenges

Gait recognition process can drastically be degraded in term of accuracy by the effects of covariate changes and gait related challenges. In this section, we highlight some factors that have direct influence on the performance of biometric gait based methods. Some of these factors are external such as walking surface, shoes type, object carrying, clothes, lighting, viewing angle, environment (indoor or outdoor) and walking speed. The other factors cause subjects to abnormally walk due to physical and physiological conditions such as injuries, limbs disabilities, gait related diseases (e.g. Parkinson), mental disabilities, pregnancy, and body weight changes.

Several efforts for tackling such challenges have been reported in literature. View transformation model (VTM) is the most popular solution for alleviating the effect of the change in viewing angles as reported in [114] [115] [119] [117] [120] [121]. The framework proposed in [125] shows the dramatic reduction in correct classification rate due to variations in view angle, clothes and carrying conditions. Normalization as well as proposing view-invariant gait features [116] [118] [123] also proved some flexibility to viewing angle changes challenge‘ in gait recognition. Moreover, human silhouette is greatly negatively affected by variations in the speed of walking. It changes stride length as well as silhouette dimensions (height and width).

Table 2.2: Publicly Available Gait Datasets

DB Name	Year	Angle	Sub.	Seq./sub.	Cycles	#Cams	Highest CCR (%)
UCSD [126]	1998	n.a.	6	7	3	1	92.20% [127]
UMD	2001	T-shape	55	220	n.a.	2	100%
UMD3 [128]	2004	15/30/45/60	12	n.a.	n.a.	2	91%
CASIA A	2001	45	20	12	3	2	98.23%[44]
CASIA B [125]	2005	11 angles	124	110	3	11	98%[116]
CASIA C	2005	11 angles	153	110	3	11	51.61%
CMU MoBo [129]	2001	Various	25	16	n.a.	6	96%[42]
LAB5	2008	n.a.	5	4	n.a.	1	n.a.
SOTON(large) [130]	2001	6	∼100	2128	1.5	2	94%[85]
MIT	2001	n.a.	24	225	3	1	n.a.
OU-ISIR A [131]	2012	Various	34	n.a.	n.a.	25	100%[53]
OU-ISIR B	2013	Various	68	n.a.	n.a.	25	90.72%
OU-ISIR D	2013	Various	185	n.a.	n.a.	25	90.80%
GA Tech	2001	45/135	20	194	n.a.	3	94.32%[91]
USF [70]	2005	2	122	n.a.	n.a.	2	94%[82]
MMUGait [132]	2013	Side/Oblique	82	194	n.a.	3	98.20%

2.13 Publicly Available Gait Databases

Table 2.2 shows a description for the main publicly available gait databases. Some variations happened from time to time due to the frequent update from the publishers. Some common notes on these databases are listed as follow:

- All are unimodal; focus on one biometric type which is here the gait.
- Cameras are positioned at mid of human body.
- Most of them use low resolution video recording and just few use (DV) technology. DV is a format for storing digital video. It was launched in 1995 with joint efforts of leading producers of video camera recorders.
- Use lossy encoding.
- Have 15-30 fps frame rates.

CHAPTER 3

GEI-BASED GAIT FEATURES

3.1 Gait Recognition Workflow

As demonstrated in Figure 3.1, the worlflow of gait recognition starts with the acquisition of human motion (which can be either through a video camera or from prestored videos). Next, silhouette extraction is performed in which the background is subtracted and the person's silhouette is formed. Background subtraction aims to separate the static background to enable the focus on moving subjects. The object of interest is isolated and passed into the subsequent component for silhouette formation. The silhouette over a gait cycle is converted into a single image known as gait energy image (GEI). Feature extraction, which is our scope in this chapter, converts the high dimensional video data into a low-dimensional representative set of features in order to perform classification. Optionally, the extracted features can be further reduced using a feature selection technique. Finally, a computational model is constructed for classification. This model will be deployed to identify a moving subject by going through a similar

process to extracted relevant features as input for the model.

In the following subsections, we describe several approaches for gait features extraction based on gait energy image.

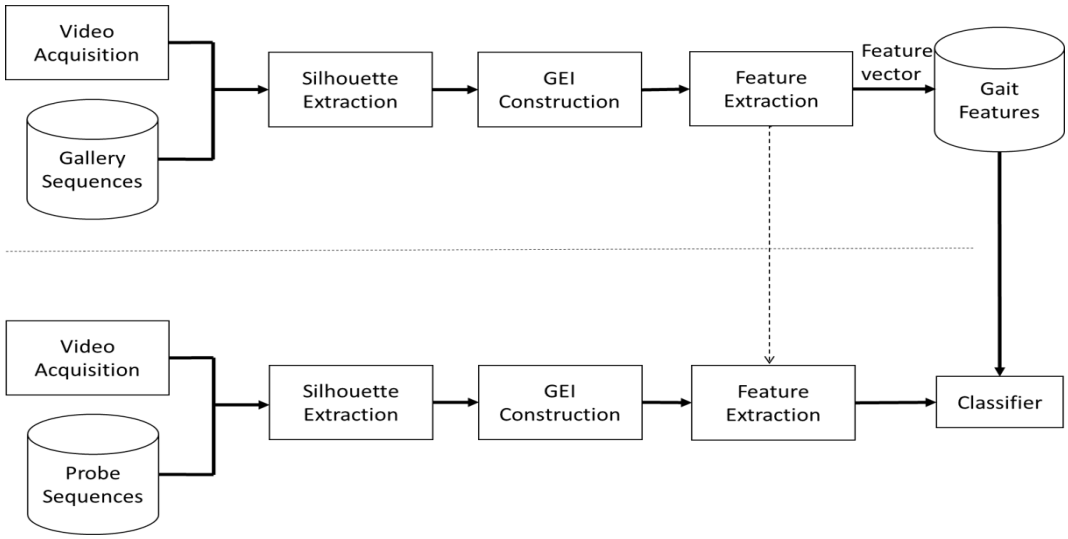

Figure 3.1: Outline of the main steps in gait recognition

3.2 GEI Construction

We have reimplemented the gait cycle detection algorithm of Wang et al. [38]. First, the aspect ratio of the width and height of moving subject's silhouette bounding box is extracted as a function of time. Then, the background component is removed from the aspect ratio signal by subtracting its mean and dividing by its standard deviation. After that, the signal is smoothed with symmetric average filter. Further, autocorrelation is computed to find the peaks. Finally, first order derivative is computed to find peak positions. The real period is estimated as the average distance between each pair of consecutive peaks.

GEI image is constructed from one gait cycle of a given gait sequence of human

silhouettes. First, each gait silhouette is normalized into 240 × 240 and then aligned to address the variations in the distance between the camera and the subject. Then, the binary aligned silhouettes are averaged to construct the GEI image as follows [9]:

$$G(x, y) = \frac{1}{M} \sum_{t=1}^{M} B_t(x, y) \tag{3.1}$$

where M is the number of silhouettes in the sequence; $B_t(x, y)$ is the binary silhouette at time t in the sequence. Figure 3.2 demonstrates an example of GEI construction from CASIA B gait sequence.

Figure 3.2: An example of GEI construction from CASIA B gait sequence.

We then extract the GEI bounding box around the target subject to discard the black region and focus the feature extraction on the main GEI region. Figure 3.3 shows an example of a bounding box over GEI of a male carrying a bag.

To enhance the performance of gait recognition, the GEI can be partitioned into predefined different-sized overlapping and non-overlapping regions. The partitioning has been conducted as a fraction of the subject's height and width as denoted by horizontal and vertical lines in the figure. For example, after normalization and alignment of GEI, we found that the head part is about 19% of the whole subject's height.

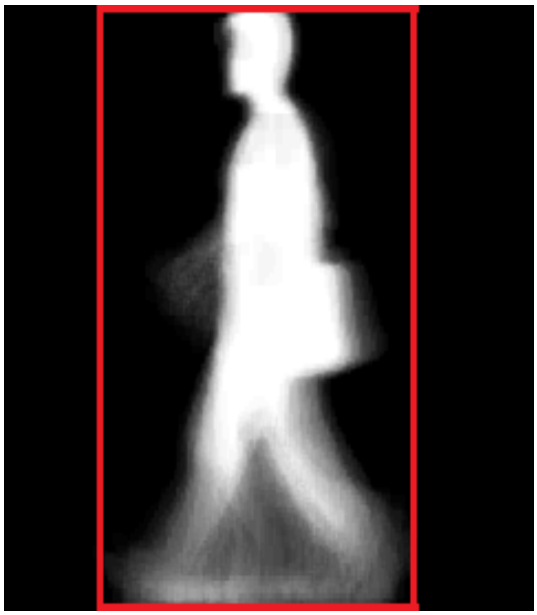

Figure 3.3: GEI bounding box detection

Different partitioning scenarios are designed and implemented to test which partitioning scenario is more effective for gait recognition. Figure 3.4 shows a demonstration example of a GEI partitioning of 7 main non-overlapping and overlapping body regions. In Fig. 3.4b, each color represents the boundary of one region. We set 10 pixels as the length of the overlapping area between two adjacent regions.

Experimental results reported in Chapter 5 show that features from overlapping regions of GEI can capture more discriminative gait information than the non-overlapping regions as well as the holistic GEI.

3.3 Feature Extraction Approaches

In this section, we discuss six approaches for texture representation of the gait energy image. Two of them have been already applied in the literature for gait

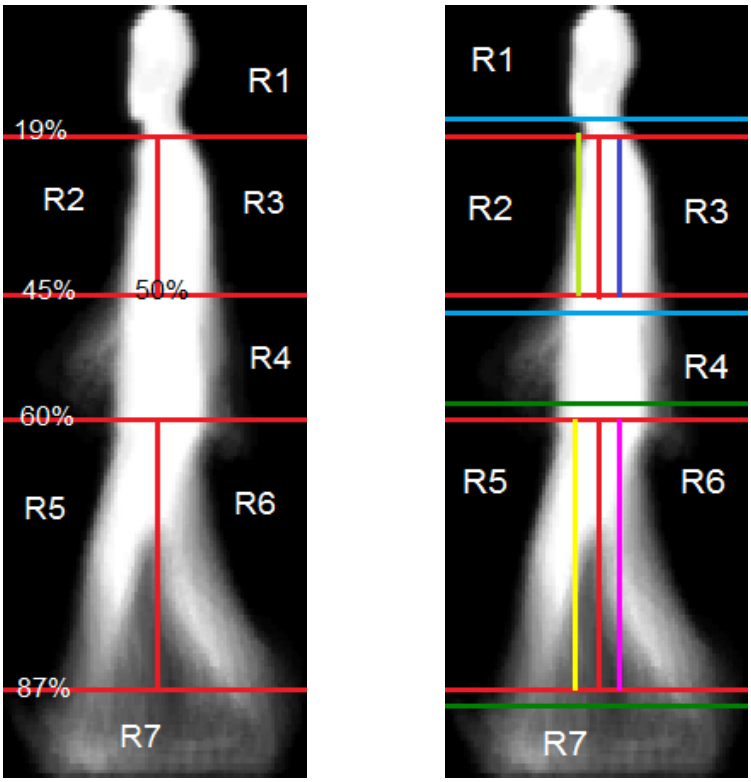

(a) Non-Overlapped Regions (b) Overlapped Regions

Figure 3.4: Overlapping and Non-overlapping Partitioning

recognition, which are Local Binary Pattern (LBP) and Gabor Filters (GF). The other four are the main contribution of this thesis for gait recognition, which are FLBP, KFLBP, FLGBP, and MFLGBP. The details of these methods will be explained in the following subsections.

3.3.1 Local Binary Patterns (LBP)

Local binary pattern (LBP) is a well-known texture operator first proposed in 1996 by Ojala et al. [133]. It has been extensively utilized in a wide spectrum of research and has demonstrated notable performance [12]. In medical studies, LBP has been investigated to recognize malignant breast cells [133]. In biometrics,

Figure 3.5: Demonstration of 5 Non-Overlapped Regions

LBP has been used in face identification [134] and expression recognition [135]. A few attempts are reported in the literature that utilize some variants of LBP for gait recognition. For example, Kellokumpu et al. [52] proposed a new gait recognition method based on using Local Binary Patterns from Three Orthogonal Planes (LBP-TOP) that spatiotemporally analyzes the human movements and extract LBP-based gait features. In [136], LBP was employed to describe the texture information of optical flow. This representation is called LBP flow, which performs well as a static representation of gait movement.

LBP uses the properties of the neighborhood pixels to describe each pixel. It is computationally simple, very efficient, and resistant to gray level changes made by lighting variations. It also has the ability to capture fine details. The main idea behind LBP is to extract the local micropattern in an image and to describe

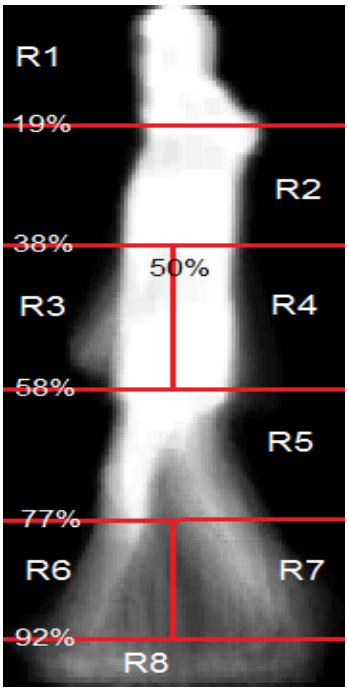

Figure 3.6: Demonstration of 8 Non-Overlapped Regions

their distribution through a histogram. Initially, two parameters have to be set: N and R (where N is the number of surrounding pixels around pixel-of-interest, and R is the radius in pixels). Each pixel in the image is investigated by applying the following LBP operator [12]:

$$LBP(N,R) = \sum_{n=0}^{N-1} s(I_n - I_c) \tag{3.2}$$

where $s(x) = 1$ if $x \geq 0$, and $s(x) = 0$ otherwise. I_c is the pixel-of-interest, and I_n is the n^{th} neighbor pixel. After passing the operator over the whole image or block, a histogram of the binary patterns is constructed to be used as the feature vector. Figure 3.8 illustrates the computational scheme of the basic LBP.

In general, LBP can generate two types of binary patterns: uniform and non-

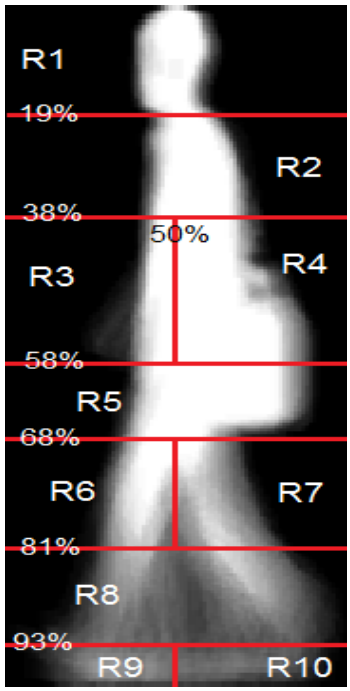

Figure 3.7: Demonstration of 10 Non-Overlapped Regions

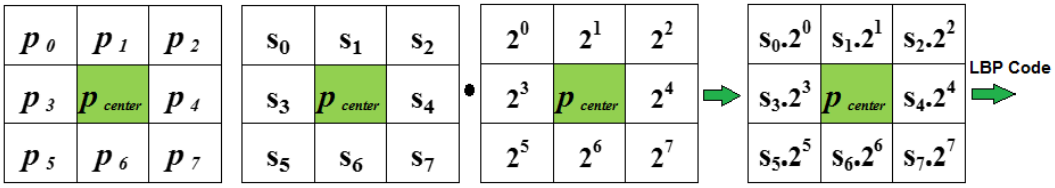

Figure 3.8: An example of LBP computation for $N = 8$ and $R = 1$

uniform patterns [12]. A uniform binary code must be circular and has at most two binary transitions from 1 to 0, or vice versa. In other words, uniform LBP code should have at most two homogenous regions of binaries. For example, the binary patterns $(\mathbf{11111111})_2$, $(\mathbf{10001111})_2$ and $(\mathbf{00100000})_2$ are uniform LBP patterns.

Despite of all its features, LBP cannot handle all the machine learning related problems. The basic LBP uses hard thresholding in computing its code. This makes it more sensitive to noise and decreases its discrimination power.

3.3.2 Fuzzy Local Binary Patterns (FLBP)

FLBP [137] incorporates fuzzy logic with LBP in order to alleviate the effect of noise on LBP and increase its distinguishing capability. The difference between basic LBP and FLBP is that each pixel in FLBP can be characterized by more than one LBP code which in turn contributes in more than one bin of FLBP histogram.

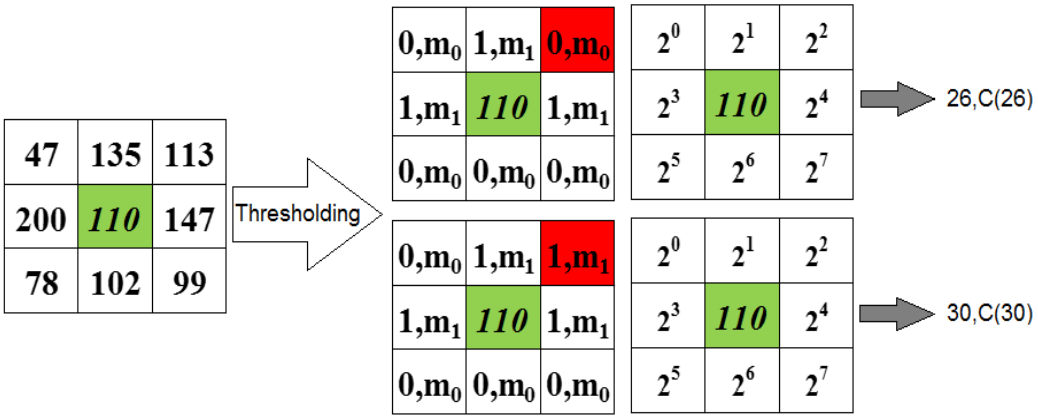

Figure 3.9: An example of FLBP computation, C is the LBP code contribution

Two membership functions are computed $m_1()$ and $m_0()$ which indicate to what extent a neighboring pixel p_i has a greater or smaller gray value than p_{center}, respectively. T is the threshold parameter and set to $T = 5$ in our experiments. Figure 3.9 illustrates the computation scheme of FLBP. It shows the generation of two binary codes for one central pixel of gray level 110. Each binary code will contribute to a different bin of the FLBP histogram; bins 26 and 30. The

contribution value is computed using Eq. 3.5

$$m_0(i) = \begin{cases} 0 & p_i \geq \ p_{center} + T \\ \frac{T - p_i + p_{center}}{2.T} & p_{center} - T < p_i < p_{center} + T \\ 1 & p_i \leq \ p_{center} - T \end{cases} \tag{3.3}$$

$$m_1(i) = 1 - m_0(i) \tag{3.4}$$

Unlike LBP, each pixel can be characterized by more than one LBP code. The member functions $m_1()$ and $m_0()$ is used to determine the contribution of each LBP code to a single bin of the FLBP histogram. The contribution of each LBP code is defined as follows:

$$C(LBP) = \prod_{i=0}^{8} m_{s_i}(i) \tag{3.5}$$

where $s_i \in \{0, 1\}$ can be determined from Eq. 3.2. The sum of contributions of all computed binary codes is always equal to unity as follows:

$$\sum_{LBP=0}^{255} C(LBP) = 1 \tag{3.6}$$

LBP histograms may have bins of zero value. However, FLBP histograms have no zero-valued bins and thus are more informative than the basic LBP. Figures 3.10 and 3.11 illustrate LBP and FLBP histograms, respectively.

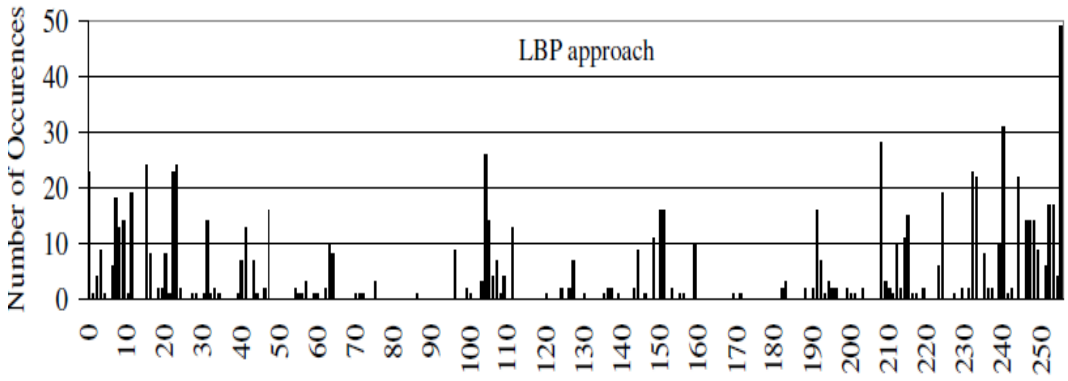

Figure 3.10: LBP Histogram

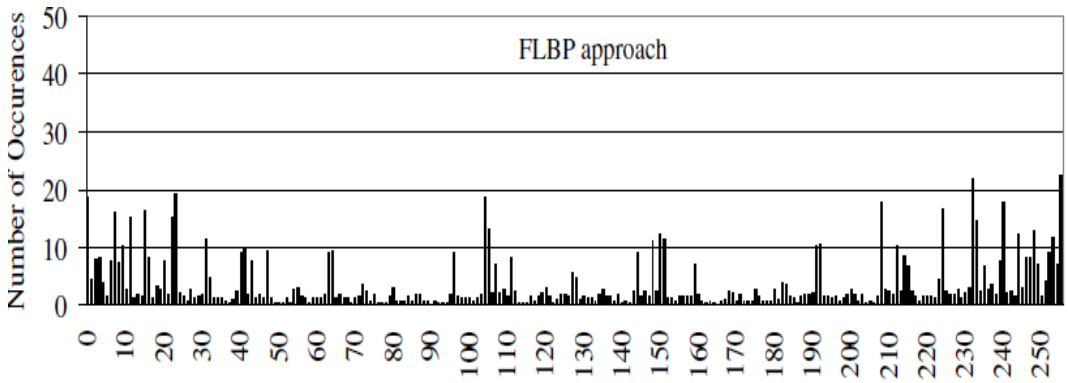

Figure 3.11: FLBP Histogram

3.3.3 Kernel-Based FLBP (KFLBP)

To increase the resistance of FLBP to gray-level changes due to noises and change in illumination and enhance its discrimination performance, we propose a multi-kernel version of FLBP. In KFLBP, instead of sampling all points over one radius, multiple radii R (kernels) with multiple neighbors N are utilized and the information provided by multiple operators is combined. Figure 3.12 illustrates the proposed idea using an example of two kernels and eight sampling points for each one.

Sampling points are first spread over multiple radii and then incorporated in a

clockwise alternative manner to form the kernel-based FLBP binary code. Consequently, more important gait information can be captured. Moreover, it alleviates the effect of changes in gray-level as well as illumination variation. Figure 3.13 illustrates the proposed idea using an example of two kernels and four sampling points for each kernel.

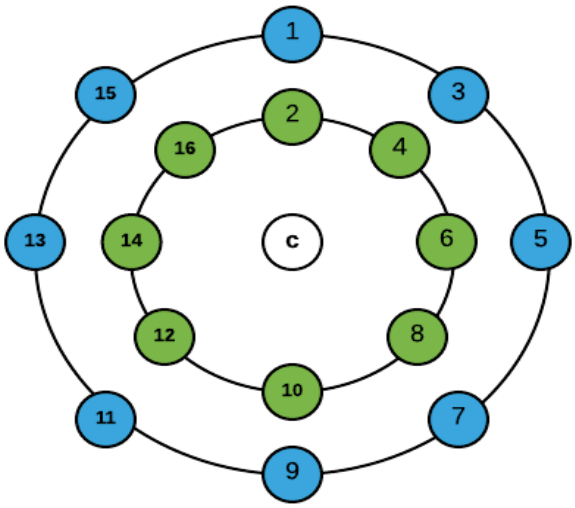

Figure 3.12: KFLBP scheme where $K = 2$, $N_1 = N_2 = 8$

KFLBP has the same formulation of FLBP with the difference of having multiple FLBP operators; each kernel has a separate operator with the same or different neighbor points N.

$$LBP_{N_k,R_k} = \sum_{n=0}^{N_k-1} s(I_n - I_c)2^n \tag{3.7}$$

where N_k is the number of neighbors; R_k is the radius; and k is the index of the radius.

The output of each operator is then combined together in a clockwise alter-

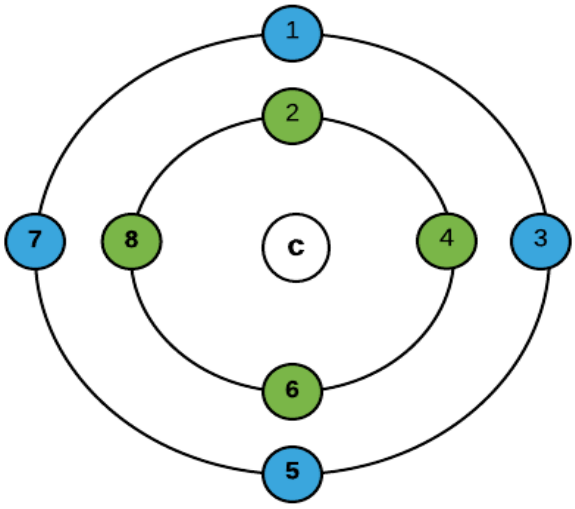

Figure 3.13: KFLBP scheme where $K = 2$, $N_1 = N_2 = 4$

native manner as illustrated by node numbers in Figures 3.12 and 3.13 to form the kernel-based FLBP binary code. In this work, for simplicity and to prove the effectiveness of the proposed feature, we chose $K = 2$ and $N = 4$ for each kernel. So, we have two FLBP operators at two different radii R_1 and R_2 as follows:

$$LBP_{N_1,R_1} = \sum_{n=0}^{N_1-1} s(I_n - I_c)2^n \tag{3.8}$$

$$LBP_{N_2,R_2} = \sum_{n=0}^{N_2-1} s(I_n - I_c)2^n \tag{3.9}$$

Although KFLBP preserves a lot of structural and statistical information by combining information from different kernels, KFLBP histogram length is still the same as that of the traditional FLBP.

3.3.4 Gabor Based Fuzzy Gait Features

Due to its robustness against local distortion and noise, Gabor filters have been widely used as an effective feature extraction approach in many fields of research [138]. They have been also utilized in many biometric applications such as iris recognition [139], face recognition [140], and gait recognition [96, 95, 97].

In this section, we describe our proposed Gabor-based fuzzy features for gait recognition purposes. Our method is based on the convolution of GEI and Gabor filters.

In our work, the GEI gait image, $GEI(x, y)$ is convolved with a bank of Gabor filters with 5 different scales and 8 different orientations. The result of the convolution process is given by [141]:

$$G_{v,\mu}(x, y) = GEI(x, y) * \psi_{v,\mu}(x, y) \tag{3.10}$$

where * represents convolution, $\psi_{v,\mu}(x, y)$ is a 2D Gabor wavelet kernel function at orientation μ and scale v, and $G_{v,\mu}(x, y)$ represents the convolution output. The kernel is defined by [141]:

$$\psi_{v,\mu}(z) = \frac{\|k_{v,\mu}\|^2}{\sigma^2} \mathbf{e}^{-(\|k_{v,\mu}\|^2 \|z\|^2 / 2\sigma^2)} [\mathbf{e}^{ik_{v,\mu}z} - \mathbf{e}^{-\sigma^2/2}] \tag{3.11}$$

where $z = (x, y)$, $\| \bullet \|$ is the Euclidean norm operator, $k_{v,\mu} = k_v \mathbf{e}^{i\varphi_\mu}$ with $k_v = k_{max}/\lambda^v$, $\lambda = 1.2$ is the spacing factor between Gabor kernels in the frequency

domain, $\phi_\mu = \pi\mu/8$ is the orientation where $\mu = 0, 1, 2, ..., 6, 7$, the scale $v = 0, 1, 2, 3, 4$, and $k_{max} = 0.35$. The Gabor response contains two main parts: real part $R_{v,\mu}(x, y)$ and imaginary part $Im_{v,\mu}(x, y)$. In our experiments, we utilized the magnitude of the Gabor response which is computed as follows:

$$Mag_{v,\mu}(x, y) = \sqrt{R^2_{v,\mu}(x, y) + Im^2_{v,\mu}(x, y)} \tag{3.12}$$

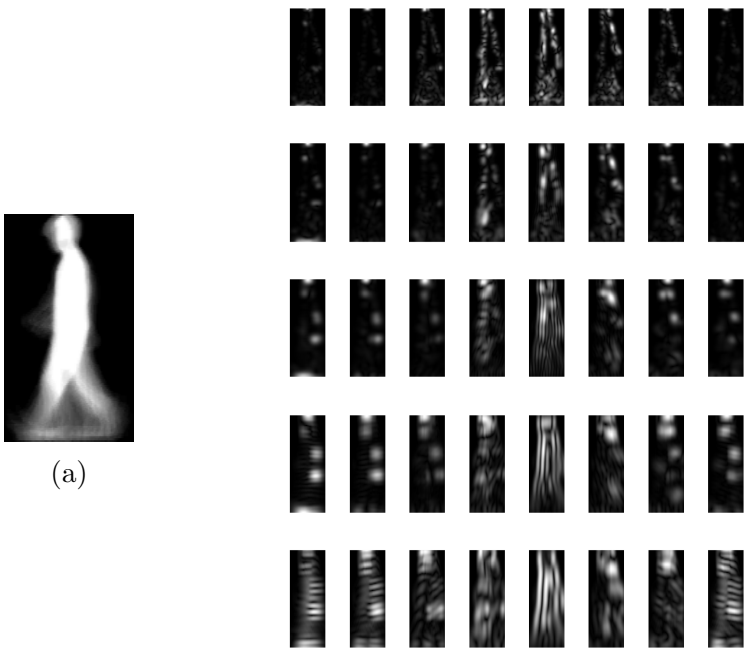

(a) (b)

Figure 3.14: (a) Original GEI, (b) GEI Gabor convolution using filter bank of 5 scales and 8 orientations

Then, the output Gabor responses are combined with FLBP and the proposed KFLBP operators to generate two different types of features, which we refer to them as FLGBP and MFLGBP, respectively. Figure 3.15 illustrates the overall process of extracting these features.

FLGBP descriptor encodes the variations in the magnitude of Gabor responses

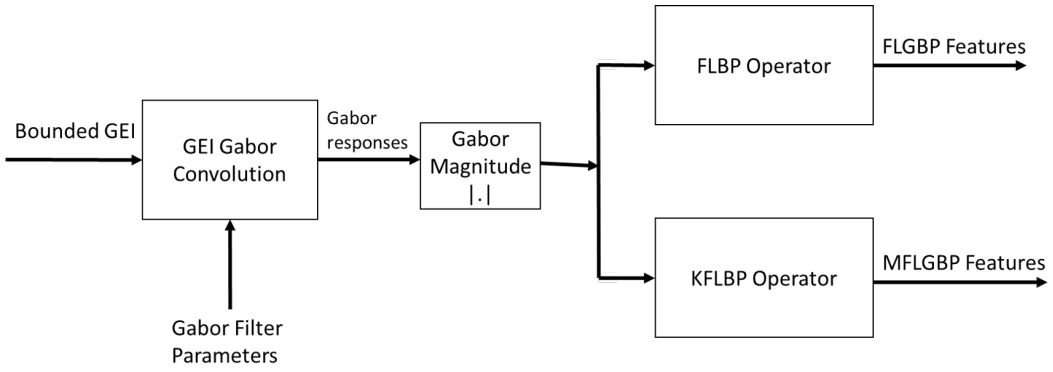

Figure 3.15: Flowchart of the two alternatives FLGBP and MFLGBP

by using FLBP operator. The binary patterns extracted from the magnitude of Gabor response at scale v and orientation μ are formulated as follows:

$$FLGBP_{v,\mu}(p_c) = \sum_{n=0}^{N-1} FLGBP_{v,\mu}^{n} \cdot 2^n \tag{3.13}$$

where p_c denotes the central pixel, N is the number of neighbor pixels around p_c, and $FLGBP_{v,\mu}^{n}$ denotes a single binary calculated as follows:

$$FLGBP_{v,\mu}^{n} = FLBP(Mag_{v,\mu}(p_c), Mag_{v,\mu}(p_n)) \tag{3.14}$$

FLBP operator is applied on the magnitude of Gabor response to generate the binary patterns as follows:

$$FLBP_{v,\mu}(N,R) = \sum_{n=0}^{N-1} s(Mag_{v,\mu}(p_n) - Mag_{v,\mu}(p_c))2^n \tag{3.15}$$

where $s(x) = 1$ if $x \geq 0$, $s(x) = 0$ otherwise, R is the radius of FLBP operator.

With the defined FLGBP patterns, one pattern histogram is calculated from each Gabor response and then all histograms of all scales and orientations com-

binations (40 combinations in our setup) are concatenated to form the FLGBP description of the GEI gait image.

The computation of MFLGBP is similar to FLGBP with the difference of utilizing two radii and through two KFLBP operators as follows:

$$MFLGBP_{v,\mu}(p_c) = \sum_{n=0}^{N-1} MFLGBP_{v,\mu}^{n} \cdot 2^n \tag{3.16}$$

$$MFLGBP_{v,\mu}^{n} = KFLBP(Mag_{v,\mu}(p_c), Mag_{v,\mu}(p_n)) \tag{3.17}$$

$$KFLBP_{v,\mu}^{N_1,R_1} = \sum_{n=0}^{N_1-1} s(Mag_{v,\mu}(p_n) - Mag_{v,\mu}(p_c))2^n \tag{3.18}$$

$$KFLBP_{v,\mu}^{N_2,R_2} = \sum_{n=0}^{N_2-1} s(Mag_{v,\mu}(p_n) - Mag_{v,\mu}(p_c))2^n \tag{3.19}$$

The output of each operator is then combined together to form the final MFLGBP binary code. In this work, for simplicity and to prove the effectiveness of the proposed feature, we chose $K = 2$ and $N = 8$ for each kernel. So, we have two KFLBP operators at two different radius R_1 and R_2.

CHAPTER 4

EVALUATION

This chapter demonstrates the experimental work that we adopt during the evaluation of the proposed methods. It reports the obtained results of the proposed features KFLBP, FLGBP, and MFLGBP. Comparison is also conducted with several gait recognition methods to measure the enhancement degree achieved by the proposed features.

Two benchmark gait datasets were chosen: CASIA B and OU-ISIR-A. CASIA B includes variations in viewing angles and covariates. Subjects were captured using 11 different views from 0° to 180° and with three different covariates: normal walking, walking with bags and with coats. OU-ISIR-A includes variations in walking speeds from 2 km/h to 10 km/h with 1 km/h interval.

4.1 Datasets

4.1.1 CASIA B Gait Dataset

The proposed methods are evaluated on CASIA B gait database [125]. It includes sequence samples of 124 subjects of 93 males and 31 females. Gait sequences for each subject were captured from 11 different views (0°, 18°, 36°, 54°, 72°, 90°, 108°, 126°, 144°, 162°, and 180°). Each subject was asked to walk 10 times through a straight line of concrete ground (6 normal walking, 2 wearing a coat, 2 carrying a bag). At each walking, there were 11 cameras capturing the subject's walking. Consequently, each subject has 110 video sequences and the database contains $110 \times 124 = 13640$ total sequences for all subjects. See Figures 4.1a and 4.1b for a sample of GEI images under three different covariates for male and female, respectively.

4.1.2 OU-ISIR-A Dataset

The OU-ISIR Gait Database [142] is meant to aid research efforts in the general area of developing, testing and evaluating algorithms for gait-based human identification. The Institute of Scientific and Industrial Research (ISIR), Osaka University (OU) has copyright in the collection of gait video and associated data and serves as a distributor of this database. The Treadmill Dataset A is composed of 34 subjects walking on a treadmill from side view with speed variation from 2 km/h to 10 km/h at 1 km/h interval. Each subject has one sequence as gallery

(training) and one as probe (test) under each speed variant.

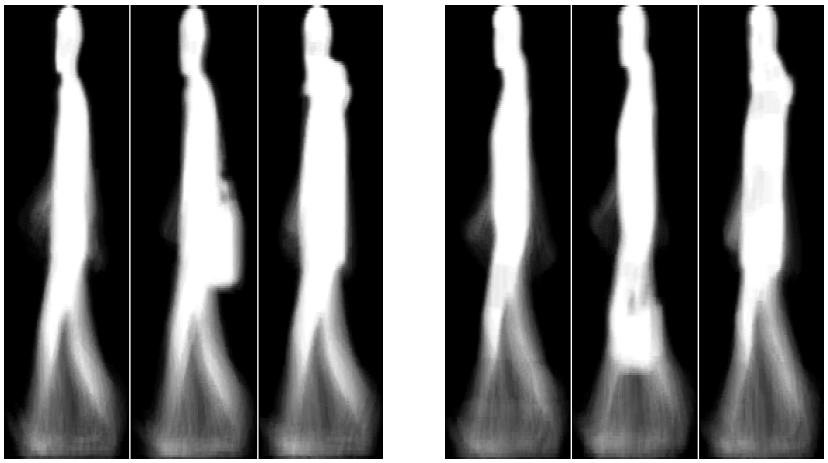

(a) Male different covariates (b) Female different covariates

Figure 4.1: Samples of CASIA B GEI images of male and female with three different covariates and viewing angle 90°

4.2 Gait Classification

In this stage, a support vector machine (SVM) classifier with a linear kernel function is used for gait recognition using the extracted feature vectors. There are several implementations of SVM. In our study, we built our model using LibSVM which implements one-against-one for multi-class classification. If k is the number of subjects under investigation, then $k(k-1)/2$ binary classifiers are constructed. Each classifier is trained on data belonging to two classes. Then max-win voting scheme is used to decide the predicted class. If there is a tie (more than one class has identical max vote), the one with the smaller index is chosen.

4.3 Experimental Setup

The proposed features are evaluated on the benchmark CASIA B and OU-ISIR-A datasets. Similar to the authors of CASIA B [125], we used the gallery set of normal walking of all subjects to train the SVM model and three sets under different covariates are used as the probe sets as follows:

1. Probe Set **A**: when subject is normally walking.

2. Probe Set **B**: when subject is carrying a bag.

3. Probe Set **C**: when subject is wearing a coat.

For OU-ISIR-A, we used the gallery set to the classifier and the probe set to test the classifier.

Moreover, to evaluate the impact of GEI partitioning, the experiments on both databases were conducted over two scenarios:

1. Scenario **1**: without partitioning.

2. Scenario **2**: with partitioning.

All partitions are given the same weight. The length of the feature vector is 256 for all experiments. After extracting the features, we used LibSVM for classification. We choose the linear kernel with a regularization parameter $C = 1$.

4.4 Performance Measures

The performance of the proposed features is measured in identification mode. Identification mode is the process of determining the identity of an unknown subject. Moreover, we adopted the closed-set identification strategy which guarantees the existence of the unknown subject within the database gallery.

4.4.1 Correct Classification Rate (CCR)

The experimental results are reported using the correct classification rate (CCR) metric which represents the performance at rank-1. CCR (rank-1) indicates that the probe sample is matching with the only one returned candidate. Eq. 4.1 represents the CCR percentage.

$$CCR(\%) = \frac{s_c}{s_t} * 100 \tag{4.1}$$

where s_t is the total number of tested subjects and s_c is the number of correctly identified subjects.

4.4.2 Precision (Positive Predictive Value)

Precision measures the relevancy of results. In other words, it is the fraction of relevant retrieved instances. High value of precision indicates a low false positive rate and show that the classifier and features are more accurate.

Precision (P) is defined as the number of true positive instances (T_P) over the

sum of true positives and false positives (F_P):

$$P = \frac{T_P}{T_P + F_P} \tag{4.2}$$

4.4.3 Recall (Sensitivity)

Recall measures how many relevant instances are correctly retrieved. High value of recall indicates a low false negative rate and show that the classifier is returning majority of the positive instances.

Recall (R) is defined as the number of true positive instances (T_P) over the sum of true positives and false negatives (F_N), i.e.,

$$R = \frac{T_P}{T_P + F_N} \tag{4.3}$$

4.4.4 F_1 Score

F_1 score (sometimes called F_1 measure) is the harmonic mean of the precision and recall, i.e.,

$$F_1 = 2 \cdot \frac{Precision \times Recall}{Precision + Recall} \tag{4.4}$$

4.5 Performance Analysis of KFLBP

In this section, we report the obtained experimental results of the proposed KFLBP using CASIA-B and OU-ISIR-A gait datasets. It also compares the per-

formance in term of correct classification rate (CCR), precision, recall, and F_1 score.

For CASIA B dataset, we first conduct the evaluation when the targeted subject is normally walking. Then, the subject is carrying a bag during his walk. Finally, we test the performance when the targeted subject is wearing a coat. For OU-ISIR-A gait dataset, each subject has two sequences for each speed. One sequence is used as a gallery and the other as a probe.

4.5.1 Discussion

We compared our features against several methods: GEI [9], LBP [143], LTP [144], GEI+PCA [145], FLBP [146]. In addition, other Gabor-based approaches that have been exploited for different machine learning problems such as face recognition [147, 148] are involved the comparison. Some methods have been applied on silhouette images on the original papers but we reimplemented and applied them on GEI images such as pyramid of Histogram of Gradient (pHOG) [149].

First, the proposed approach was applied on the GEI image without any partitioning. Several gait recognition approaches were implemented and compared to our proposed features. All comparisons were conducted in terms of four performance measures: correct classification rate (CCR), Precision (P), Recall (R), and (F_1) score.

Tables 4.1, 4.2, and 4.3, show the performance of KFLBP using CASIA B

dataset. KFLBP feature is always outperforming all other methods involved in the comparison under all the three scenarios in term of CCR. Moreover, the performance was superior in the case of probe set A when subjects are normally walking. It proves that KFLBP has the ability to capture more discriminative gait information than FLBP and all methods involved in the comparison. We need to investigate the applicability of KFLBP for different machine learning problems such as face recognition and other biometrics.

In addition, we evaluated the performance of KFLBP using several performance measures: precision, recall, and F_1 score. Figures 4.2, 4.5, and 4.8 show the precision of KFLBP as well as of the compared methods. Recall is represented in Figures 4.3, 4.6, and 4.9; and F_1 Score is illustrated in Figures 4.4, 4.7, and 4.10. It is obvious that KFLBP has the higher performance over relevant involved approaches under the three covariates and in most viewing angles.

Tables 4.4, 4.5, 4.6, and 4.7 show the performance of KFLBP using OU-ISIR-A gait dataset using four different performance measures. Several implemented methods are involved in the performance comparison of our proposed method under nine speed variations. Results demonstrated that KFLBP outperformed all other methods under most speeds and using the four performance measures.

4.5.2 Effect of Partitioning on Performance

To evaluate the effect of partitioning on the overall performance, a group of experiments is designed. Experiments were conducted in two modes: overlapping and

non-overlapping. Also, a set of different-sized regions is applied and investigated as an attempt to discover the efficient and effective partitioning strategy for gait recognition purposes.

The shown experimental results demonstrate that using partitioning (overlapping or non-overlapping) is always enhancing the performance at almost all viewing angles and under the three tested covariates. Tables 4.8, 4.10, and 4.12 show the performance of non-overlapping partitioning for the three scenarios. Similarly for overlapping partitioning, the results are shown in Tables 4.9, 4.11, and 4.13. It is obvious that using the holistic GEI to extract gait feature without any partitioning can't compete against the partitioning strategy. In addition, we utilized mean and standard deviation analysis to measure the partitioning degree of confidence. Table 4.14 and 4.15 show the results for the non-overlapping and overlapping partitioning on OU-ISIR-A dataset, respectively.

Moreover, there is an edge for overlapping over the non-overlapping partitioning in most cases. Also, it is clear that partitioning GEI into 10 overlapping regions has the best performance in almost all viewing angles and under the three scenarios. However, it is not a guarantee that with this number of regions we can always get the best performance in all cases.

4.5.3 Effect of Covariates on Performance

It is obvious from reported tables that normal walking covariate achieves the best result over carrying a bag and wearing a coat covariates. It is due to the deformity

in the normal shape of human body during normal walking. This causes difficulties in capturing the basic discriminative features originated from the normal walking. The performance under carrying a bag covariate is moderate. Bag is occupying region in the middle of the human body and cause deformity for that part of body during walking. However, coat causes the largest amount of deformity of the human body. Consequently, wearing a coat covariate is the most difficult and hardest scenario to discover and extract representative features.

Table 4.1: Comparison of correct classification rates under Normal-Walking covariate without partitioning

Method	**Angle**										
	0°	18°	36°	54°	72°	90°	108°	126°	144°	162°	180°
GEI	89.11	87.50	**85.08**	82.25	87.90	**89.11**	**88.30**	85.88	83.87	83.46	**89.11**
GEI+pHOG	82.76	74.57	76.72	76.72	81.47	86.21	81.04	77.59	76.72	78.45	83.62
GEI+PCA	83.06	73.38	75	72.58	85.08	84.67	83.46	83.06	77.41	75.80	87.09
GEI+LXP	61.64	61.21	53.02	56.04	60.78	62.07	63.36	57.33	57.33	63.79	53.02
GEI+LBP	56.9	66.81	60.35	56.9	68.54	73.28	68.97	62.5	61.21	68.97	57.33
GEI+SLBP	68.54	65.52	61.21	63.79	68.54	68.97	65.52	68.54	66.81	75.43	66.38
GEI+LTP	49.59	43.95	37.9	45.96	49.59	50.81	50.81	41.53	41.53	52.01	54.43
GEI+FLBP	74.14	78.45	67.24	74.14	75.43	78.02	76.29	75.86	75	77.59	70.69
GEI+KFLBP	**89.66**	**92.24**	82.33	**82.76**	**90.95**	88.79	87.93	**87.07**	**85.35**	**91.38**	82.76

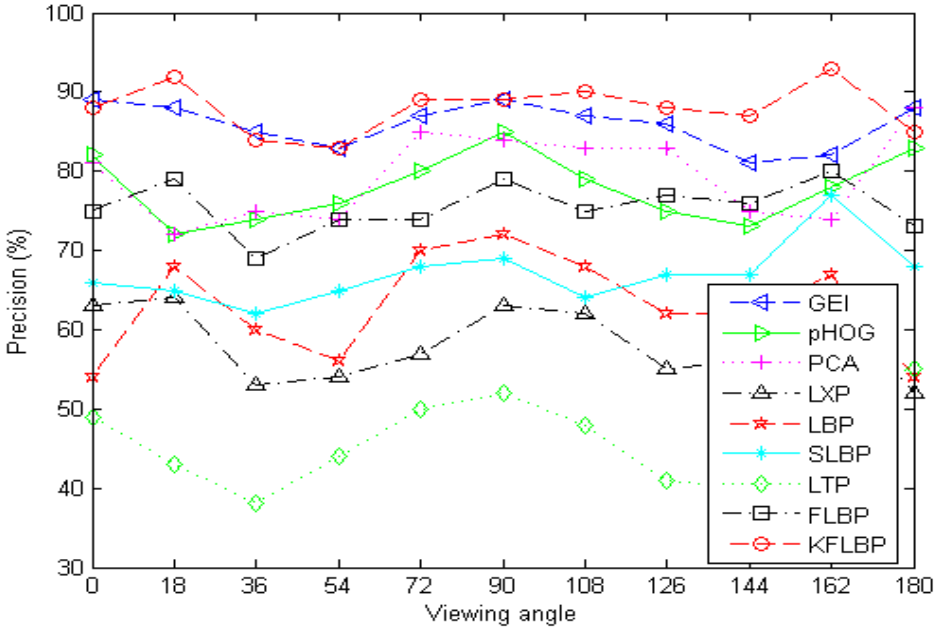

Figure 4.2: Comparison of precision under Normal-Walking covariate without partitioning

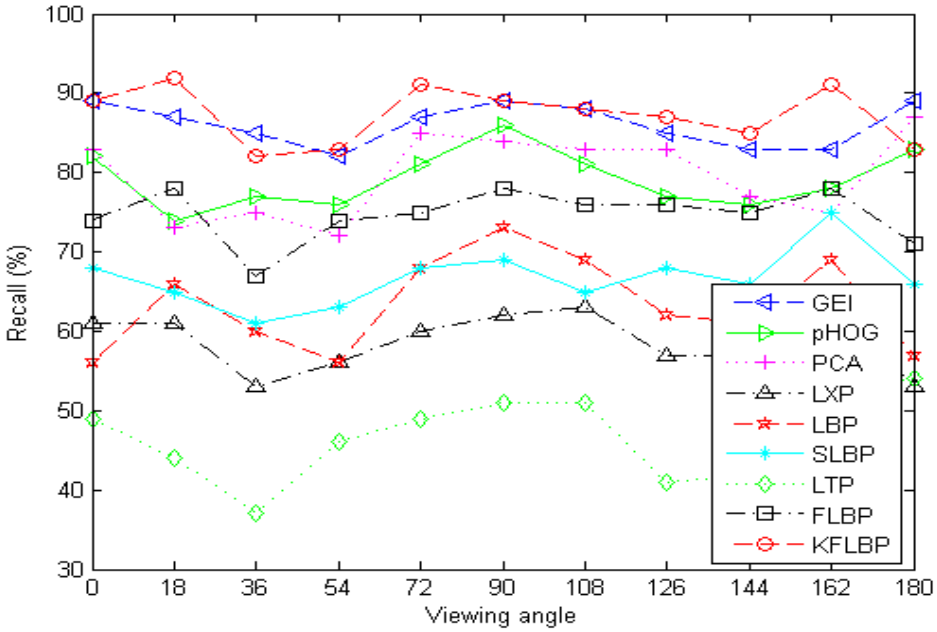

Figure 4.3: Comparison of recall under Normal-Walking covariate without partitioning

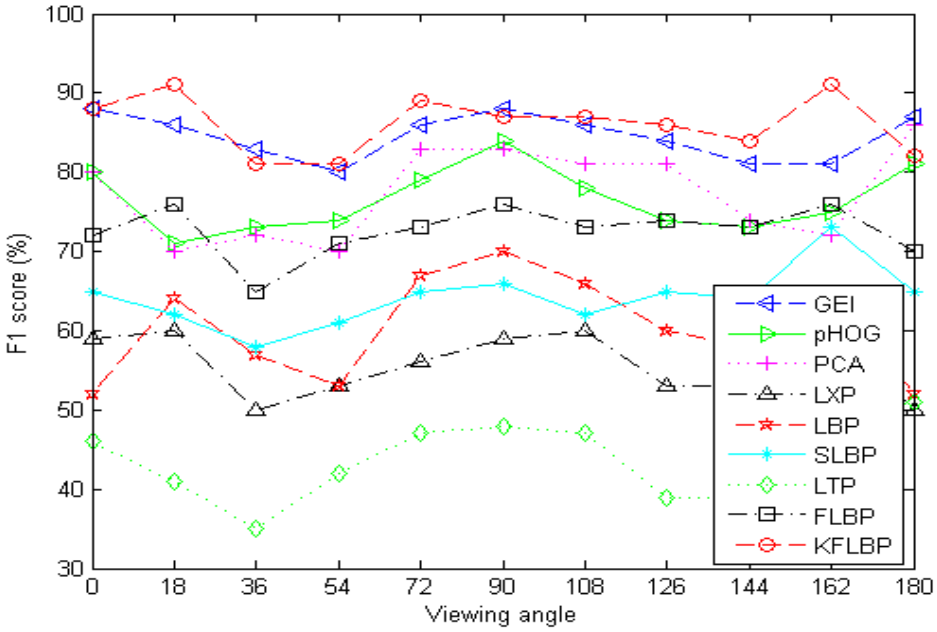

Figure 4.4: Comparison of F_1 score under Normal-Walking covariate without partitioning

Table 4.2: Comparison of correct classification rates under Carrying-Bag covariate without partitioning

Method	**Angle**										
	0°	18°	36°	54°	72°	90°	108°	126°	144°	162°	180°
GEI	50.8	42.74	**45.56**	**41.53**	**45.16**	41.12	41.12	**37.5**	**40.72**	46.37	51.2
GEI+pHOG	45.26	30.6	30.6	24.57	20.26	22.41	18.54	21.98	20.26	35.78	42.67
GEI+PCA	40.32	35.48	35.88	30.64	37.5	33.46	39.51	33.06	29.83	34.67	41.93
GEI+LXP	26.72	18.54	15.95	15.95	9.91	18.54	18.1	18.1	8.62	21.55	20.69
GEI+LBP	28.02	43.1	34.05	30.6	34.05	37.5	34.48	31.47	28.02	35.35	29.74
GEI+SLBP	28.45	28.88	23.71	25	29.74	35.78	31.04	26.72	31.9	27.16	28.45
GEI+LTP	21.37	17.74	19.75	11.69	10.48	14.91	9.67	13.31	13.31	15.32	19.35
GEI+FLBP	40.85	43.54	36.91	33.62	36.72	40.1	38.9	31.16	30.16	40.55	37.35
GEI+KFLBP	**55.17**	**53.45**	40.09	37.93	40.52	**42.24**	**42.67**	31.04	33.62	**46.98**	**51.72**

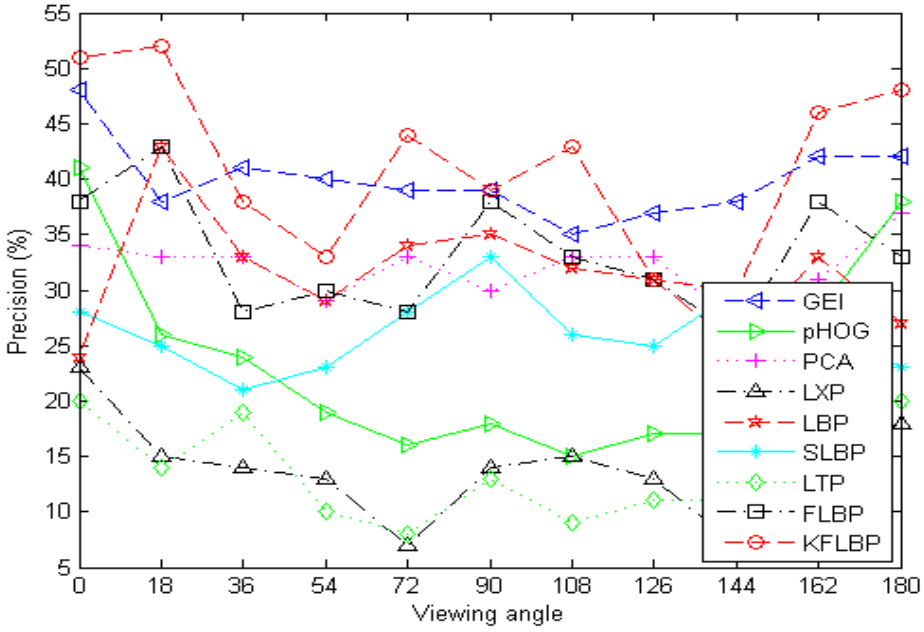

Figure 4.5: Comparison of precision under Carrying-Bag covariate without partitioning

Table 4.3: Comparison of correct classification rates under Wearing-Coat covariate without partitioning

Method	**Angle**										
	0°	18°	36°	54°	72°	90°	108°	126°	144°	162°	180°
GEI	**22.98**	20.07	20.07	15.32	10.88	16.12	13.7	16.12	**23.79**	**22.98**	**23.38**
GEI+pHOG	12.93	13.79	12.07	9.05	9.48	8.19	9.48	10.78	11.21	13.79	12.93
GEI+PCA	17.33	15.72	18.54	12.5	19.75	19.35	18.54	19.07	24.19	19.75	16.93
GEI+LXP	7.33	9.05	7.33	12.07	12.07	6.47	9.48	9.48	13.79	7.33	6.9
GEI+LBP	9.91	9.91	15.95	18.1	16.38	15.09	13.79	17.24	10.78	10.78	11.21
GEI+SLBP	7.33	12.07	13.79	11.64	12.07	13.79	11.64	13.36	11.21	12.07	7.33
GEI+LTP	5.64	8.06	10.48	8.87	9.67	9.27	11.29	10.88	9.27	6.04	7.66
GEI+FLBP	11.33	16.5	17.62	20.64	20.36	21.07	16.5	18.52	14.81	13.91	13.9
GEI+KFLBP	13.36	**20.26**	**20.26**	**24.57**	**26.29**	**25.43**	**20.69**	**19.4**	18.1	15.95	15.52

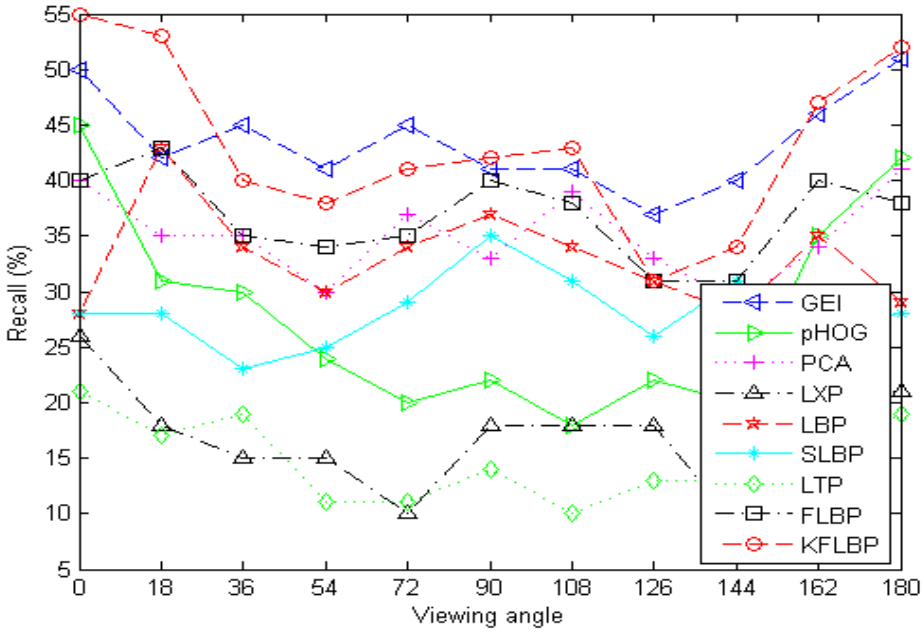

Figure 4.6: Comparison of recall under Carrying-Bag covariate without partitioning

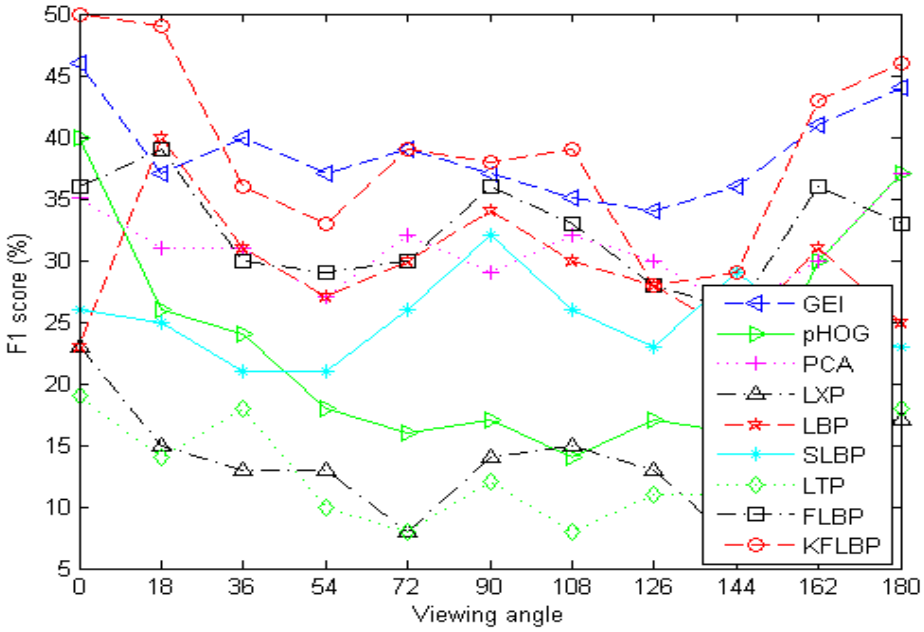

Figure 4.7: Comparison of F_1 score under Carrying-Bag covariate without partitioning

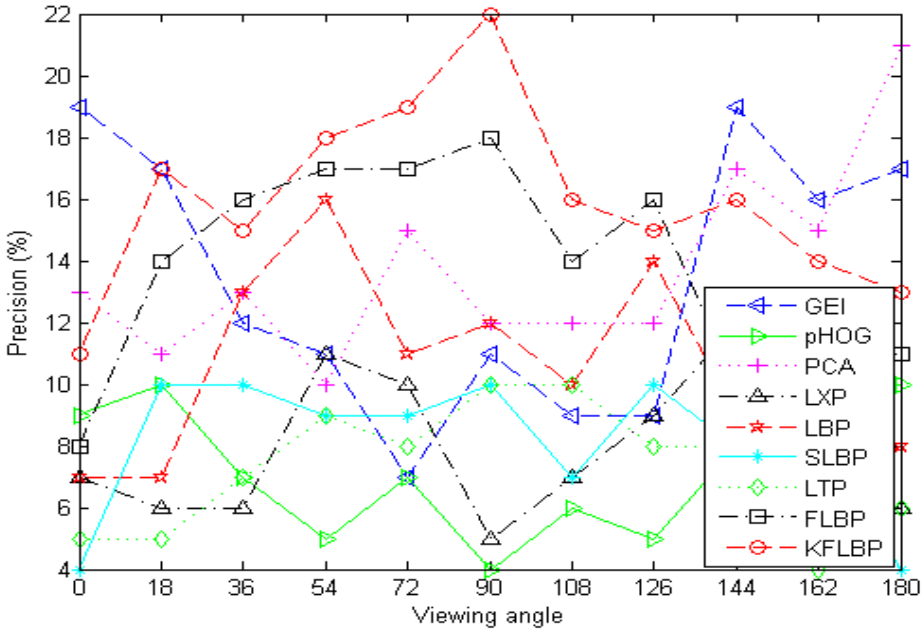

Figure 4.8: Comparison of precision under Wearing-Coat covariate without partitioning

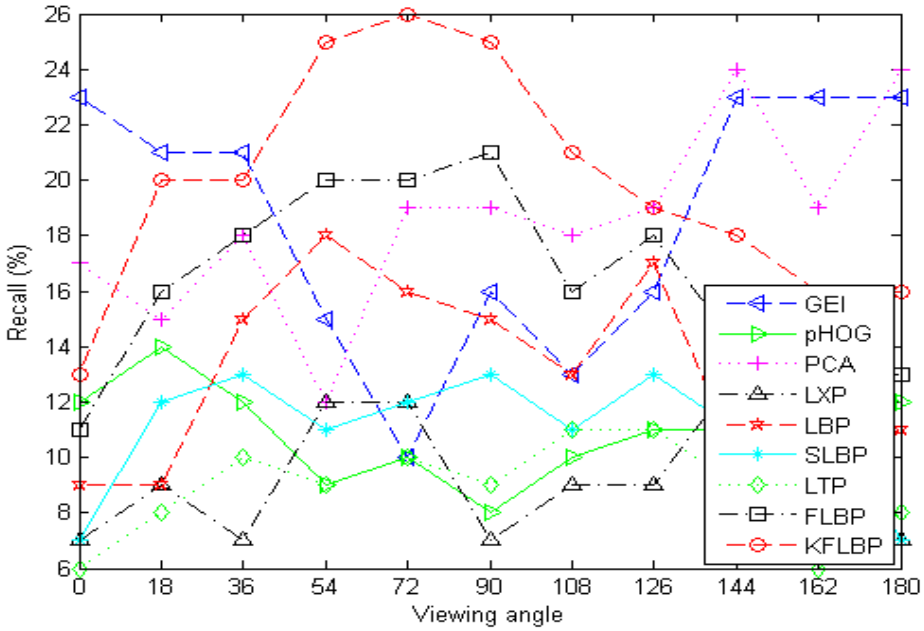

Figure 4.9: Comparison of recall under Wearing-Coat covariate without partitioning

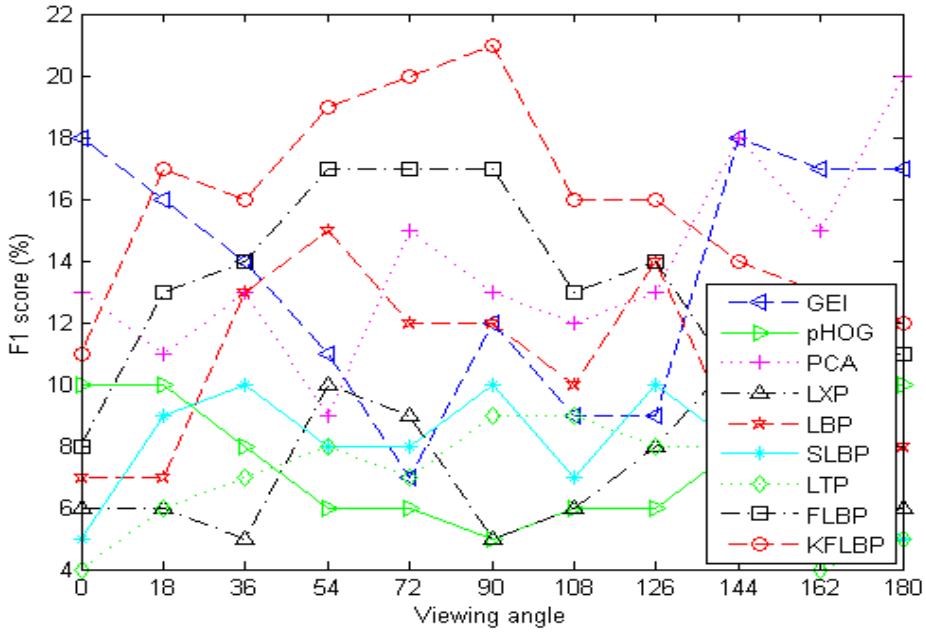

Figure 4.10: Comparison of F_1 score under Wearing-Coat covariate without partitioning

Table 4.4: Comparison of correct classification rates under different walking speeds without partitioning

Method	**Speed**								
	2 km/h	3 km/h	4 km/h	5 km/h	6 km/h	7 km/h	8 km/h	9 km/h	10 km/h
GEI	94.11	91.17	**97.05**	85.29	88.23	85.29	85.29	79.41	91.17
GEI+pHOG	91.17	88.23	82.35	76.47	82.35	91.17	91.17	94.11	91.17
GEI+PCA	94.11	94.11	94.11	94.11	88.23	88.23	91.17	82.35	91.17
GEI+LXP	67.64	55.88	52.94	38.23	47.05	32.35	47.05	47.05	50
GEI+LBP	73.52	67.64	64.7	64.7	58.82	58.82	61.76	61.76	79.41
GEI+SLBP	67.64	61.76	55.88	47.05	55.88	44.11	67.64	55.88	64.7
GEI+LTP	67.64	70.58	58.82	50	58.82	44.11	52.94	67.64	52.94
GEI+FLBP	73.52	67.64	70.58	70.58	76.47	61.76	76.47	76.47	79.41
GEI+KFLBP	**94.11**	**97.05**	94.11	**97.05**	**97.05**	**97.05**	**94.11**	**97.05**	**97.05**

Table 4.5: Comparison of precisions under different walking speeds without partitioning

Method	**Speed**								
	2 km/h	3 km/h	4 km/h	5 km/h	6 km/h	7 km/h	8 km/h	9 km/h	10 km/h
GEI	91	88	**95**	80	83	77	79	72	86
GEI+pHOG	86	82	75	69	75	87	87	91	86
GEI+PCA	91	91	91	91	82	82	86	76	89
GEI+LXP	59	45	43	26	36	25	37	36	40
GEI+LBP	64	54	53	51	47	48	47	51	70
GEI+SLBP	53	52	49	35	45	36	57	45	52
GEI+LTP	55	59	47	38	50	32	42	59	40
GEI+FLBP	65	53	61	65	69	52	64	67	70
GEI+KFLBP	**91**	**95**	91	**96**	**95**	**95**	**91**	**95**	**96**

Table 4.6: Comparison of recalls under different walking speeds without partitioning

Method	**Speed**								
	2 km/h	3 km/h	4 km/h	5 km/h	6 km/h	7 km/h	8 km/h	9 km/h	10 km/h
GEI	94	91	**97**	85	88	85	85	79	91
GEI+pHOG	91	88	82	76	82	91	91	94	91
GEI+PCA	94	94	94	94	88	88	91	82	91
GEI+LXP	67	55	52	38	47	32	47	47	50
GEI+LBP	73	67	64	64	58	58	61	61	79
GEI+SLBP	67	61	55	47	55	44	67	55	64
GEI+LTP	67	70	58	50	58	44	52	67	52
GEI+FLBP	73	67	70	70	76	61	76	76	79
GEI+KFLBP	**94**	**97**	94	**97**	**97**	**97**	**94**	**97**	**97**

Table 4.7: Comparison of F_1 score under different walking speeds without partitioning

Method	**Speed**								
	2 km/h	3 km/h	4 km/h	5 km/h	6 km/h	7 km/h	8 km/h	9 km/h	10 km/h
GEI	92	89	**96**	81	85	80	81	74	88
GEI+pHOG	88	84	77	71	77	88	88	92	88
GEI+PCA	92	92	92	92	84	84	88	78	89
GEI+LXP	62	48	45	29	39	27	40	39	43
GEI+LBP	66	58	57	55	50	51	51	54	73
GEI+SLBP	58	55	51	38	48	37	60	48	56
GEI+LTP	59	63	51	41	52	36	45	62	44
GEI+FLBP	68	57	64	66	71	55	68	70	73
GEI+KFLBP	**92**	**96**	92	**96**	**96**	**96**	**92**	**96**	**96**

Table 4.8: Impact of *non-overlapping* partitioning on CCR of KFLBP under Normal-Walking covariate

Angle(°)	**Number of Regions**					
	Holistic	**5**	**7**	**8**	**10**	**16**
0	89.66	96.12	98.71	98.28	**99.1**	96.98
18	92.24	97.41	**97.85**	96.98	97.12	95.26
36	82.33	95.26	94.4	96.12	**98.54**	94.83
54	82.76	95.26	95.69	96.12	**97.12**	93.54
72	90.95	95.69	96.12	96.55	**97.12**	96.55
90	88.79	93.54	94.83	95.26	**96.98**	96.98
108	87.93	94.83	96.12	96.12	**96.55**	95.69
126	87.07	97.41	96.55	97.84	**97.84**	94.83
144	85.35	96.55	96.98	97.85	**98.28**	92.67
162	91.38	96.98	97.85	98.28	**99.1**	92.24
180	82.76	96.55	97.85	97.85	**98.71**	96.98

Table 4.9: Impact of *overlapping* partitioning on CCR of KFLBP under Normal-Walking covariate

Angle(°)	**Number of Regions**					
	Holistic	**5**	**7**	**8**	**10**	**16**
0	89.66	97.41	98.71	97.41	**99.14**	96.12
18	92.24	96.98	**98.28**	97.41	97.41	95.69
36	82.33	96.98	96.98	97.41	**98.28**	94.4
54	82.76	96.12	96.12	96.98	**97.85**	93.97
72	90.95	95.69	96.98	96.55	**97.41**	96.12
90	88.79	95.69	96.55	96.55	96.55	**96.98**
108	87.93	96.55	**96.98**	96.55	96.55	95.26
126	87.07	97.41	97.41	**97.85**	97.41	94.83
144	85.35	96.12	96.12	97.41	**98.28**	92.67
162	91.38	98.71	**99.14**	98.71	**99.14**	92.67
180	82.76	95.26	96.98	97.41	**98.71**	96.55

Table 4.10: Impact of *non-overlapping* partitioning on CCR of KFLBP under Carrying-Bag covariate

Angle(°)	**Number of Regions**					
	Holistic	**5**	**7**	**8**	**10**	**16**
0	55.17	71.98	77.16	68.54	**78.12**	59.91
18	53.45	59.91	59.48	64.22	**75.16**	56.04
36	40.09	50.43	54.74	53.88	**64.66**	53.02
54	37.93	47.85	57.33	58.19	**63.36**	50.43
72	40.52	56.04	61.21	61.21	**70.69**	46.98
90	42.24	62.5	68.1	60.35	**75.16**	46.98
108	42.67	61.21	**68.54**	59.05	68.54	50.43
126	31.04	52.59	63.36	46.55	**68.54**	47.85
144	33.62	53.02	60.78	56.04	**65.09**	53.88
162	46.98	61.64	66.38	54.31	**70.26**	56.04
180	51.72	68.54	69.83	60.78	**71.12**	50.43

Table 4.11: Impact of *overlapping* partitioning on CCR of KFLBP under Carrying-Bag covariate

Angle(°)	**Number of Regions**					
	Holistic	**5**	**7**	**8**	**10**	**16**
0	55.17	75	**82.76**	78.45	78.45	59.05
18	53.45	65.95	75	75	**75.43**	56.03
36	40.09	54.31	61.21	59.91	**64.66**	53.88
54	37.93	53.88	59.48	62.5	**63.79**	50.43
72	40.52	62.5	**71.98**	71.55	70.26	46.98
90	42.24	74.14	73.28	75	**75.43**	47.85
108	42.67	64.22	**72.85**	65.95	68.1	50.86
126	31.04	61.21	65.09	62.07	**68.1**	47.85
144	33.62	53.45	60.35	63.79	**65.95**	52.59
162	46.98	62.5	**71.12**	70.26	70.69	55.17
180	51.72	68.1	**75.43**	69.83	71.98	50.43

4.6 Performance Analysis of MFLGBP

In this section we conduct set of experiments to evaluate the performance of the proposed Gabor-based fuzzy features FLGBP and MFLGBP. It also compares the

Table 4.12: Impact of *non-overlapping* partitioning on CCR of KFLBP under Wearing-Coat covariate

Angle(°)	**Number of Regions**					
	Holistic	**5**	**7**	**8**	**10**	**16**
0	13.36	31.04	34.48	36.21	**49.14**	31.47
18	20.26	37.5	31.9	37.5	**50.43**	34.48
36	20.26	29.31	32.76	37.07	**49.57**	29.74
54	24.57	27.16	36.64	44.4	**48.89**	26.72
72	26.29	34.91	45.69	**49.14**	48.28	27.59
90	25.43	34.05	45.26	46.55	**48.28**	31.47
108	20.69	31.9	**45.69**	40.09	41.81	22.41
126	19.4	31.04	**45.26**	35.35	39.22	21.98
144	18.1	25.86	37.07	39.22	**46.98**	26.72
162	15.95	33.62	36.21	35.78	**49.57**	32.76
180	15.52	32.76	34.91	37.5	**50.43**	34.91

performance of our methods with several Gabor-based gait recognition approaches reported in the literature.

Our main goals is to evaluate the performance of the proposed methods when different covariates are presented using the three probe sets A, B, and C. Consequently, we first evaluate the performance when the subject is normally walking. Then, the subject is carrying a bag during his walk. Finally, we test the performance when the targeted subject is walking and wearing a coat. To evaluate the performance of MFLGBP and FLGBP, we utilized four different performance measures: CCR, precision, recall, and F_1 score.

Table 4.16 demonstrates the performance of FLGBP and MFLGBP under normal walking covariate using CCR measure. MFLGBP enhanced the performance in term of correct classification rate under all viewing angles. Similarly, MFLGBP and FLGBP are always outperforming in case of walking with bag and coat as shown in Tables 4.17 and 4.18, respectively. Moreover, several experiments were

Table 4.13: Impact of *overlapping* partitioning on CCR of KFLBP under Wearing-Coat covariate

Angle(°)	**Number of Regions**					
	Holistic	**5**	**7**	**8**	**10**	**16**
0	13.36	33.62	40.52	46.55	**49.57**	30.6
18	20.26	34.48	46.98	49.14	**50.43**	34.91
36	20.26	29.74	41.81	44.4	**49.14**	30.6
54	24.57	21.98	35.78	42.67	**48.28**	26.72
72	26.29	28.88	40.52	43.1	**47.41**	28.45
90	25.43	27.59	42.67	45.26	**47.41**	33.62
108	20.69	25	39.66	38.36	**41.38**	23.71
126	19.4	24.14	35.78	35.35	**39.22**	21.98
144	18.1	22.41	36.64	36.64	**46.12**	28.88
162	15.95	31.47	38.36	43.1	**49.14**	34.91
180	15.52	31.9	44.83	46.12	**50.43**	36.64

conducted on OU-ISIR-A using four different the utilized performance measures. The proposed MFLGBP is outperforming all involved methods using the four measures: CCR, precision, recall, and F_1 score as shown in Tables 4.19, 4.20, 4.21, and 4.22, respectively.

In addition, Figures 4.11, 4.14, and 4.17 show the precision of MFLGBP as well as of the compared methods for the three tested scenario: normal walking, carrying bag, and wearing coat, respectively. Recall is represented in Figures 4.12, 4.15, and 4.18; and F_1 score is illustrated in Figures 4.13, 4.16, and 4.19. It is obvious that MFLGBP has the higher performance over relevant involved approaches under the three covariates and in most viewing angles.

The presented results prove that MFLGBP has the ability to capture more discriminative gait information than all methods involved in the comparison. We need to investigate the applicability of MFLGBP for different machine learning problems such as face recognition and other biometrics.

Table 4.14: Impact of *non-overlapping* partitioning on CCR of KFLBP under different speeds

Speed	**Number of Regions**					
	Holistic	**5**	**7**	**8**	**10**	**16**
2 km/h	94.11	91.17	**97.05**	91.17	94.11	79.41
3 km/h	**97.05**	91.17	94.11	94.11	88.23	85.29
4 km/h	94.11	91.17	**100**	**100**	94.11	85.29
5 km/h	**97.05**	88.23	91.17	91.17	88.23	82.35
6 km/h	97.05	91.17	94.11	**97.05**	**97.05**	91.17
7 km/h	**97.05**	91.17	91.17	82.35	82.35	88.23
8 km/h	94.11	**94.11**	91.17	85.29	82.35	88.23
9 km/h	97.05	94.11	94.11	91.17	**97.05**	82.35
10 km/h	**97.05**	94.11	94.11	91.17	91.17	88.23

Table 4.15: Impact of *overlapping* partitioning on CCR of KFLBP under different speeds

Speed	**Number of Regions**					
	Holistic	**5**	**7**	**8**	**10**	**16**
2 km/h	94.11	94.11	**97.05**	94.11	94.11	91.17
3 km/h	97.05	94.11	**97.05**	**97.05**	94.11	91.17
4 km/h	94.11	94.11	**100**	**100**	97.05	88.23
5 km/h	97.05	85.29	91.17	**97.05**	94.11	91.17
6 km/h	97.05	**97.05**	**97.05**	94.11	**97.05**	88.23
7 km/h	97.05	94.11	**97.05**	94.11	94.11	91.17
8 km/h	94.11	**97.05**	**97.05**	94.11	**97.05**	88.23
9 km/h	**97.05**	91.17	91.17	91.17	94.11	91.17
10 km/h	97.05	94.11	**97.05**	**97.05**	94.11	91.17

Table 4.16: Comparison of correct classification rates of Gabor-based Fuzzy Gait Features under Normal-Walking covariate

Angle(°)	**CCR (%)**				
	LGXP	**LGBP**	**SLGBP**	**FLGBP**	**MFLGBP**
0	88.71	88.31	85.08	90.52	**94.4**
18	79.84	80.65	77.82	88.31	**93.54**
36	77.02	78.23	77.82	84.91	**92.67**
54	77.82	77.42	79.44	87.93	**93.54**
72	83.87	83.87	83.87	88.79	**93.1**
90	83.47	85.08	85.89	87.93	**95.69**
108	86.29	87.5	85.48	92.24	**96.12**
126	87.09	87.09	85.48	90.09	**94.4**
144	81.85	81.45	81.05	87.5	**92.67**
162	84.27	83.47	84.27	86.64	**93.54**
180	87.9	86.29	83.87	89.66	**95.69**

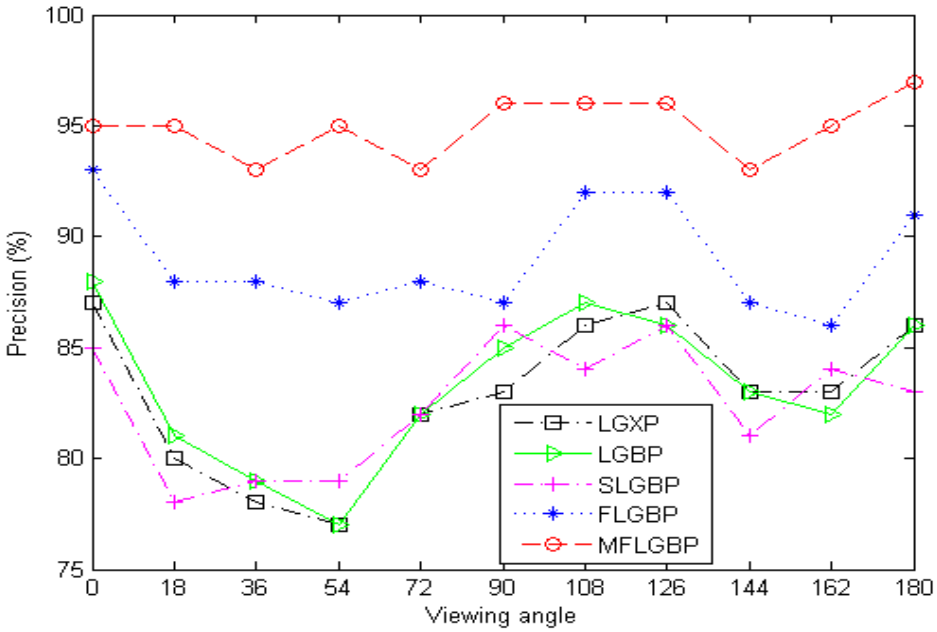

Figure 4.11: Comparison of precision of Gabor-based Fuzzy Gait Features under Normal-Walking covariate

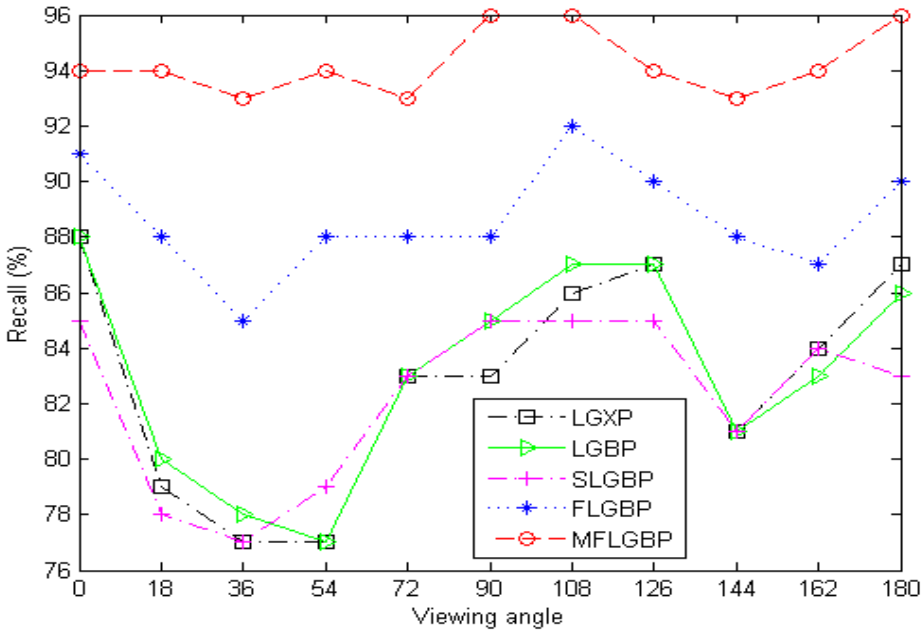

Figure 4.12: Comparison of recall of Gabor-based Fuzzy Gait Features under Normal-Walking covariate

4.7 Comparison with Existing Methods

In this section, we compare our proposed approach against several state-of-art gait recognition approaches as shown in Table 4.23. The table shows the correct classification rates on CASIA B and OU-ISIR A of the proposed approach as well as several existing gait recognition approaches. Using CASIA B, it is clear from the reported table that our proposed MFLGBP is outperforming most of the listed approaches. Arora et al. [150] achieved better performance of 98% on CASIA B using its gait recognition approach named as Gait Gaussian Image (GGI). However, they follow an expensive computation procedure to construct the final GGI which is then used for recognition. A fuzzification process of all pixels of the same coordinate over the whole gait cycle is done using Gaussian membership functions

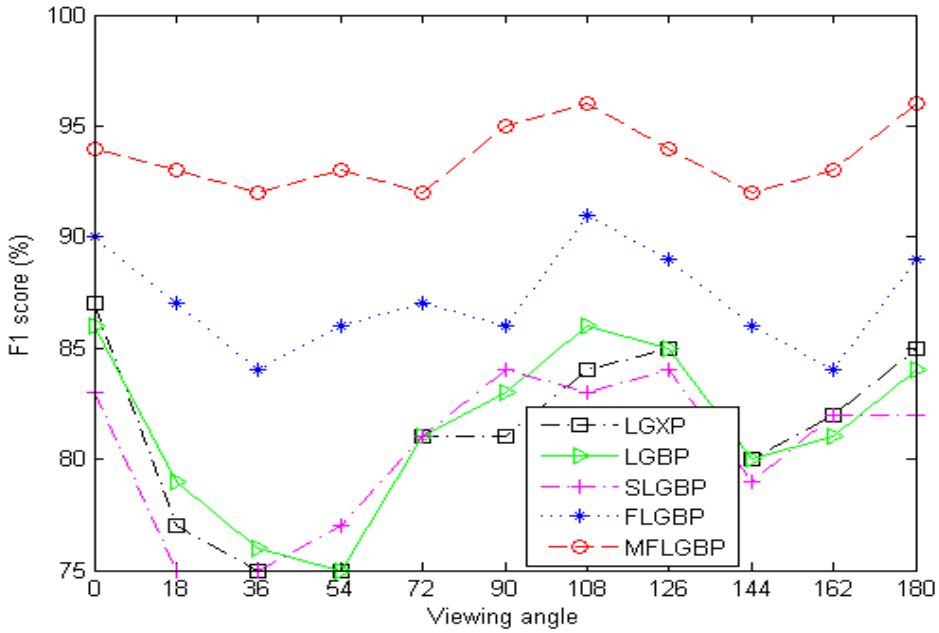

Figure 4.13: Comparison of F_1 score of Gabor-based Fuzzy Gait Features under Normal-Walking covariate

and by computing the mean and variance of these pixels. This process is repeated for the all pixels. Unlike GGI, the proposed MFLGBP constructs the GEI gait representation as the average of frames within one gait cycle. Hence, MFLGBP reduces the required computation burden. Kusakunniran et al. [151] also achieved better performance of 97% on CASIA B using Procrustes Shape Analysis (PSA) and Pairwise Shape Configuration (PSC). Also, a shape re-sampling method was proposed and applied as a prior step to PSC which encodes local shape information by investigating local relation between a point on the re-sampled shape boundary and its neighboring point. PSC embeds both distance and direction into a uniform complex coordinate system. The shape description was constructed for each frame within the gait cycle. Then, Procrustes Mean Shape (PMS) was applied to combine all these descriptions of one gait cycle to generate gait features.

Table 4.17: Comparison of correct classification rates of Gabor-based Fuzzy Gait Features under Carrying-Bag covariate

Angle(°)	**CCR (%)**				
	LGXP	**LGBP**	**SLGBP**	**FLGBP**	**MFLGBP**
0	48.39	50	44.35	54.74	**62.07**
18	33.87	34.68	29.44	46.55	**51.72**
36	34.68	36.29	28.23	42.74	**55.17**
54	35.48	33.87	24.59	38.79	**46.12**
72	29.84	33.87	29.03	49.57	**52.16**
90	31.45	34.68	30.24	53.45	**53.45**
108	31.85	33.06	26.61	46.12	**48.71**
126	35.48	34.68	31.05	40.95	**53.45**
144	39.92	41.94	32.66	38.79	**55.17**
162	42.74	43.95	33.06	48.71	**62.07**
180	47.18	48.39	41.53	46.55	**64.45**

Although this approach has better recognition performance, it requires a high computational process.

The table also shows the results of the proposed approach (MFLGBP) on the OU-ISIR-A (at 6km/h) and comparison with two other approaches. The training for the three approaches is conducted at 6 km/h and the test is conducted also at the same speed. Although each approach achieved 100% accuracy, we found that the performance drastically decreases when testing at a different speed than the one used in training.

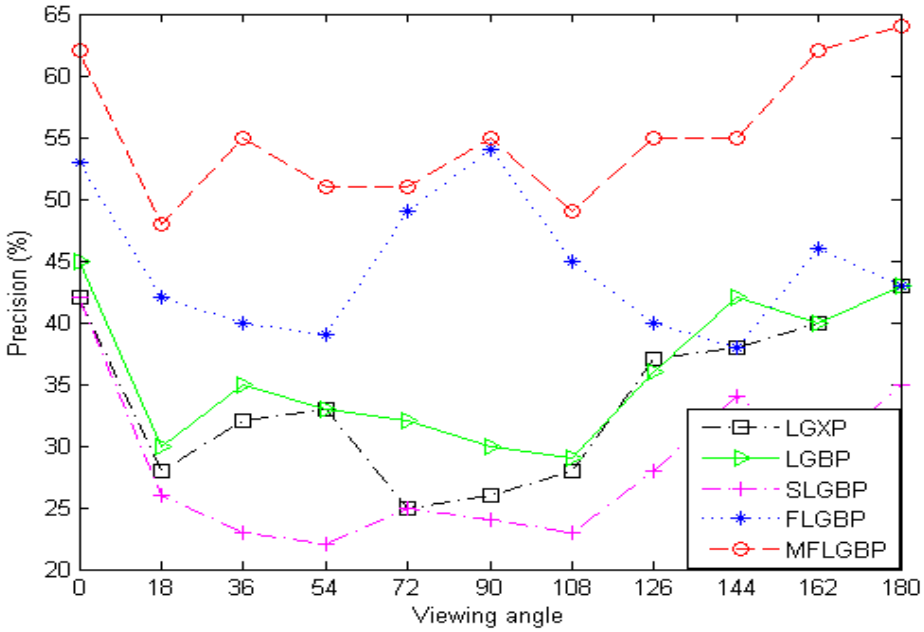

Figure 4.14: Comparison of precision of Gabor-based Fuzzy Gait Features under Carrying-Bag covariate

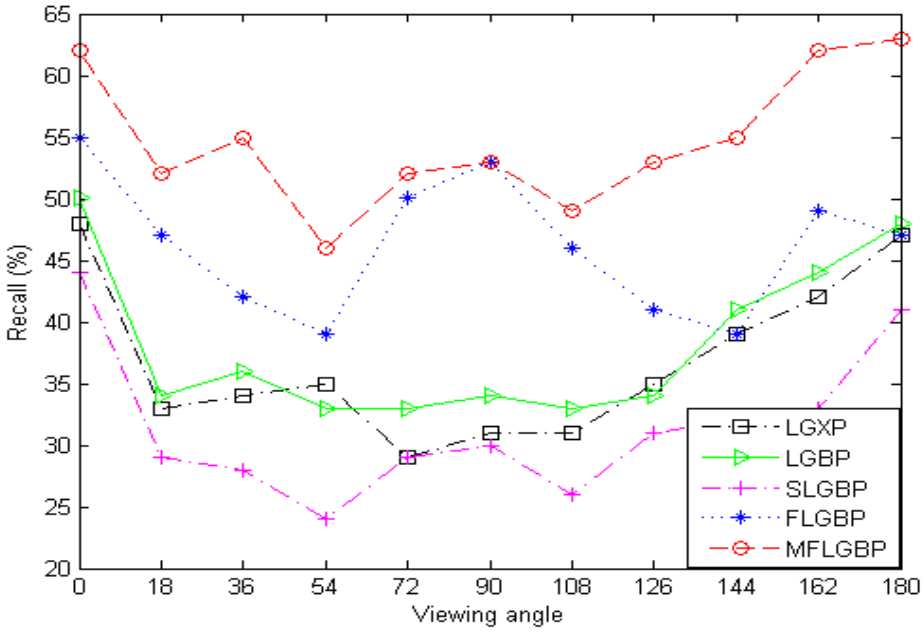

Figure 4.15: Comparison of recall of Gabor-based Fuzzy Gait Features under Carrying-Bag covariate

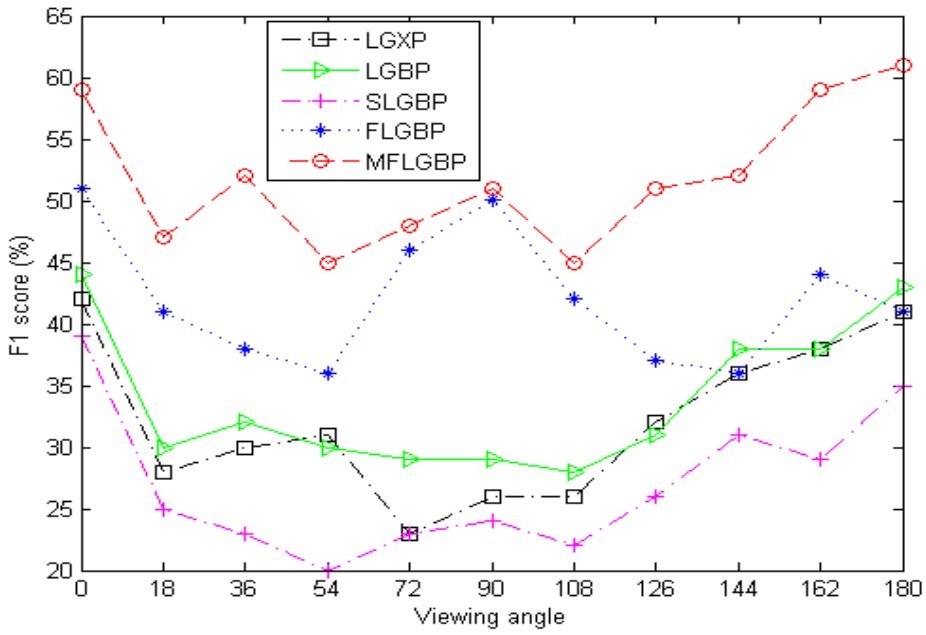

Figure 4.16: Comparison of F_1 score of Gabor-based Fuzzy Gait Features under Carrying-Bag covariate

Table 4.18: Comparison of correct classification rates of Gabor-based Fuzzy Gait Features under Wearing-Coat covariate

Angle(°)	**CCR (%)**				
	LGXP	**LGBP**	**SLGBP**	**FLGBP**	**MFLGBP**
0	16.13	22.85	16.13	38.79	**40.09**
18	17.74	24.86	15.32	32.33	**34.68**
36	16.94	27.59	12.9	34.68	**40.09**
54	16.94	27.16	16.53	41.81	**43.54**
72	18.95	31.47	11.69	44.4	**47.41**
90	20.56	29.74	8.06	41.81	**43.97**
108	15.73	31.47	10.48	40.95	**47.41**
126	15.73	23.71	14.92	**45.26**	43.97
144	16.94	24.14	12.9	42.67	**43.97**
162	15.32	17.24	13.71	30.6	**35.41**
180	20.56	22.85	20.97	32.76	**40.09**

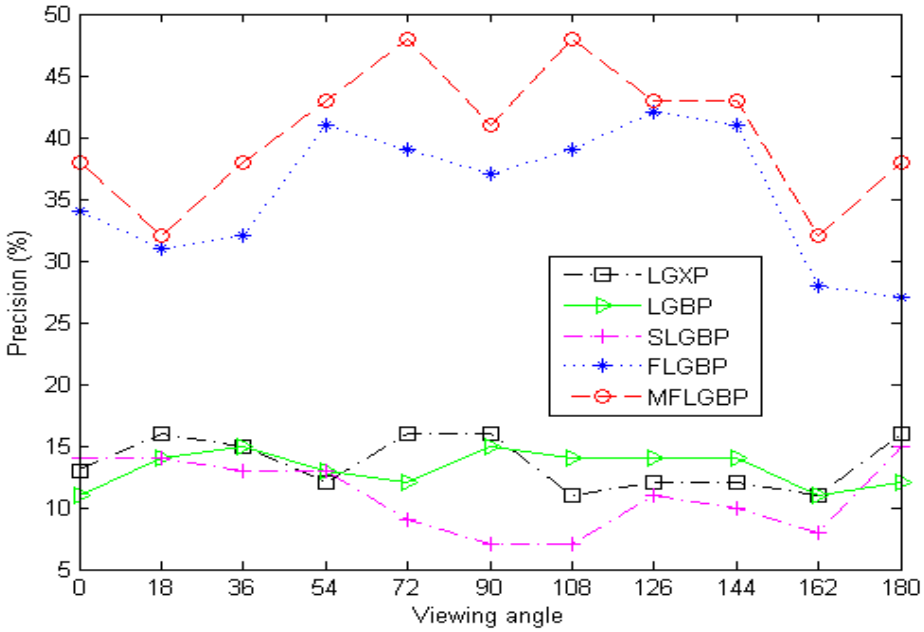

Figure 4.17: Comparison of precision of Gabor-based Fuzzy Gait Features under Wearing-Coat covariate

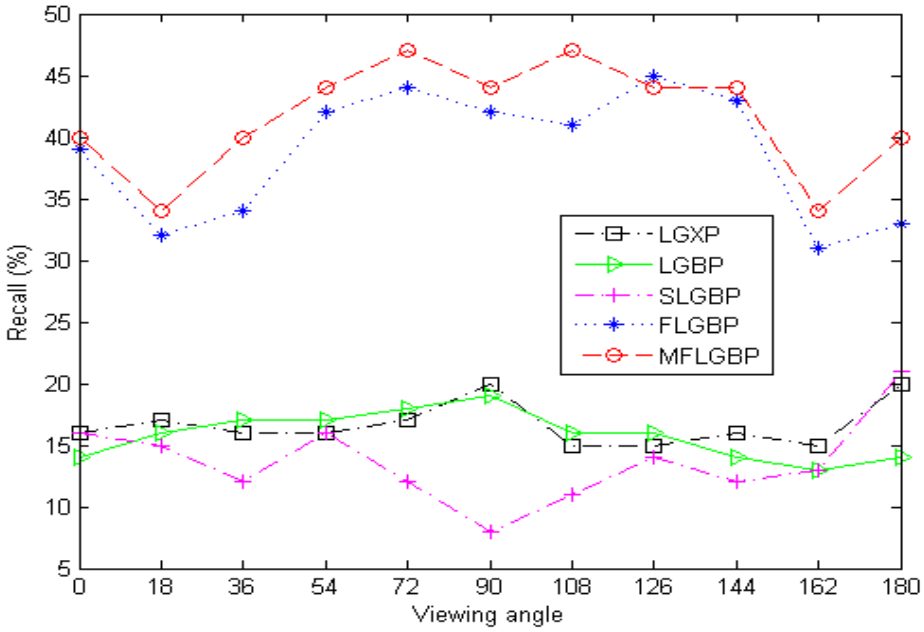

Figure 4.18: Comparison of recall of Gabor-based Fuzzy Gait Features under Wearing-Coat covariate

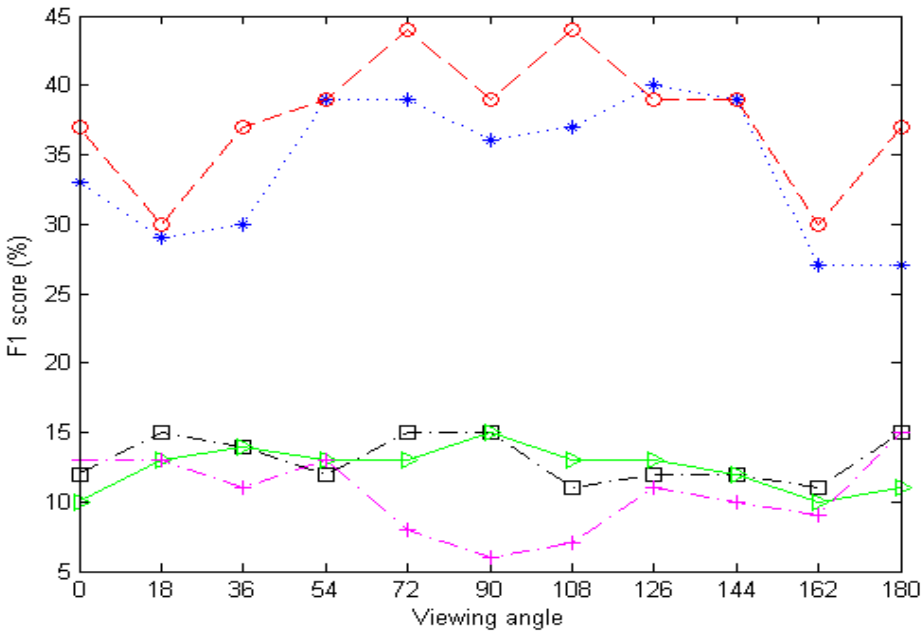

Figure 4.19: Comparison of F_1 score of Gabor-based Fuzzy Gait Features under Wearing-Coat covariate

Table 4.19: Comparison of correct classification rates of Gabor-based Fuzzy Gait Features under different speeds

Speed	**CCR (%)**				
	LGXP	**LGBP**	**SLGBP**	**FLGBP**	**MFLGBP**
2 km/h	88.23	91.17	91.17	94.11	**97.05**
3 km/h	85.29	91.17	88.23	**97.05**	**97.05**
4 km/h	79.41	82.35	88.23	94.11	**100**
5 km/h	88.23	88.23	91.17	91.17	**94.11**
6 km/h	85.29	97.05	94.11	91.17	**100**
7 km/h	82.35	79.41	85.29	**94.11**	**94.11**
8 km/h	82.35	88.23	91.17	88.23	**97.05**
9 km/h	79.41	88.23	82.35	82.35	**94.11**
10 km/h	82.35	91.17	82.35	82.35	**94.11**

Table 4.20: Comparison of precisions of Gabor-based Fuzzy Gait Features under different speeds

Speed	**Precision**				
	LGXP	**LGBP**	**SLGBP**	**FLGBP**	**MFLGBP**
2 km/h	82	86	87	91	**95**
3 km/h	78	89	83	**95**	**95**
4 km/h	70	74	83	91	**100**
5 km/h	82	82	86	86	**91**
6 km/h	80	95	92	86	**100**
7 km/h	73	74	77	**91**	**91**
8 km/h	79	83	86	82	**95**
9 km/h	74	84	77	74	**92**
10 km/h	75	87	74	75	**91**

Table 4.21: Comparison of recalls of Gabor-based Fuzzy Gait Features under different speeds

Speed	**Recall**				
	LGXP	**LGBP**	**SLGBP**	**FLGBP**	**MFLGBP**
2 km/h	88	91	91	94	**97**
3 km/h	85	91	88	97	**97**
4 km/h	79	82	88	94	**100**
5 km/h	88	88	91	91	**94**
6 km/h	85	97	94	91	**100**
7 km/h	82	79	85	**94**	**94**
8 km/h	82	88	91	88	**97**
9 km/h	79	88	82	82	**94**
10 km/h	82	91	82	82	**94**

Table 4.22: Comparison of F_1 score of Gabor-based Fuzzy Gait Features under different speeds

Speed	**F_1 score**				
	LGXP	**LGBP**	**SLGBP**	**FLGBP**	**MFLGBP**
2 km/h	84	88	88	92	**96**
3 km/h	80	90	84	**96**	**96**
4 km/h	73	77	85	92	**100**
5 km/h	84	84	88	88	**92**
6 km/h	81	96	92	88	**100**
7 km/h	76	76	80	**92**	**92**
8 km/h	80	84	88	84	**96**
9 km/h	75	85	78	77	**92**
10 km/h	77	88	77	77	**92**

Table 4.23: Comparison with existing methods in the literature

Approach	**CCR%**		**Notes**
	CASIA B (90^o)	**OU-ISIR-A (6km/h)**	
MFLGBP [proposed]	95.69	100	Best proposed
Kumar et al. [143]	85.66	-	
Yan-qiu Liu et al. [152]	83.00	-	
Jeevan et al. [153]	51.18	-	
Arora et al. [150]	98.00	-	Gait Gaussian Image
Han et al. [9]	93.00	-	Gait Energy Image
Kusakunniran et al. [53]	-	100	DCM
Bashir et al. [154]	95.00	-	Gait Entropy Image
Goffredo et al. [155]	87.00	-	View rectification
Wang et al. [156]	85.00	-	CSC+PSA
Kusakunniran et al. [151]	97.00	-	PSC+PSA
Worapan et al. [121]	93.00	-	GEI+SVR
Guan et al. [104]	-	100	RSM

CHAPTER 5

CONCLUSIONS AND FUTURE WORK

5.1 Thesis Contributions

The main contributions of this thesis are as follows:

1. It investigates the application of fuzzy local binary patterns (FLBP) for extracting more discriminative features from the spatio-temporal gait representation to help in improving the process of human identification.

2. It proposes an effective extension of FLBP kernel-based fuzzy binary patterns (KFLBP) which achieved notable and robust performance against different gait covariates.

3. It proposes two Gabor-based fuzzy features (FLGBP) and (MFLGBP) for gait recognition purposes with enhanced performance.

4. It introduces a region-based partitioning which is robust against gait variations in covariates and environmental conditions.

5.2 Conclusions

In this thesis, we have reviewed most of the previous and current state-of-the-art gait recognition approaches. Most of these approaches can fit into two main categories: Model-Free and Model-Based. Research in model-free is much more than that in model-based due to the computation expensiveness and complexity of model-based methods. Model-free approaches can be temporal or spatio-temporal. Approaches under temporal subcategory analyze features on a frame by frame basis. On the other hand, spatio-temporal methods summarize the whole frame sequence and then extract summary features.

Temporal gait recognition approaches are expensive in terms of storage and computation due to the frame by frame feature extraction and classification. Consequently, we adopt the Gait Energy Image (GEI) as the spatio-temporal gait representation. GEI represents the human walking in a single image conserving motion temporal properties. Several gait recognition approaches relied on features extracted from GEIs. However, they use reduced-dimensionality GEIs or apply the feature extraction algorithm on the holistic GEI. We conducted different-sized partitioning strategy as an attempt to deserve as much discriminative gait information as possible.

Moreover, we extended the fuzzy local binary patterns (FLBP) to improve its discriminatory power for gait recognition purposes. Kernel-based FLBP was proposed to enhance the performance. KFLBP utilizes more than one kernel

(radius) instead of one kernel as in the original FLBP. The reported experimental results demonstrate the outperformance of KFLBP over several gait recognition approaches. Moreover, partitioning has notably enhanced the overall performance of the proposed feature.

In addition, two Gabor-based fuzzy features were proposed and evaluated. GEI is convolved with a Gabor filter bank of 5 different scales and 8 different orientations to produce Gabor responses. Then, FLBP and KFLBP operators are combined with each Gabor response to extract FLGBP and MFLGBP feature vector respectively. The global feature vector is then formed by merging all extracted feature vectors. PCA is applied to reduce the high dimensional global feature vector. Experimental results demonstrate the ouperformance of FLGBP and MFLGBP over several Gabor-based gait recognition methods.

5.3 Future Work

This work can be improved and extended in many directions as follows:

1. More sophisticated preprocessing could be applied to improve the performance.

2. Further investigation of the proposed methods could be done to demonstrate its applicability for other machine learning research problems.

3. More gait recognition approaches could be included in the comparison.

4. Experiments could involve more covariates to prove practicality of the proposed methods for real applications.

5. Further investigation could be done to testify the applicability of the proposed methods for cross viewing angles and cross speed variations.

6. In our experiments, we used only SVM classifier. Several classifiers could be utilized and compared.

7. Several gait databases could be involved in experiments to prove the robustness of our proposed methods.

Bibliography

[1] D. Cunado, M. S. Nixon, and J. N. Carter, "Using gait as a biometric, via phase-weighted magnitude spectra," in *Proceedings of the First International Conference on Audio- and Video-Based Biometric Person Authentication (AVBPA)*. London, UK: Springer-Verlag, 1997, pp. 95–102.

[2] C. Yam, M. S. Nixon, and J. N. Carter, "Gait recognition by walking and running: A model-based approach," in *Proceedings Asian Conference on Computer Vision (ACCV)*, January 2002, pp. 1–6.

[3] J. hee Yoo, M. S. Nixon, and C. J. Harris, "Extracting gait signatures based on anatomical knowledge," in *in Proc. BMVA Symposium on Advancing Biometric Techniques at the Royal Statistical Society, London*, 2002.

[4] L. Lee and W. E. L. Grimson, "Gait analysis for recognition and classification," in *Proceedings of Fifth IEEE International Conference on Automatic Face Gesture Recognition*, May 2002, pp. 148–155.

[5] R. Zhang, C. Vogler, and D. Metaxas, "Human gait recognition at sagittal plane," *Image Vision Comput.*, vol. 25, no. 3, pp. 321–330, Mar. 2007.

[6] S. L. Dockstader, M. J. Berg, and A. M. Tekalp, "Stochastic kinematic modeling and feature extraction for gait analysis," *IEEE Transactions on Image Processing*, vol. 12, no. 8, pp. 962–976, Aug 2003.

[7] H. Lu, K. N. Plataniotis, and A. N. Venetsanopoulos, "A full-body layered deformable model for automatic model-based gait recognition," *EURASIP Journal on Advances in Signal Processing*, vol. 2008, no. 1, p. 261317, 2007.

[8] E. Zhang, Y. Zhao, and W. Xiong, "Active energy image plus 2DLPP for gait recognition," *Signal Processing*, vol. 90, no. 7, pp. 2295 – 2302, 2010.

[9] J. Han and B. Bhanu, "Individual recognition using gait energy image," *IEEE Transactions on Pattern Analysis and Machine Intelligence*, vol. 28, no. 2, pp. 316–322, Feb 2006.

[10] E. Mordini and D. Tzovaras, *Second Generation Biometrics: The Ethical, Legal and Social Context*. Springer-Verlag Berlin Heidelberg, 2012.

[11] A. Jain, A. A. Ross, and K. Nandakumar, *Introduction to Biometrics*. Springer, 2008.

[12] S. Brahnam, L. C. Jain, L. Nanni, and A. Lumini, *Local Binary Patterns - New Variants and Applications*. Springer-Verlag Berlin Heidelberg, 2014.

[13] H. Benaliouche and M. Touahria, "Comparative study of multimodal biometric recognition by fusion of iris and fingerprint," *The Scientific World Journal*, Jan 2014.

[14] H. Iwama, D. Muramatsu, Y. Makihara, and Y. Yagi, "Gait-based person-verification system for forensics," in *IEEE Fifth International Conference on Biometrics: Theory, Applications and Systems (BTAS)*, Sept 2012, pp. 113–120.

[15] M. S. Nixon, I. Bouchrika, B. Arbab-Zavar, and J. N. Carter, "On use of biometrics in forensics: Gait and ear," in *18th European Signal Processing Conference*, Aug 2010, pp. 1655–1659.

[16] D. Muramatsu, Y. Makihara, H. Iwama, T. Tanoue, and Y. Yagi, "Gait verification system for supporting criminal investigation," in *2nd IAPR Asian Conference on Pattern Recognition*, Nov 2013, pp. 747–748.

[17] T. Lee, M. Belkhatir, and S. Sanei, "A comprehensive review of past and present vision-based techniques for gait recognition," *Multimedia Tools and Applications*, vol. 72, no. 3, pp. 2833–2869, 2014.

[18] A. Kale, A. Sundaresan, A. Rajagopalan, N. Cuntoor, A. Roy-Chowdhury, V. Kruger, and R. Chellappa, "Identification of humans using gait," *IEEE Transactions on Image Processing*, vol. 13, no. 9, pp. 1163–1173, 2004.

[19] I. Bouchrika, J. N. Carter, and M. S. Nixon, "Towards automated visual surveillance using gait for identity recognition and tracking across multiple non-intersecting cameras," *Multimedia Tools and Applications*, 2014.

[20] S. Shirke, S. Pawar, and K. Shah, "Literature review: Model free human gait recognition," in *Fourth International Conference on Communication Systems and Network Technologies (CSNT)*, April 2014, pp. 891–895.

[21] E. Tamil, M. Noor, Z. Razak, N. Noor, and A. Tamil, "A review on feature extraction and classification techniques for biosignal processing (part v: Gait signal)," in *4th Kuala Lumpur International Conference on Biomedical Engineering*, ser. IFMBE Proceedings. Springer Berlin Heidelberg, 2008, vol. 21, pp. 122–124.

[22] C. Martek, "A survey of silhouette-based gait recognition methods," 2010.

[23] D. Gafurov, "A survey of biometric gait recognition: Approaches, security and challenges," in *Norsk Informatic Conference (NIK)*, November 2007.

[24] Z. Zhang, M. Hu, and Y. Wang, "A survey of advances in biometric gait recognition," in *Biometric Recognition*, ser. Lecture Notes in Computer Science. Springer Berlin Heidelberg, 2011, vol. 7098, pp. 150–158.

[25] L.-F. Liu, W. Jia, and Y.-H. Zhu, "Survey of gait recognition," in *Emerging Intelligent Computing Technology and Applications with Aspects of Artificial Intelligence*, ser. Lecture Notes in Computer Science. Springer Berlin Heidelberg, 2009, vol. 5755, pp. 652–659.

[26] J. Wang, M. She, S. Nahavandi, and A. Kouzani, "A review of vision-based gait recognition methods for human identification," in *Digital Image Com-*

puting: Techniques and Applications (DICTA), 2010 International Conference on, Dec 2010, pp. 320–327.

[27] S. Sebastian, "Literature survey on automated person identification techniques," *International Journal of Computer Science and Mobile Computing*, vol. 2, p. 232237, 2013.

[28] J. Unar, W. C. Seng, and A. Abbasi, "A review of biometric technology along with trends and prospects," *Pattern Recognition*, vol. 47, no. 8, pp. 2673 – 2688, 2014.

[29] G. Goudelis, A. Tefas, and I. Pitas, "Emerging biometric modalities: a survey," *Journal on Multimodal User Interfaces*, vol. 2, no. 3-4, pp. 217–235, 2008.

[30] S. Chauhan, A. Arora, and A. Kaul, "A survey of emerging biometric modalities," *Procedia Computer Science*, vol. 2, no. 0, pp. 213 – 218, 2010.

[31] D. Cunado, M. S. Nixon, and J. N. Carter, "Automatic extraction and description of human gait models for recognition purposes," *Computer Vision and Image Understanding*, vol. 20, no. 4, pp. 1–40, 2003.

[32] J.-H. Yoo, M. S. Nixon, and C. J. Harris, "Model-driven statistical analysis of human gait motion," in *in Proceedings of International Conference on Image Processing (ICIP)*, vol. 1, 2002, pp. I–285–I–288 vol.1.

[33] H. Yoo and M. S. Nixon, "Automated markerless analysis of human gait motion for recognition and classification," *ETRI Journal*, vol. 33, no. 2, pp. 259–266, 2011.

[34] R. Tanawongsuwan and A. Bobick, "Gait recognition from time-normalized joint-angle trajectories in the walking plane," in *Proceedings of the IEEE Computer Society Conference on Computer Vision and Pattern Recognition*, 2001, pp. II–726–II–731 vol.2.

[35] A. Y. Johnson and A. F. Bobick, "A multi-view method for gait recognition using static body parameters," in *Proceedings of the Third International Conference on Audio- and Video-Based Biometric Person Authentication (AVBPA)*. London, UK, UK: Springer-Verlag, 2001, pp. 301–311.

[36] C. B. Abdelkader, "Stride and cadence as a biometric in automatic person identification and verification," in *Proceedings of the Fifth IEEE International Conference on Automatic Face and Gesture Recognition (FGR)*. Washington, DC, USA: IEEE Computer Society, 2002, pp. 372–377.

[37] S. Niyogi and E. Adelson, "Analyzing and recognizing walking figures in XYT," in *Proceedings of IEEE Computer Society Conference on Computer Vision and Pattern Recognition*, Jun 1994, pp. 469–474.

[38] L. Wang, T. Tan, H. Ning, and W. Hu, "Silhouette analysis-based gait recognition for human identification," *IEEE Transactions on Pattern Analysis and Machine Intelligence*, vol. 25, no. 12, pp. 1505–1518, Dec 2003.

[39] A. Kale, N. Cuntoor, B. Yegnanarayana, A. N. Rajagopalan, and R. Chellappa, "Gait analysis for human identification," in *Proceedings of the 4th International Conference on Audio- and Video-based Biometric Person Authentication (AVBPA)*. Berlin, Heidelberg: Springer-Verlag, 2003, pp. 706–714.

[40] S. Hong, H. Lee, I. Nizami, and E. Kim, "A new gait representation for human identification: Mass vector," in *2nd IEEE Conference on Industrial Electronics and Applications (ICIEA)*, May 2007, pp. 669–673.

[41] H. Ng, W.-H. Tan, H.-L. Tong, J. Abdullah, and R. Komiya, "Extraction of human gait features from enhanced human silhouette images," in *2009 IEEE International Conference on Signal and Image Processing Applications (ICSIPA)*, Nov 2009, pp. 425–430.

[42] S. Shaikh, K. Saeed, and N. Chaki, "Gait recognition using partial silhouette-based approach," in *2014 International Conference on Signal Processing and Integrated Networks (SPIN)*, Feb 2014, pp. 101–106.

[43] A. Sabir, N. Al-jawad, and S. Jassim, "Gait recognition using spatio-temporal silhouette-based features," *Proceeding of SPIE on Mobile Multimedia/Image Processing, Security, and Applications*, vol. 8755, pp. 87 550R–87 550R–10, 2013.

[44] G. Yang, Y. Yin, J. Park, and H. Man, "Human gait recognition by pyramid of hog feature on silhouette images," *Proceeding of SPIE on Optical Pattern*

Recognition, vol. 8748, pp. 87 480J–87 480J–6, 2013.

[45] H. Lee, J. Baek, and E. Kim, "A probabilistic image-weighting scheme for robust silhouette-based gait recognition," *Multimedia Tools and Applications*, vol. 70, no. 3, pp. 1399–1419, 2014.

[46] R. Collins, R. Gross, and J. Shi, "Silhouette-based human identification from body shape and gait," in *Fifth IEEE International Conference on Automatic Face and Gesture Recognition*, May 2002, pp. 366–371.

[47] S. Sengupta, U. Halder, R. Panda, and A. Chowdhury, "A frequency domain approach to silhouette based gait recognition," in *Fourth National Conference on Computer Vision, Pattern Recognition, Image Processing and Graphics (NCVPRIPG)*, Dec 2013, pp. 1–4.

[48] S. Benbakreti and M. Benyettou, "Gait recognition based on leg motion and contour of silhouette," in *International Conference on Information Technology and e-Services (ICITeS)*, March 2012, pp. 1–5.

[49] A. Kochhar, D. Gupta, M. Hanmandlu, and S. Vasikarla, "Novel features for silhouette based gait recognition systems," in *IEEE Applied Imagery Pattern Recognition Workshop (AIPR)*, Oct 2012, pp. 1–6.

[50] Z. Liu and S. Sarkar, "Simplest representation yet for gait recognition: averaged silhouette," in *Proceedings of the 17th International Conference on Pattern Recognition (ICPR)*, vol. 4, Aug 2004, pp. 211–214.

[51] F. Dadashi, B. Araabi, and H. Soltanian-Zadeh, "Gait recognition using wavelet packet silhouette representation and transductive support vector machines," in *2nd International Congress on Image and Signal Processing (CISP)*, Oct 2009, pp. 1–5.

[52] V. Kellokumpu, G. Zhao, S. Li, and M. Pietikinen, "Dynamic texture based gait recognition," in *Advances in Biometrics*, ser. Lecture Notes in Computer Science. Springer Berlin Heidelberg, 2009, vol. 5558, pp. 1000–1009.

[53] W. Kusakunniran, Q. Wu, J. Zhang, and H. Li, "Gait recognition across various walking speeds using higher order shape configuration based on a differential composition model," *IEEE Transactions on Systems, Man, and Cybernetics, Part B (Cybernetics)*, vol. 42, no. 6, pp. 1654–1668, Dec 2012.

[54] L. Wang, H. Ning, T. Tan, and W. Hu, "Fusion of static and dynamic body biometrics for gait recognition," *IEEE Transactions on Circuits and Systems for Video Technology*, vol. 14, no. 2, pp. 149–158, Feb 2004.

[55] A. I. Bazin and M. S. Nixon, "Probabilistic combination of static and dynamic gait features for verification," in *SPIE Defense and Security Symposium on Biometric Technology for Human Identification II*, A. K. Jain and N. K. Ratha, Eds., vol. 5779, 2005, pp. 23–30.

[56] D. K. Wagg and M. S. Nixon, "Automated markerless extraction of walking people using deformable contour models: Research articles," *Comput. Animat. Virtual Worlds*, vol. 15, no. 3-4, pp. 399–406, 2004.

[57] G. V. Veres, L. Gordon, J. N. Carter, and M. S. Nixon, "What image information is important in silhouette-based gait recognition?" in *Proceedings of the IEEE Computer Society Conference on Computer Vision and Pattern Recognition (CVPR)*, vol. 2, June 2004, pp. 776–782.

[58] C. Nandini and C. N. RaviKumar, "An approach to gait recognition," in *International Symposium on Biometrics and Security Technologies*, April 2008, pp. 1–3.

[59] C. Nandini, K. Sindhu, and C. Kumar, "Gait recognition by combining wavelets and geometrical features," in *2nd International Conference on Intelligent Agent and Multi-Agent Systems (IAMA)*, Sept 2011, pp. 52–56.

[60] C. Nandini and K. Sindhu, "Gait authentication based on fusion of wavelet and Hough transform," *International Journal of Engineering and Technology (IJET)*, vol. 2, no. 3, pp. 347–351, March 2012.

[61] I. Nizami, S. Hong, H. Lee, S. Ahn, K.-A. Toh, and E. Kim, "Multi-view gait recognition fusion methodology," in *3rd IEEE Conference on Industrial Electronics and Applications*, June 2008, pp. 2101–2105.

[62] S. Hong, H. Lee, and E. Kim, "Fusion of multiple gait cycles for human identification," in *ICROS-SICE International Joint Conference*, Aug 2009, pp. 3171–3175.

[63] B. Lee, S. Hong, H. Lee, and E. Kim, "Gait recognition system using decision-level fusion," in *Proceedings of the 5th IEEE Conference on Industrial Electronics and Applications (ICIEA)*, June 2010, pp. 313–316.

[64] T. H. Lam, R. S. Lee, and D. Zhang, "Human gait recognition by the fusion of motion and static spatio-temporal templates," *Pattern Recognition*, vol. 40, no. 9, pp. 2563 – 2573, 2007.

[65] J. Lu and E. Zhang, "Gait recognition for human identification based on ICA and fuzzy SVM through multiple views fusion," *Pattern Recognition Letters*, vol. 28, no. 16, pp. 2401 – 2411, 2007.

[66] C. Ran, Y. qiu Liu, and X. Wang, "Human gait recognition for multiple views," *Procedia Engineering, Advanced in Control Engineering and Information Science (CEIS)*, vol. 15, pp. 1832 – 1836, 2011.

[67] J. Han and B. Bhanu, "Statistical feature fusion for gait-based human recognition," in *Proceedings of the IEEE Computer Society Conference on Computer Vision and Pattern Recognition (CVPR)*, vol. 2, June 2004, pp. II–842–II–847.

[68] S. Hong, H. Lee, S. J. An, and E. Kim, "Fusion of multiple gait features for human identification," in *International Conference on Control, Automation and Systems (ICCAS)*, Oct 2008, pp. 2121–2125.

[69] A. Kale, A. Chowdhury, and R. Chellappa, "Towards a view invariant gait recognition algorithm," in *Proceedings of IEEE Conference on Advanced Video and Signal Based Surveillance*, July 2003, pp. 143–150.

[70] S. Sarkar, P. Phillips, Z. Liu, I. Vega, P. Grother, and K. Bowyer, "The human ID gait challenge problem: data sets, performance, and analysis," *IEEE Transactions on Pattern Analysis and Machine Intelligence*, vol. 27, no. 2, pp. 162–177, Feb 2005.

[71] Y. Ran, I. Weiss, Q. Zheng, and L. Davis, "Pedestrian detection via periodic motion analysis," *International Journal of Computer Vision*, vol. 71, no. 2, pp. 143–160, 2007.

[72] M.-F. Ho, K.-Z. Chen, and C.-L. Huang, "Gait analysis for human walking paths and identities recognition," in *IEEE International Conference on Multimedia and Expo ICME*, June 2009, pp. 1054–1057.

[73] A. Kale, A. Rajagopalan, N. Cuntoor, and V. Kruger, "Gait-based recognition of humans using continuous HMMs," in *Proceedings of the fifth IEEE International Conference on Automatic Face and Gesture Recognition*, May 2002, pp. 336–341.

[74] A. Kale, A. Sundaresan, A. Rajagopalan, N. Cuntoor, A. Roy-Chowdhury, V. Kruger, and R. Chellappa, "Identification of humans using gait," *IEEE Transactions on Image Processing*, vol. 13, no. 9, pp. 1163–1173, Sept 2004.

[75] L. Wang, W. Hu, and T. Tan, "A new attempt to gait-based human identification," in *Proceedings of the 16th International Conference on Pattern Recognition*, vol. 1, 2002, pp. 115–118 vol.1.

[76] C. BenAbdelkader, R. Cutler, H. Nanda, and L. Davis, "Eigengait: Motion-based recognition of people using image self-similarity," in *Audio- and Video-Based Biometric Person Authentication,*, ser. Lecture Notes in Computer Science, J. Bigun and F. Smeraldi, Eds. Springer Berlin Heidelberg, 2001, vol. 2091, pp. 284–294.

[77] R. Cutler and L. Davis, "Robust real-time periodic motion detection, analysis, and applications," *IEEE Transactions on Pattern Analysis and Machine Intelligence*, vol. 22, no. 8, pp. 781–796, Aug 2000.

[78] L. Lee, "Gait dynamics for recognition and classification," in *Proceedings of the 5th IEEE International Conference on Automatic Face and Gesture Recognition (AFGR)*, September 2001.

[79] J. Davis and A. Bobick, "The representation and recognition of human movement using temporal templates," in *Proceedings of IEEE Computer Society Conference on Computer Vision and Pattern Recognition*, Jun 1997, pp. 928–934.

[80] C. Chen, J. Zhang, and R. Fleischer, "Distance approximating dimension reduction of riemannian manifolds," *IEEE Transactions on Systems, Man, and Cybernetics, Part B: Cybernetics*, vol. 40, no. 1, pp. 208–217, Feb 2010.

[81] I. F. Nizami, S. Hong, H. Lee, B. Lee, and E. Kim, "Automatic gait recognition based on probabilistic approach," *International Journal of Imaging Systems and Technology*, vol. 20, no. 4, pp. 400–408, Dec. 2010.

[82] S. Rahati, R. Moravejian, and F. Kazemi, "Gait recognition using wavelet transform," in *Fifth International Conference on Information Technology: New Generations, (ITNG)*, April 2008, pp. 932–936.

[83] S. Wei, C. Ning, and Y. Gao, "Biomimetic gait recognition based on motion contours wavelets analysis and mutual information," in *3rd International Congress on Image and Signal Processing (CISP)*, vol. 1, Oct 2010, pp. 404–408.

[84] K. Arai and R. Andrie, "Gait recognition method based on wavelet transformation and its evaluation with Chinese Academy of Sciences (CASIA) gait database as a human gait recognition dataset," in *Ninth International Conference on Information Technology: New Generations (ITNG)*, April 2012, pp. 656–661.

[85] L. Du and W. Shao, "Recognizing gait using Haar wavelet and support vector machine," in *Soft Computing in Information Communication Technology*, ser. Advances in Intelligent and Soft Computing. Springer Berlin Heidelberg, 2012, vol. 158, pp. 221–227.

[86] D. Ming, C. Zhang, Y. Bai, B. Wan, Y. Hu, and K. Luk, "Gait recognition based on multiple views fusion of wavelet descriptor and human skele-

ton model," in *IEEE International Conference on Virtual Environments, Human-Computer Interfaces and Measurements Systems, VECIMS*, May 2009, pp. 246–249.

[87] J. Lu, E. Zhang, and C. Jing, "Gait recognition using wavelet descriptors and independent component analysis," in *Advances in Neural Networks - ISNN*, ser. Lecture Notes in Computer Science. Springer Berlin Heidelberg, 2006, vol. 3972, pp. 232–237.

[88] C.-R. Li, J.-P. Li, X.-C. Yang, and Z.-W. Liang, "Gait recognition using the magnitude and phase of quaternion wavelet transform," in *International Conference on Wavelet Active Media Technology and Information Processing (ICWAMTIP)*, Dec 2012, pp. 322–324.

[89] H. Zhang and Z. Liu, "Gait representation and recognition using Haar wavelet and Radon transform," in *WASE International Conference on Information Engineering (ICIE)*, vol. 1, July 2009, pp. 83–86.

[90] A. Sabir, N. Al-Jawad, S. Jassim, and A. Al-Talabani, "Human gait gender classification based on fusing spatio-temporal and wavelet statistical features," in *5th Computer Science and Electronic Engineering Conference (CEEC)*, Sept 2013, pp. 140–145.

[91] T. Amin and D. Hatzinakos, "Wavelet analysis of cyclic human gait for recognition," in *16th International Conference on Digital Signal Processing*, July 2009, pp. 1–6.

[92] K. Arai and R. Asmara, "Human gait gender classification using 3D discrete wavelet transform feature extraction," *International Journal of Advanced Research in Artificial Intelligence (IJARAI)*, vol. 3, no. 2, pp. 12–17, 2014.

[93] S. Chen, W. Huang, Q. Guo, and L. Dong, "Wavelet moments for gait recognition represented by motion templates," in *Seventh International Conference on Fuzzy Systems and Knowledge Discovery (FSKD)*, vol. 2, Aug 2010, pp. 620–624.

[94] N. Boulgouris and Z. Chi, "Gait representation and recognition based on Radon transform," in *IEEE International Conference on Image Processing*, Oct 2006, pp. 2665–2668.

[95] D.-Y. Huang, T.-W. Lin, W.-C. Hu, and C.-H. Cheng, "Gait recognition based on Gabor wavelets and modified gait energy image for human identification," *Journal of Electronic Imaging*, vol. 22, no. 4, Oct 2013.

[96] M. Hu, Y. Wang, Z. Zhang, and Y. Wang, "Combining spatial and temporal information for gait based gender classification," in *20th International Conference on Pattern Recognition (ICPR)*, Aug 2010, pp. 3679–3682.

[97] D. Tao, X. Li, X. Wu, and S. Maybank, "General tensor discriminant analysis and Gabor features for gait recognition," *IEEE Transactions on Pattern Analysis and Machine Intelligence*, vol. 29, no. 10, pp. 1700–1715, Oct 2007.

[98] X. Yang, J. Dai, Y. Zhou, and J. Yang, "Gabor-based discriminative common vectors for gait recognition," in *Congress on Image and Signal Processing (CISP)*, vol. 4, May 2008, pp. 191–195.

[99] X. Yang, Y. Zhou, T. Zhang, G. Shu, and J. Yang, "Gait recognition based on dynamic region analysis," *Signal Processing*, vol. 88, no. 9, pp. 2350 – 2356, 2008.

[100] W. Zhang, S. Shan, W. Gao, X. Chen, and H. Zhang, "Local Gabor binary pattern histogram sequence (LGBPHS): a novel non-statistical model for face representation and recognition," in *Tenth IEEE International Conference on Computer Vision (ICCV)*, vol. 1, Oct 2005, pp. 786–791.

[101] W. Zhang, S. Shan, X. Chen, and W. Gao, "Are Gabor phases really useless for face recognition?" in *Proceedings of International Conference on Pattern Recognition (ICPR'06)*, 2006, pp. 606–609.

[102] B. Zhang, S. Shan, X. Chen, and W. Gao, "Histogram of Gabor phase patterns (HGPP): A novel object representation approach for face recognition," *IEEE Transactions on Image Processing*, vol. 16, no. 1, pp. 57–68, Jan 2007.

[103] S. Xie, S. Shan, X. Chen, and J. Chen, "Fusing local patterns of Gabor magnitude and phase for face recognition," *IEEE Transactions on Image Processing*, vol. 19, no. 5, pp. 1349–1361, May 2010.

[104] Y. Guan and C. T. Li, "A robust speed-invariant gait recognition system for walker and runner identification," in *2013 International Conference on Biometrics (ICB)*, June 2013, pp. 1–8.

[105] T. Guang-Jian, H. Fu-Yuan, and Z. Rong-chun, "Gait recognition based on fourier descriptors," in *Proceedings of International Symposium on Intelligent Multimedia, Video and Speech Processing*, Oct 2004, pp. 29–32.

[106] Z. Ling, C. Zhao, Q. Pan, Y. Wang, and Y. Cheng, "Analyzing human movements from silhouettes via fourier descriptor," in *IEEE International Conference on Automation and Logistics*, Aug 2007, pp. 231–236.

[107] D.-Y. Huang, W.-C. Hu, C.-W. Chuang, M.-S. Chen, and C.-C. Ko, "Gait recognition of different people groups based on fourier descriptor and support vector machine," in *11th International Conference on Hybrid Intelligent Systems (HIS)*, Dec 2011, pp. 601–604.

[108] Y. Ran, I. Weiss, Q. Zheng, and L. Davis, "Pedestrian detection via periodic motion analysis," *International Journal of Computer Vision*, vol. 71, no. 2, pp. 143–160, 2007.

[109] M.-F. Ho, K.-Z. Chen, and C.-L. Huang, "Gait analysis for human walking paths and identities recognition," in *IEEE International Conference on Multimedia and Expo (ICME)*, June 2009, pp. 1054–1057.

[110] K. Iwamoto, K. Sonobe, and N. Komatsu, "A gait recognition method using HMM," in *SICE Annual Conference*, vol. 2, Aug 2003, pp. 1936–1941 Vol.2.

[111] A. Kale, A. Rajagopalan, N. Cuntoor, and V. Kruger, "Gait-based recognition of humans using continuous hmms," in *Proceedings of the Fifth IEEE International Conference on Automatic Face and Gesture Recognition*, May 2002, pp. 336–341.

[112] A. Kale, A. Sundaresan, A. Rajagopalan, N. Cuntoor, A. Roy-Chowdhury, V. Kruger, and R. Chellappa, "Identification of humans using gait," *IEEE Transactions on Image Processing*, vol. 13, no. 9, pp. 1163–1173, Sept 2004.

[113] K. Wang, X. Xing, T. Yan, and Z. Lv, "Couple metric learning based on separable criteria with its application in cross-view gait recognition," in *Biometric Recognition*, ser. Lecture Notes in Computer Science. Springer International Publishing, 2014, vol. 8833, pp. 347–356.

[114] W. Kusakunniran, Q. Wu, H. Li, and J. Zhang, "Multiple views gait recognition using view transformation model based on optimized gait energy image," in *IEEE 12th International Conference on Computer Vision Workshops (ICCV Workshops)*, Sept 2009, pp. 1058–1064.

[115] Y. Makihara, R. Sagawa, Y. Mukaigawa, T. Echigo, and Y. Yagi, "Gait recognition using a view transformation model in the frequency domain," in *Computer Vision ECCV*, ser. Lecture Notes in Computer Science. Springer Berlin Heidelberg, 2006, vol. 3953, pp. 151–163.

[116] W. Kusakunniran, Q. Wu, J. Zhang, Y. Ma, and H. Li, "A new view-invariant feature for cross-view gait recognition," *IEEE Transactions on*

Information Forensics and Security, vol. 8, no. 10, pp. 1642–1653, Oct 2013.

[117] M. Hu, Y. Wang, Z. Zhang, J. Little, and D. Huang, "View-invariant discriminative projection for multi-view gait-based human identification," *IEEE Transactions on Information Forensics and Security*, vol. 8, no. 12, pp. 2034–2045, Dec 2013.

[118] J. Han, B. Bhanu, and A. Roy-Chowdhury, "A study on view-insensitive gait recognition," in *IEEE International Conference on Image Processing (ICIP)*, vol. 3, Sept 2005, pp. III–297–300.

[119] A. Mansur, Y. Makihara, D. Muramatsu, and Y. Yagi, "Cross-view gait recognition using view-dependent discriminative analysis," in *IEEE International Joint Conference on Biometrics (IJCB)*, Sept 2014, pp. 1–8.

[120] D. Muramatsu, Y. Makihara, and Y. Yagi, "View transformation-based cross-view gait recognition using transformation consistency measure," in *International Workshop on Biometrics and Forensics (IWBF)*, March 2014, pp. 1–6.

[121] W. Kusakunniran, Q. Wu, J. Zhang, and H. Li, "Support vector regression for multi-view gait recognition based on local motion feature selection," in *IEEE Conference on Computer Vision and Pattern Recognition (CVPR)*, June 2010, pp. 974–981.

[122] X. Huang and N. Boulgouris, "Gait recognition using multiple views," in *IEEE International Conference on Acoustics, Speech and Signal Processing (ICASSP)*, March 2008, pp. 1705–1708.

[123] X. Chen, T. Yang, and J. Xu, "Cross-view gait recognition based on human walking trajectory," *Journal of Visual Communication and Image Representation*, vol. 25, no. 8, pp. 1842 – 1855, 2014.

[124] A. Kale, A. Chowdhury, and R. Chellappa, "Towards a view invariant gait recognition algorithm," in *Proceedings of IEEE Conference on Advanced Video and Signal Based Surveillance*, July 2003, pp. 143–150.

[125] S. Yu, D. Tan, and T. Tan, "A framework for evaluating the effect of view angle, clothing and carrying condition on gait recognition," in *18th International Conference on Pattern Recognition (ICPR)*, vol. 4, 2006, pp. 441–444.

[126] J. Little and J. Boyd, "Recognizing people by their gait: The shape of motion," in *Videre*, vol. 1, no. 2, 1998, pp. 1–33.

[127] Y. Chai, J. Ren, R. Zhao, and J. Jia, "Automatic gait recognition using dynamic variance features," in *7th International Conference on Automatic Face and Gesture Recognition (FGR06)*, April 2006, pp. 475–480.

[128] A. Kale, N. Cuntoor, B. Yegnanarayana, A. Rajagopalan, and R. Chellappa, "Gait-based human identification using appearance matching," in *Optical and Digital Techniques for Information Security*, ser. Advanced Sciences and

Technologies for Security Applications. Springer New York, 2005, vol. 1, pp. 271–295.

[129] R. Gross and J. Shi, "The CMU motion of body (MoBo) database," *Technical report CMU-RI-TR-01-18, Robotics Institute, Carnegie Mellon University*, 2001.

[130] J. Shutler, M. Grant, M. Nixon, and J. Carter, "On a large sequence-based human gait database," in *Applications and Science in Soft Computing*, ser. Advances in Soft Computing. Springer Berlin Heidelberg, 2004, vol. 24, pp. 339–346.

[131] Y. Makihara, H. Mannami, A. Tsuji, M. Hossain, K. Sugiura, A. Mori, and Y. Yagi, "The OU-ISIR gait database comprising the treadmill dataset," *IPSJ Transactions on Computer Vision and Applications*, vol. 4, pp. 53–62, April 2012.

[132] H. Ng, C. Ho, W.-H. Tan, H.-L. Tong, K.-W. Ng, T.-V. Yap, P.-F. Chong, L.-K. Tan, J. Abdullah, and C. Eswaran, "MMUGait database and baseline results," in *Advances in Visual Informatics*, ser. Lecture Notes in Computer Science. Springer International Publishing, 2013, vol. 8237, pp. 458–469.

[133] T. Ojala, M. Pietikainen, and T. Maenpaa, "Multiresolution gray-scale and rotation invariant texture classification with local binary patterns," *IEEE Transactions on Pattern Analysis and Machine Intelligence*, vol. 24, no. 7, pp. 971–987, Jul 2002.

[134] T. Ahonen, A. Hadid, and M. Pietikainen, "Face description with local binary patterns: Application to face recognition," *IEEE Transactions on Pattern Analysis and Machine Intelligence*, vol. 28, no. 12, pp. 2037–2041, Dec 2006.

[135] G. Zhao and M. Pietikainen, "Dynamic texture recognition using local binary patterns with an application to facial expressions," *IEEE Transactions on Pattern Analysis and Machine Intelligence*, vol. 29, no. 6, pp. 915–928, June 2007.

[136] M. Hu, Y. Wang, Z. Zhang, D. Zhang, and J. Little, "Incremental learning for video-based gait recognition with LBP flow," *IEEE Transactions on Cybernetics*, vol. 43, no. 1, pp. 77–89, Feb 2013.

[137] D. Iakovidis, E. Keramidas, and D. Maroulis, "Fuzzy local binary patterns for ultrasound texture characterization," in *Image Analysis and Recognition*, ser. Lecture Notes in Computer Science, A. Campilho and M. Kamel, Eds. Springer Berlin Heidelberg, 2008, vol. 5112, pp. 750–759.

[138] D. Tao, X. Li, X. Wu, and S. J. Maybank, "General tensor discriminant analysis and Gabor features for gait recognition," *IEEE Transactions on Pattern Analysis and Machine Intelligence*, vol. 29, no. 10, pp. 1700–1715, 2007.

[139] Y. Du, C. Belcher, and Z. Zhou, "Scale invariant Gabor descriptor-based noncooperative iris recognition," *EURASIP Journal on Advances in Signal*

Processing, pp. 37:1–37:13, Feb. 2010.

[140] L. Shen and L. Bai, "A review on Gabor wavelets for face recognition," *Pattern Analysis and Applications*, vol. 9, no. 2-3, pp. 273–292, 2006.

[141] M. Lades, J. Vorbruggen, J. Buhmann, J. Lange, C. von der Malsburg, R. Wurtz, and W. Konen, "Distortion invariant object recognition in the dynamic link architecture," *IEEE Transactions on Computers*, vol. 42, no. 3, pp. 300–311, 1993.

[142] H. Iwama, M. Okumura, Y. Makihara, and Y. Yagi, "The OU-ISIR gait database comprising the large population dataset and performance evaluation of gait recognition," *IEEE Transactions on Information Forensics and Security*, vol. 7, no. 5, pp. 1511–1521, Oct 2012.

[143] H. P. M. Kumar and H. S. Nagendraswamy, "LBP for gait recognition: A symbolic approach based on GEI plus RBL of GEI," in *International Conference on Electronics and Communication Systems (ICECS)*, Feb 2014, pp. 1–5.

[144] K. B. Low and U. U. Sheikh, "Gait recognition using local ternary pattern (LTP)," in *IEEE International Conference on Signal and Image Processing Applications (ICSIPA)*, Oct 2013, pp. 167–171.

[145] H. Ali, J. Dargham, C. Ali, and E. Moung, "Gait recognition using gait energy image," *International Journal of Signal Processing, Image Processing and Pattern Recognition*, vol. 4, no. 3, pp. 141–152, Sept 2011.

[146] A. G. Binsaadoon and E.-S. M. El-Alfy, "Gait-based recognition for human identification using fuzzy local binary patterns," in *Proceedings of the 8th International Conference on Agents and Artificial Intelligence*, 2016, pp. 314–321.

[147] S. Xie, S. Shan, X. Chen, and J. Chen, "Fusing local patterns of Gabor magnitude and phase for face recognition," *IEEE Transactions on Image Processing*, vol. 19, no. 5, pp. 1349–1361, 2010.

[148] W. Zhang, S. Shan, W. Gao, X. Chen, and H. Zhang, "Local Gabor binary pattern histogram sequence (LGBPHS): a novel non-statistical model for face representation and recognition," in *Tenth IEEE International Conference on Computer Vision ICCV*, vol. 1, 2005, pp. 786–791.

[149] G. Yang, Y. Yin, J. Park, and H. Man, "Human gait recognition by pyramid of HOG feature on silhouette images," *Proceeding SPIE Optical Pattern Recognition*, vol. 8748, no. 1, pp. 87 480J–87 480J–6, April 2013.

[150] P. Arora and S. Srivastava, "Gait recognition using gait gaussian image," in *2nd International Conference on Signal Processing and Integrated Networks (SPIN)*, Feb 2015, pp. 791–794.

[151] W. Kusakunniran, Q. Wu, J. Zhang, and H. Li, "Pairwise shape configuration-based psa for gait recognition under small viewing angle change," in *8th IEEE International Conference on Advanced Video and Signal Based Surveillance (AVSS)*, Aug 2011, pp. 17–22.

[152] Y. qiu Liu and X. Wang, "Human gait recognition for multiple views," *Procedia Engineering, Advanced in Control Engineering and Information Science (CEIS)*, vol. 15, pp. 1832 – 1836, 2011.

[153] M. Jeevan, N. Jain, M. Hanmandlu, and G. Chetty, "Gait recognition based on gait pal and pal entropy image," in *IEEE International Conference on Image Processing*, Sept 2013, pp. 4195–4199.

[154] K. Bashir, T. Xiang, and S. Gong, "Gait recognition using gait entropy image," in *3rd International Conference on Imaging for Crime Detection and Prevention (ICDP)*, Dec 2009, pp. 1–6.

[155] M. Goffredo, I. Bouchrika, J. N. Carter, and M. S. Nixon, "Self-calibrating view-invariant gait biometrics," *IEEE Transactions on Systems, Man, and Cybernetics, Part B (Cybernetics)*, vol. 40, no. 4, pp. 997–1008, Aug 2010.

[156] L. Wang, T. Tan, W. Hu, and H. Ning, "Automatic gait recognition based on statistical shape analysis," *IEEE Transactions on Image Processing*, vol. 12, no. 9, pp. 1120–1131, Sept 2003.

Appendix .1. Thesis Outcomes

- **Published**

1. Amer G. Binsaadoon and El-Sayed M. El-Alfy, "Statistical Gabor-Based Gait Recognition Using Region-Level Analysis," *in Proceedings of the* 9^{th} *IEEE European Modeling Symposium (EMS'15)*, Madrid, Spain, 2015.

2. Amer G. Binsaadoon and El-Sayed M. El-Alfy, "Gait-Based Human Identification Using Fuzzy Local Binary Patterns," in *Proceedings of the* 8^{th} *International Conference on Agents and Artificial Intelligence (ICAART'16)*, Vol. 2, pp. 314-321, Rome, Italy, 2016.

3. Amer G. Binsaadoon and El-Sayed M. El-Alfy, "FLGBP: Improved Method for Gait Representation and Recognition," *in Proceedings of IEEE World Symposium on Computer Applications and Research (WS-CAR'16)*, pp. 59-64, Cairo, Egypt, March, 2016.

4. Amer G. Binsaadoon and El-Sayed M. El-Alfy, "Kernel-Based Fuzzy Local Binary Patterns for Gait Recognition," in *Proceedings of the* 9^{th} *IEEE European Modeling Symposium (EMS'16)*, Pisa, Italy, 2016.

5. Amer G. Binsaadoon and El-Sayed M. El-Alfy, "Multi-Kernel Fuzzy-Based Local Gabor Patterns for Gait Recognition," in *Advances in Visual Computing, Lecture Notes in Computer Science, Vol. 10072, Springer, also presented at the* 12^{th} *International Symposium on Visual*

Computing (ISVC'16), Las Vegas, Nevada, USA, December, 2016.

6. Amer G. Binsaadoon and El-Sayed M. El-Alfy, "Statistical Gabor-Based Gait Recognition Using Region-Level Analysis," *International Journal of Simulation, Systems, Science, and Technology (IJSSST)*, vol. 17, no. 33, 2016.

- **Submitted**

1. El-Sayed M. El-Alfy and Amer G. Binsaadoon, "Silhouette-Based Gender Recognition in Smart Environments Using Fuzzy Local Binary Patterns and Support Vector Machines," *Procedia Computer Science, Elsevier, the* 8^{th} *International Conference on Ambient Systems, Networks and Technologies*, Madeira, Portugal, May, 2017.

- **Under Preparation**

1. Amer G. Binsaadoon, and El-Sayed M. El-Alfy, "Fusion of Gabor Filters with Multiscale Fuzzy Local Binary Patterns for Gait Recognition".

2. El-Sayed M. El-Alfy and Amer G. Binsaadoon, "Evaluation of Local Binary Pattern Variants for Texture Recognition".

3. El-Sayed M. El-Alfy and Amer G. Binsaadoon, "A Survey of Gait Recognition Techniques".

- **Patents**

1. Amer G. Binsaadoon and El-Sayed M. El-Alfy,"APARATUS AND METHOD FOR GAIT RECOGNITION," September, 2016.

2. Amer G. Binsaadoon and El-Sayed M. El-Alfy, "MFLGBP: MULTI-KERNEL FUZZY-BASED LOCAL GABOR PATTERNS FOR GAIT RECOGNITION," 2017.

Vitae

- Name: Amer Ghazi Abdullah Binsaadoon
- Nationality: Yemen
- Date of Birth: November 16, 1985
- Email: *agbinsaadoon@gmail.com*
- Permenant Address: Hadramout, Yemen
- Educational Qualification:

  M.S. IN COMPUTER SCIENCE

  January, 2017

  King Fahd University of Petroleum and Minerals

  Dhahran, Saudi Arabia

  B.S. IN INFORMATION TECHNOLOGY

  July, 2009

  Cairo University

  Cairo, Egypt